

MARTIN MARIETTA ENERGY SYSTEMS LIBRARIES



3 4456 0349686 6

ORNL 1770 4A
Reactors-Research and Power

AEIC RESEARCH AND DEVELOPMENT REPORT

PRELIMINARY CRITICAL ASSEMBLIES OF THE
REFLECTOR MODERATOR REACTOR

R. M. Spencer



CENTRAL RESEARCH LIBRARY
DOCUMENT COLLECTION

LIBRARY LOAN COPY

DO NOT TRANSFER TO ANOTHER PERSON

If you wish someone else to see this document,
send in name with document and the library will
arrange a loan.

OAK RIDGE NATIONAL LABORATORY
OPERATED BY
CARBIDE AND CARBON CHEMICALS COMPANY
A DIVISION OF UNION CARBIDE AND CARBON CORPORATION



POST OFFICE BOX P
OAK RIDGE, TENNESSEE

RESTRICTED DATA

This document contains Restricted Data as defined in the Atomic Energy Act of 1946. Its transmission or disclosure of its contents in any manner to an unauthorized person is prohibited.

ORNL 1770

This document contains 89 pages
This is copy 4 of 197 Series A

Subject Category Reactors - Research
and Power

PRELIMINARY CRITICAL ASSEMBLIES
of the
REFLECTOR MODERATOR REACTOR

Experimentation by D V P Williams
R C Keen (Louisiana State University)
J J Lynn
Dixon Callihan

Reported by R M Spencer, USAF

DATE ISSUED

NOV 22 1954

PHYSICS DIVISION

A H Snell
Director

Contract No W-7405, Eng 26
OAK RIDGE NATIONAL LABORATORY

Operated by

CARBIDE AND CARBON CHEMICALS COMPANY
A Division of Union Carbide and Carbon Corporation
Post Office Box P
Oak Ridge, Tennessee



3 4456 0349686 6

INTERNAL DISTRIBUTION

1	C E Center	46	C P Keim
2	Biology Library	47	C S Harrill
3	Health Physics Library	48	C E Winters
4-5	Central Research Library	49	D S Billington
6	Reactor Experimental Engineering Library	50	D W Cardwell
7-20	Laboratory Records Department	51	E M King
21	Laboratory Records, ORNL R C	52	E O Wollan
22	C E Larson	53	A J Miller
23	L B Emlet (K-25)	54	J A Lane
24	J P Murray (Y-12)	55	R B Briggs
25	A M Weinberg	56	L D Roberts
26	E H Taylor	57	R N Lyon
27	E D Shipley	58	W C Koehler
28	A H Snell	59	E P Blizzard
29	F C VonderLage	60	M E Rose
30	W H Jordan	61	D D Cowen
31	S J Cromer	62	W M Breazeale (consultant)
32	G E Boyd	63	M J Skinner
33	R A Charpie	64	J E Sherwood
34	J A Swartout	65	Dixon Callihan
35	S C Lind	66	A P Fraas
36	F L Culler	67	T A Welton
37	A Hollaender	68	D K Holmes
38	J H Frye, Jr	69	R R Coveyou
39	W M Good	70	E S Bettis
40	M T Kelley	71	C B Mills
41	G H Clewett	72	R M Spencer
42	R S Livingston	73	Dunlap Scott
43	K Z Morgan	74	D V P Williams
44	T A Lincoln	75	E L Zimmerman
45	A S Householder	76-77	ORNL Document Reference Library, Y-12 Plant

EXTERNAL DISTRIBUTION

78 AF Plant Representative, Burbank
79 AF Plant Representative, Seattle
80 AF Plant Representative, Wood-Ridge
81 American Machine and Foundry Company
82 ANP Project Office, Fort Worth
83-93 Argonne National Laboratory
94 Armed Forces Special Weapons Project (Sandia)
95 Armed Forces Special Weapons Project, Washington
96-100 Atomic Energy Commission, Washington
101 Babcock and Wilcox Company
102 Battelle Memorial Institute
103 Bendix Aviation Corporation
104-106 Brookhaven National Laboratory
107 Bureau of Ships

- 108 Chicago Patent Group
- 109 Chief of Naval Research
- 110 Commonwealth Edison Company
- 111 Department of the Navy - Op-362
- 112 Detroit Edison Company
- 113-117 duPont Company, Augusta
- 118 duPont Company, Wilmington
- 119 Duquesne Light Company
- 120 Foster Wheeler Corporation
- 121-123 General Electric Company (ANPD)
- 124 General Electric Company (APS)
- 125-132 General Electric Company, Richland
- 133 Hanford Operations Office
- 134 Iowa State College
- 135-138 Knolls Atomic Power Laboratory
- 139-140 Los Alamos Scientific Laboratory
- 141 Nuclear Metals, Inc
- 142 Monsanto Chemical Company
- 143 Mound Laboratory
- 144 National Advisory Committee for Aeronautics, Cleveland
- 145 National Advisory Committee for Aeronautics, Washington
- 146-147 Naval Research Laboratory
- 148 Newport News Shipbuilding and Dry Dock Company
- 149 New York Operations Office
- 150-151 North American Aviation, Inc
- 152 Nuclear Development Associates, Inc
- 153 Patent Branch, Washington
- 154-160 Phillips Petroleum Company (NRTS)
- 161 Powerplant Laboratory (WADC)
- 162 Pratt & Whitney Aircraft Division (Fox Project)
- 163 Rand Corporation
- 164 San Francisco Field Office
- 165 Sylvania Electric Products, Inc
- 166 Tennessee Valley Authority (Dean)
- 167 USAF Headquarters
- 168 U S Naval Radiological Defense Laboratory
- 169-170 University of California Radiation Laboratory, Berkeley
- 171-172 University of California Radiation Laboratory, Livermore
- 173 Walter Kidde Nuclear Laboratories, Inc
- 174-179 Westinghouse Electric Corporation
- 180-194 Technical Information Service, Oak Ridge
- 195 Division of Research and Medicine, AEC, ORO
- 196 Pacific Northwest Power Group
- 197 Materials Laboratory (WADC)

1 1

1 1

ABSTRACT

Five preliminary critical assemblies, planned in conjunction with a full scale aircraft type circulating fuel reactor, were constructed at the Oak Ridge Critical Experiment Facility. The first assembly was constructed with a beryllium island and reflector, and had enriched uranium disks placed between sodium filled stainless steel cans arranged in a fuel annulus. The assembly was critical with 15.1 kg of U-235. The second assembly was also constructed with a beryllium island and reflector, however, a powdered mixture of sodium, zirconium and uranium fluorides packed in aluminum tubes was used as a fuel, and fuel end ducts were provided. The assembly was critical with 7.7 kg of U-235. The addition of structural poisons (fifth assembly) to this assembly increased the critical mass to 18.2 kg of U-235. In the third assembly the beryllium island and reflector were replaced by graphite. With 17.3 kg of U-235 in the fuel region, this assembly was not critical. In order to make the assembly critical approximately 80% of the graphite in the island and inner six inches of the reflector were replaced by beryllium. The fourth assembly was constructed as a two region assembly with a 1 to 1 volume ratio of graphite and powdered fuel in the core and a beryllium reflector. This assembly was critical with 15.2 kg of U-235.

Neutron flux distributions were determined in these assemblies using indium foil activation. Power distributions were determined using aluminum catcher foils in contact with uranium fuel disks.

Measurements were made on the effect on reactivity of placing various materials in the fuel and reflector regions, and an estimate of the neutron leakage was obtained for two of the assemblies.

TABLE OF CONTENTS

	Page
ABSTRACT	v
LIST OF FIGURES	vii
LIST OF TABLES . . .	ix
I INTRODUCTION	1
II DESCRIPTION OF ASSEMBLY AND MATERIALS	2
III CA-10	4
A Assembly Loading	4
B Control Rod Calibrations	4
C Temperature Effects	11
D Neutron Flux and Power Distribution	11
E Danger Coefficient Measurements	26
IV CA-11	29
A Assembly Loading	29
B Evaluation of Control Rod D	30
C Neutron Flux Distribution	30
D Power Distributions	38
E Neutron Leakage Measurements	44
F Evaluation of Boral Around Fuel End Ducts	45
G Stainless Steel and Boron Poison Rods	45
H Cadmium Importance Function	45
I Danger Coefficients	48
J Effect of Stainless Steel Around Fuel Annulus	48
V CA-12	51
VI CA-13	56
A Assembly Loading	56
B Neutron Flux Distribution	56
C Power Distributions	59
VII CA-14	63
A Critical Loadings	63
B Importance Function of Three Stainless Steel Rods	66
C Thermal Neutron Leakage	68
D Power Distribution	68
VIII APPENDICES	72
A Summary of Materials in Reactor Assemblies	72
B Analyses of Reactor Materials	79

LIST OF FIGURES

	Page
II-1 Photograph of Two Halves of Aluminum Matrix	3
III-1 Assembly Loading at Mid-plane	5
III-2 Axial Loading of Assembly in Vertical Plane Containing Reactor Axis	6
III-3 Photograph of Typical Fuel Shish	7
III-4 Calibration Curve for Control Rod D	9
III-5 Average Sensitivities of Control Rod D	10
III-6 Change in Reactivity vs Temperature	12
III-7 Bare and Cadmium Covered Indium Traverses Through Fuel Core	13
III-8 Bare and Cadmium Covered Indium Traverses Parallel to Axis Through Cell O-12	14
III-9 Bare and Cadmium Covered Indium Traverses Parallel to Axis Through Beryllium Island and Fuel	15
III-10 Indium Traverse Radially in Mid-plane of Reactor, Cell O-12 to X-12	18
III-11 Bare and Cadmium Covered Indium Traverses Across Fuel Annulus	19
III-12 Power Distribution in Cell Q-13	21
III-13 Power Distribution Across Fuel Annulus	23
III-14 Power Distribution Through 20 Mil Uranium Disk	24
III-15 Effect of Stainless Steel on Power Distribution	27
III-16 Loss in Reactivity Due to Addition of Stainless Steel Core Shells	28
IV-1 Assembly Loading at Mid-plane	31
IV-2 Axial Loading of Assembly in Vertical Plane Containing Reactor Axis	32
IV-3 Fuel Tube Arrangement	33

	Page
IV-4 Calibration Curve for Control Rod D	35
IV-5 Radial Flux Distribution at the Mid-plane .	36
IV-6 Radial Flux Distribution 6-1/4" From Mid-plane .	37
IV-7 Cadmium Fractions in CA-10 and CA-11	39
IV-8 Position of Boral Inserted Around End Ducts	40
IV-9 Axial Power Distributions in Call N-14	41
IV-10 Power Distribution Across Fuel in Mid-plane	43
IV-11 Reactivity Loss due to Poison Rods Inserted in O-12	46
IV-12 Cadmium Importance Function	47
V-1 Assembly Loading at Mid-plane	52
V-2 Assembly Loading at Mid-plane	53
V-3 Neutron Flux Distribution in Mid-plane .	54
VI-1 Assembly Loading at Mid-plane	57
VI-2 Radial Neutron Flux Distribution in Mid-plane	58
VI-3 Radial Power Distribution in Mid-plane .	60
VI-4 Axial Power Distribution Through M-12	61
VI-5 Radial Fuel Cadmium Fractions	62
VII-1 Assembly Loading at Mid-plane	64
VII-2 Axial Assembly Loading in Vertical Plane Containing Reactor Axis ()	65
VII-3 Position of Nickel Sheets	67
VII-4 Thermal Flux Leakage vs. Boral Thickness .	69
VII-5 Power Distribution Across Fuel Annulus at Mid-plane	70

LIST OF TABLES

	Page
III-1. Summary of Calibration Data for Rod D .	8
III-2 Summary of Calibration Data for Rods B and C	8
III-3 Neutron Flux Traverses in Cell Q-13	16
III-4 Neutron Flux Traverses Through Cells O-12 and P-12	16
III-5 Radial Flux Traverse in Mid-plane	. 17
III-6 Neutron Flux Distribution Across Fuel Annulus	20
III-7 Power Distribution in Cell Q-13	20
III-8 Power Distribution Across Fuel Annulus	22
III-9 Power Distribution Through 0.02" Fuel Disk	25
III-10 Fuel Cadmium Fractions for Cell Q-13	25
III-11 Effect of Stainless Steel on Power Distribution	26
IV-1 Rod D Calibration . .	. 34
IV-2 Radial Flux Distribution in Mid-plane	34
IV-3. Radial Flux Distribution 6-1/4" from Mid-plane	38
IV-4 Axial Power Distributions in N-14	42
IV-5 Power Distribution Across Fuel in Mid-plane	42
IV-6. Summary of Neutron Leakage Measurements	44
IV-7 Reactivity Loss Due to Poison Rods Inserted in O-12	45
IV-8 Cadmium Importance Function	. 48
IV-9 Danger Coefficient Measurements	. 49
V-1 Radial Neutron Flux Traverse in Mid-plane	55
VI-1. Radial Flux Distribution in Mid-plane	56
VI-2 Radial Power Distribution in Mid-plane	59
VI-3. Axial Power Distribution Through M-12	59
VI-4. Fuel Cadmium Fractions in the Mid-plane	. 63

	Page
VII-1 Importance Function of Three Stainless Steel Rods	68
VII-2 Thermal Neutron Leakage	71
VII-3 Power Distribution Across Fuel Annulus at Mid-plane	71

I INTRODUCTION

The Reflector Moderated Reactor (RMR) as presently conceived is a high power, high temperature, circulating fuel reactor, which is characterized by a central beryllium island surrounded by a uranium bearing fluoride fuel annulus and a beryllium reflector¹. Five critical assemblies have been constructed in which the essential features of the RMR were mocked-up. The series of experiments, which were carried out at room temperature and essentially zero power, provide experimental data on the critical mass and neutron flux and power distributions that can be compared to those predicted by multigroup calculation for the assembly in question. In addition, danger coefficients were obtained for a large number of materials placed at various points in the reactors.

The first assembly (CA-10) consisted essentially of a central 12" cube of beryllium partially surrounded by a 3" fuel annulus and a 12" thick beryllium reflector backed by graphite. The fuel annulus contained sodium filled stainless steel cans between which were placed 0.01" thick uranium disks. The majority of the measurements were taken with 15.1 kg of U-235 in the reactor, which provided an excess reactivity of 1.9% in k_{eff} .

The second assembly (CA-11) differed from the first in that, 1) the fuel region contained an homogeneous mixture of ZrO_2 , NaF, C, and UF_4 packed in aluminum tubes, 2) the thickness of the fuel annulus was increased to 4-1/2", and end fuel ducts were provided, 3) the central island region was arranged essentially as a 9" cube, and 4) the regions were assembled to approximate concentric spheres somewhat more closely. This assembly was critical with 7.7 kg of U-235.

The third assembly (CA-12) was originally designed to evaluate the characteristics of a graphite moderated and reflected assembly. The fuel region was built up as a cylindrical shell 21" OD, 3" thick and 36" long. The fuel used was similar to that used in CA-11 with the U-235 concentration approximately doubled. This array was not critical. Approximately 80% of the graphite in the island and the inner 6" of the reflector was then replaced by beryllium in order to make the reactor critical. The fuel region contained 17.3 kg of U-235. In the second modification of this reactor, the 17.3 kg of fuel were rearranged as an ellipsoid with the beryllium and graphite surrounding the central fuel region. This two region reactor was not critical.

1 Fraas, A. P. and Mills, C. B., "The Fireball, A Reflector Moderated Circulating - Fuel Reactor" Y-F10-104, June 20, 1952

The fourth assembly (CA-13) was composed of a central ellipsoid containing a 1 to 1 volume ratio of graphite and the fuel used in CA-12. This core was surrounded by a beryllium reflector 12" thick. The reactor was critical with 15.2 kg of U-235.

The last assembly (CA-14) was similar to CA-11 except that the fuel with the higher uranium concentration was used and an effort was made to simulate the poisons (core shells, coolants, coolant tubes, etc.) that will be present in a full scale reactor. It was critical with 18.2 kg of U-235.

II DESCRIPTION OF ASSEMBLY AND MATERIALS

The critical experiment assembly has been described in other reports, and only a brief description of the components that are necessary for an understanding of the physical make up of the reactors will be given¹.

The assembly apparatus consists basically of a matrix of square 2S aluminum tubes, which form a 6' cube and into which may be placed the reactor materials. The 6' cube is divided into two identical halves, one of which is stationary and the other movable by remote control. Each half consists of 576 tubes, stacked in a 24 x 24 cell array. These tubes are 36" in length with a 3" x 3" outside cross-section and have 0.047" thick walls. Part of the reactor materials are placed in each half and the assembly made critical by control rod adjustment after the two halves have been brought together. A reference system is used to designate each cell. A letter designation is given each column of cells and a number for each row. This system is evident from any of the loading diagrams. The assembly, with the two halves separated, can be seen in Fig. II-1. (The materials visible in the upper portion of the movable half have no relation to the subject experiments.)

The basic materials present in the reactors beside the fuel and aluminum matrix were beryllium and graphite. These materials were in the form of square blocks, either 2-7/8" x 2-7/8" or 1-7/16" x 1-7/16" and of various thicknesses. Each block had a 0.196" hole drilled through its center, normal to the square cross-section. When required, a skewer rod was inserted through these holes to form a "shish-kabob". The skewer rods had a 3/16" diameter and were composed of aluminum except for those "shishes" used as safety or control rods in which case a steel skewer was used. All safety and control rods were normal reflector or island shishes.

1 Bly, F. T. et al., NEPA Critical Experiment Facility, NEPA-1769, April 15, 1951

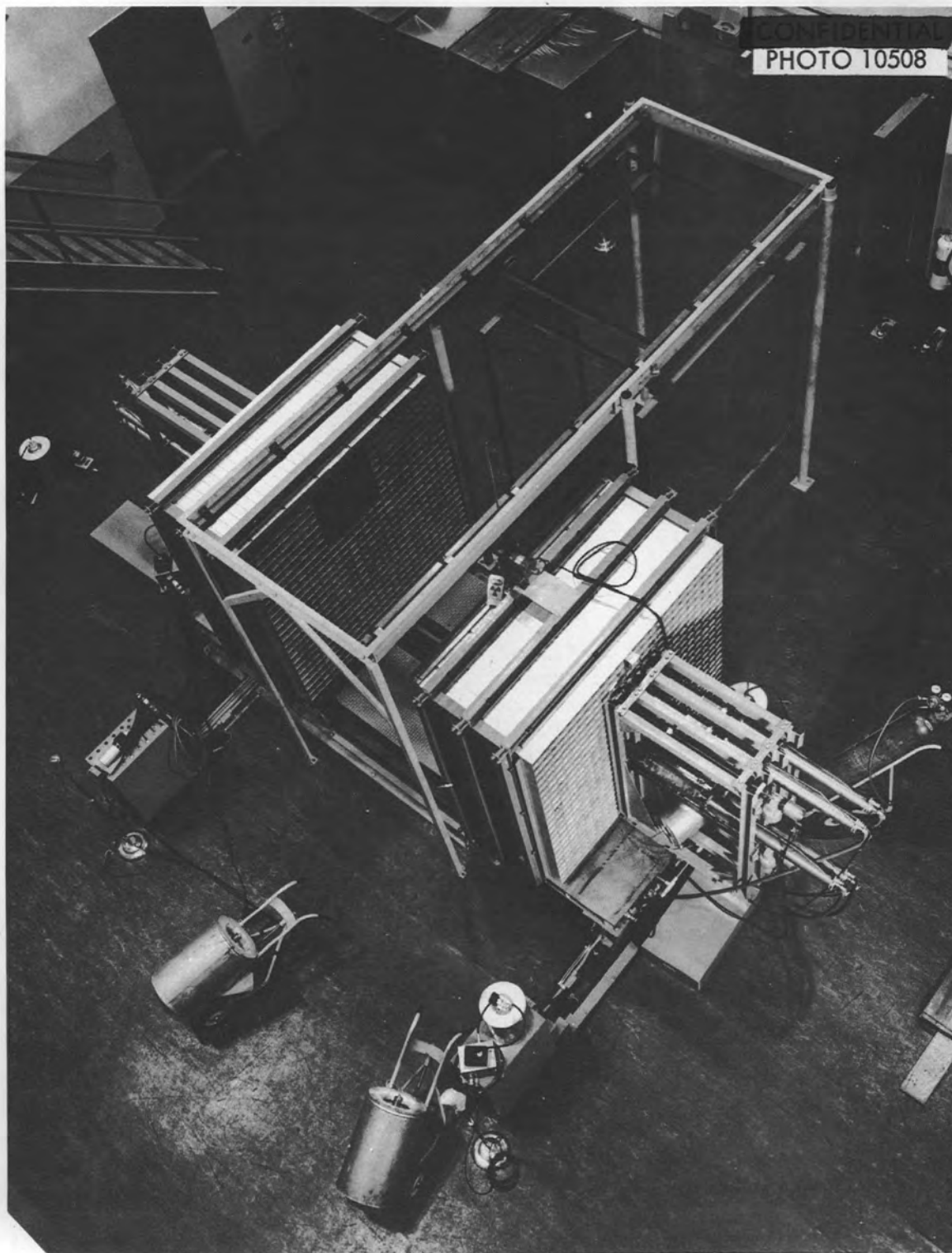


Fig. II-1 Table Assembly.

The enriched (93.3% U-235) uranium metal disks used were approximately 0.01" thick with diameters of 2.860" and 1.430" and weighed 18.0 ± 0.1 and 4.5 ± 0.1 grams respectively. The weight tolerance was obtained by punching small holes in some of the disks. Each disk had a 0.196" hole drilled through the center. The powdered fuel mixtures are described under the appropriate reactor designation.

The appendix contains quantitative information on the materials located in each region of all the assemblies, and also spectrographic analyses of some of the materials used.

III CA-10

A Assembly Loading

The initial loading for CA-10 is shown in Figs III-1 and III-2, which are cross-sections of the assembly at the mid-plane of the reactor and the vertical plane containing the central axis of the reactor, respectively. It is seen that the assembly consists of a 12" central cube of beryllium, partially surrounded by a 3" fuel annulus composed of sodium filled stainless steel cans ($2\frac{7}{8}" \times 2\frac{7}{8}" \times 1"$) between which were placed the large sized 0.01" thick uranium disks. The components and arrangement of a typical fuel shish are shown in Fig III-3. As can be noted from Fig III-2, a section 6" square at both ends of the fuel annulus was filled with beryllium rather than the uranium disks and sodium. The fuel region was loaded with two fuel disks between each sodium filled can except for the 3" end fuel regions behind the central beryllium cube, which had only one disk between each can. The fuel annulus was surrounded by a 12" thick beryllium reflector backed by 6" of graphite on the sides and 8" on the ends of the reactor.

With the loading described above the reactor contained 15.0 kg of U-235 which at a room temperature of 74°F provided an excess reactivity of 1.9% in k_{eff} . The reactor was made critical by removing the reflector from cells J-13 and 14 and I-13 (1.6%) and by adjustment of the control rods. Measurements that required more reactivity than was available on the control rods were accomplished by inserting one or more reflector shishes in the above cells. All foil and danger coefficient measurements were taken on the opposite side of the reactor where the effect of the voids on the measurements was negligible.

B Control Rod Calibrations

The change in reactivity introduced by the linear displacement of each of three control rods was determined. Rod D was cali-

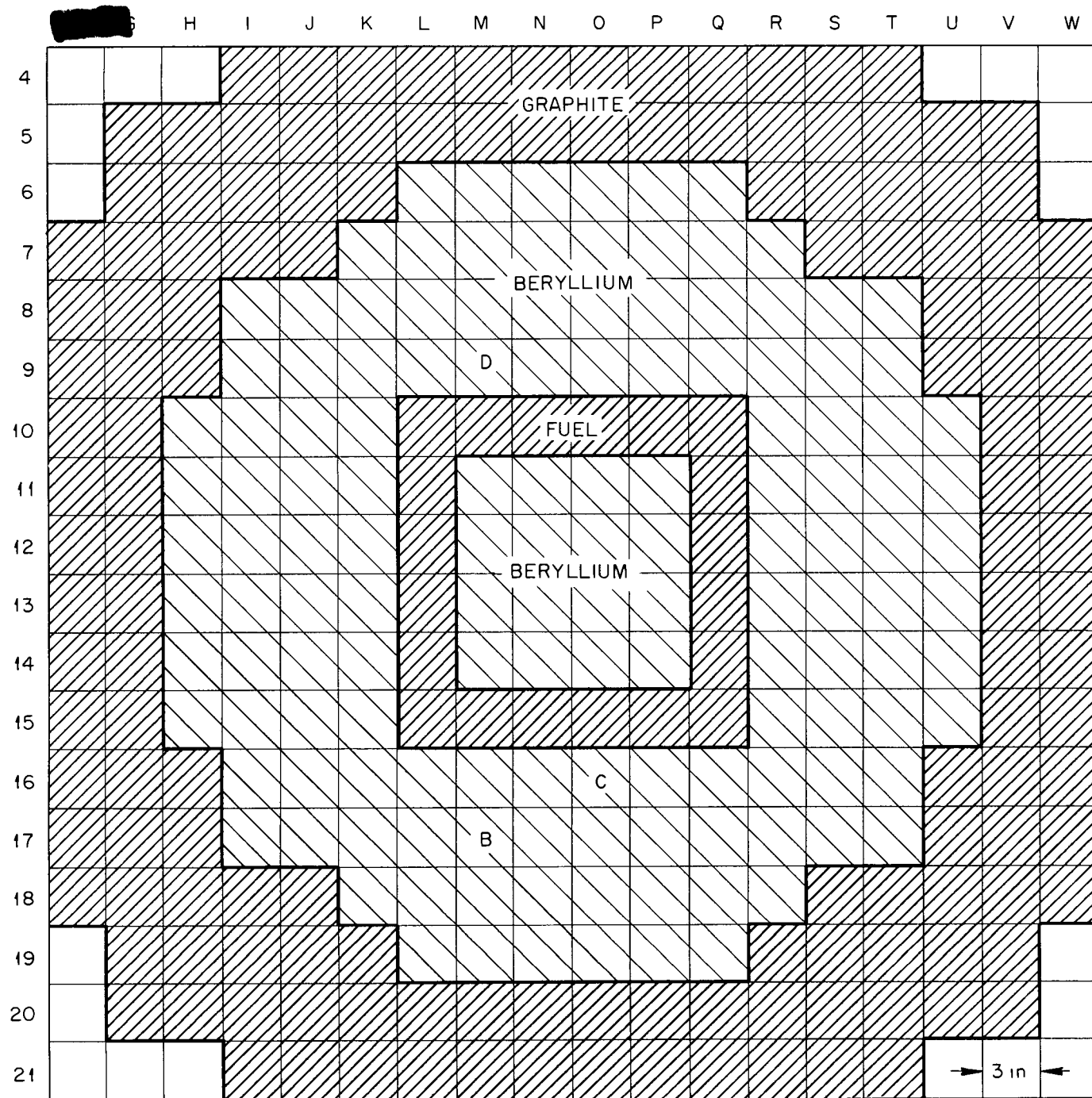


Fig III-1 Assembly Loading at Mid-Plane

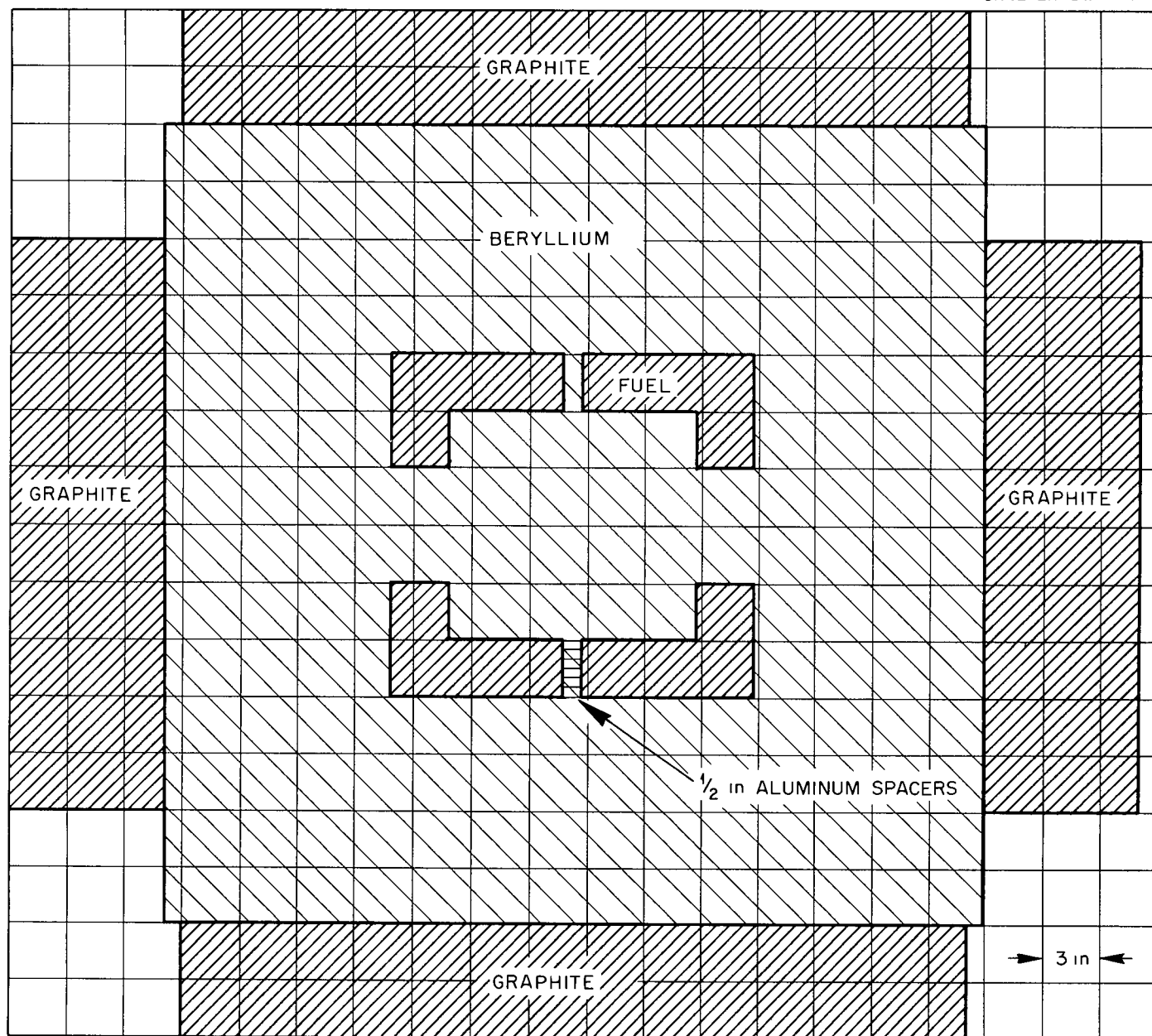
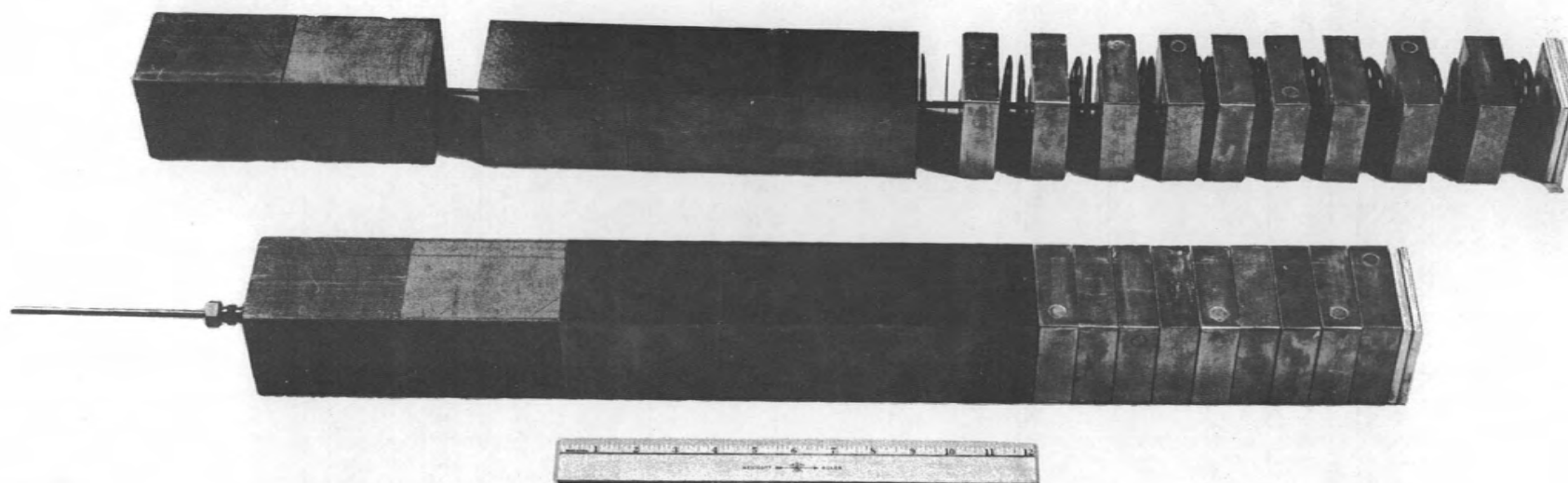


Fig III-2 Axial Loading of Assembly in Vertical Plane Containing Reactor Axis

CONFIDENTIAL
PHOTO 12013



-7-

Fig. III-3. Typical Fuel Shish.

brated by the integrated period method after which rods B and C were evaluated by direct comparison with Rod D². Detailed data for Rod D are given in Table III-1. A graph of reactivity of this rod in cents, versus its linear displacement is shown in Fig. III-4. The average change in reactivity per unit displacement for each increment of displacement is plotted for the same rod in Fig. III-5. Similar data for rods B and C are shown in Table III-2. The delayed neutron fraction has been taken as 0.0073.

TABLE III - 1

SUMMARY OF CALIBRATION DATA FOR ROD D

Position of Rod From Mid-Plane in Inches	Total Change in Reactivity Value in Cents	Average Incremental Sensitivity in Cents per Inch
0 0	0.0	-
2.555	2 01	0 79
7.844	8.98	1 32
10.245	14.62	2.35
11 987	19 80	2.97
13 560	24 74	3 14
14 921	28 98	3 12
16 290	32 50	2.57
17 623	35.02	1.89
19 194	37 79	1 76
25 697	42 69	0 75

TABLE III-2

SUMMARY CALIBRATION DATA FOR RODS B AND C

Distance of Rod From the Mid-plane in Inches	Reactivity in Cents		Average Sensitivity in Cents per Inch	
	Rod B	Rod C	Rod B	Rod C
0 0	0 0	0 0	-	-
5 0	11 3	3 5	2 26	0 70
10 0	20.9	12.2	1 92	1 74
15.0	28 5	28 2	3 20	3.20
20.0	33.0	39 3	2.22	2 27
25 0	35.0	43.2	0 78	0 78

² Callihan, D. "Critical Experiments on Direct Cycle Aircraft Reactor" ORNL-1615, October 22, 1953. p 22.

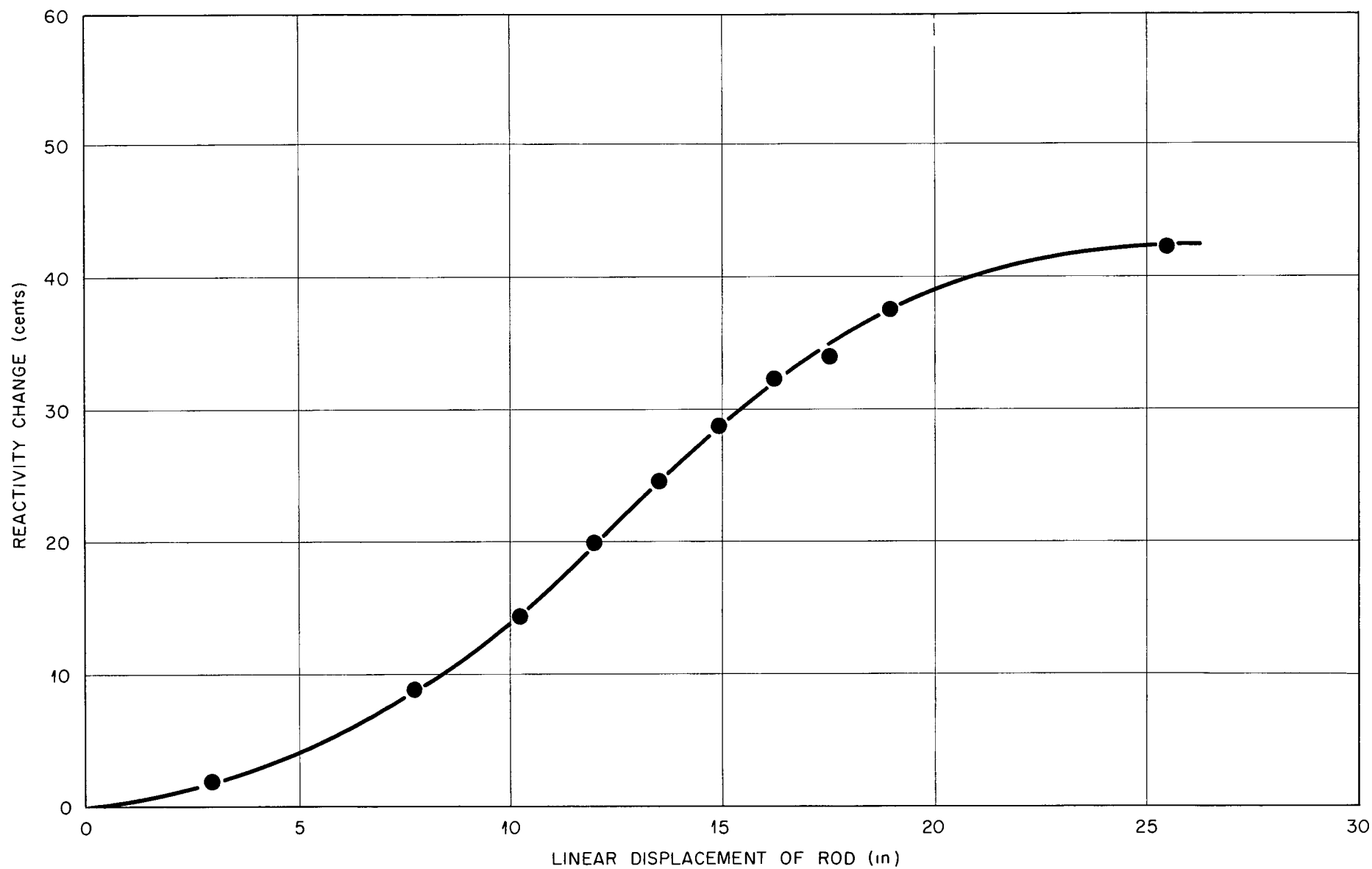


Fig III-4 Calibration Curve For Control Rod D

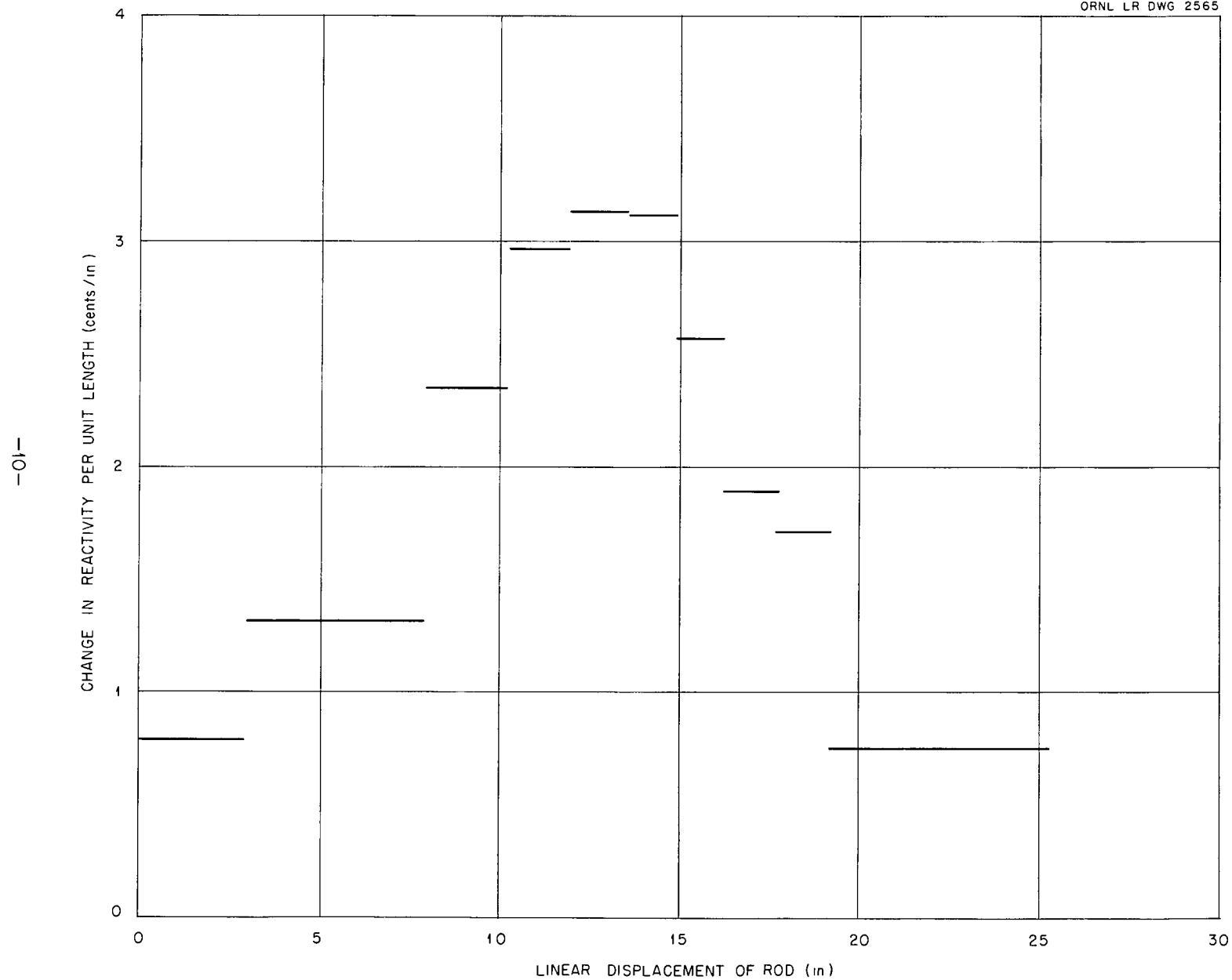


Fig III 5 Average Sensitivities of Control Rod D

C. Temperature Effects

The changes in reactivity produced by changes in temperature over a limited range were determined by changing the demand temperature of the assembly room. Several days were allowed for the reactor temperature to reach equilibrium. The reactor was made critical before and after the temperature changes, and the reactivity differences determined in terms of the calibrated control rod settings. The temperature of the reactor was determined from two iron-constantan thermocouples. Figure III-6 shows the reactivity changes plotted as a function of the assembly temperature. A systematic study was not undertaken to determine the sources of this temperature effect, it was determined primarily to correct all reactivity measurements to a common reactor temperature.

D. Neutron Flux and Power Distribution

Neutron flux distributions were obtained using bare and cadmium covered indium foils. The techniques used for these measurements have been adequately covered in previous reports and will not be repeated here.³ Power distributions were obtained using the aluminum catcher foil technique which is also described in the same reference.

1. Flux Distributions

Bare and cadmium covered indium traverses were made through the fuel core, starting at the mid-plane and extending to the edge of the graphite reflector and parallel to the axis of the reactor through cell Q-13. Table III-3 contains data showing the positions of the bare and cadmium covered foils and their relative activities. Figure III-7 shows the relative activities plotted as a function of the distances of the foils from the mid-plane.

Bare and cadmium covered indium traverses were also made through the beryllium island parallel to the axis of the reactor, starting at the mid-plane and extending to the edge of the graphite reflector, through cell O-12 and P-12. The traverses made through cell P-12 pass through the fuel core while those through O-12 do not. Table III-4 contains data showing the distances of the foils from the mid-plane in the respective cells and also the relative activity obtained for each foil. Figures III-8 and III-9 show the graph of the

³ Ibid, p 36

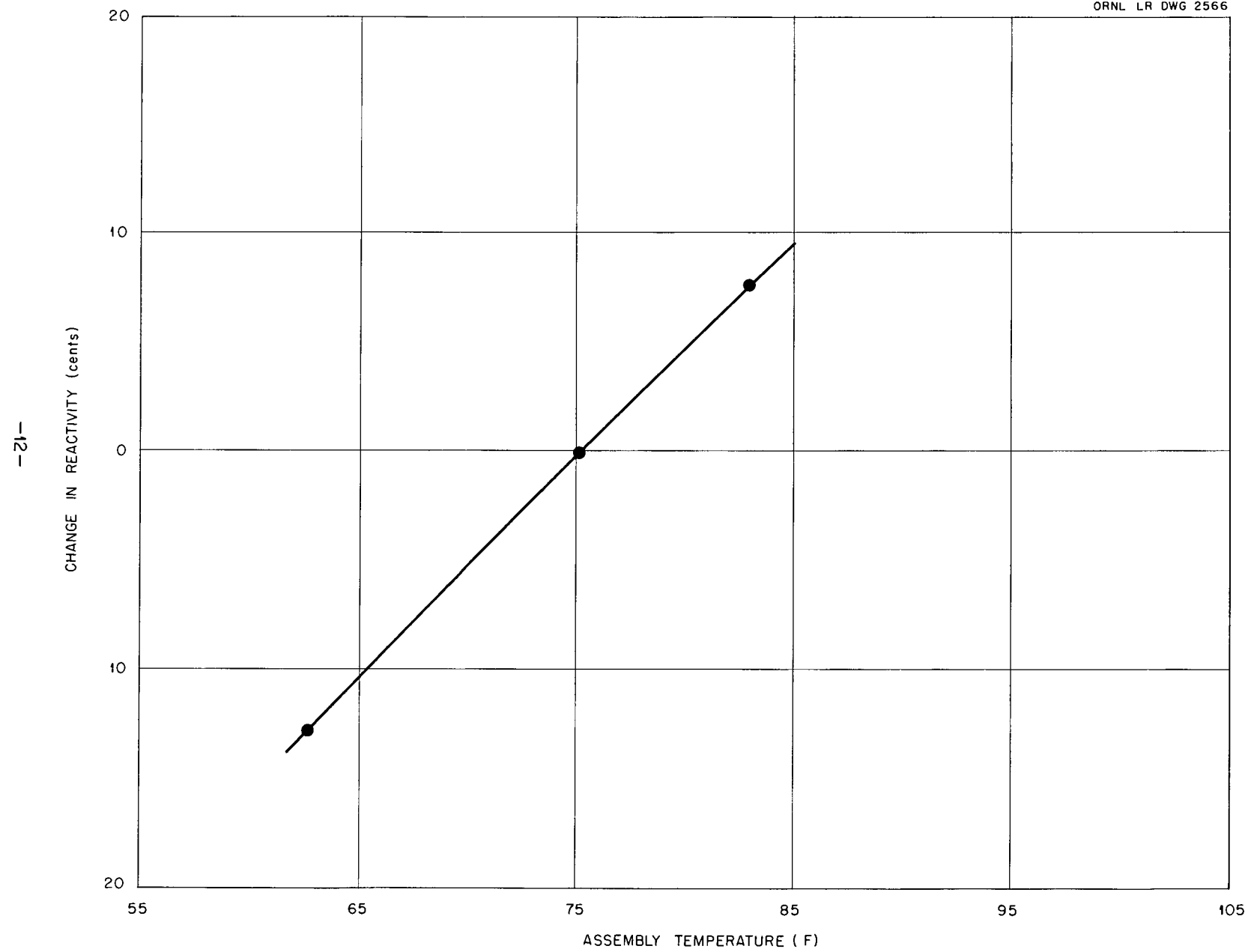


Fig III 6 Change in Reactivity vs Temperature

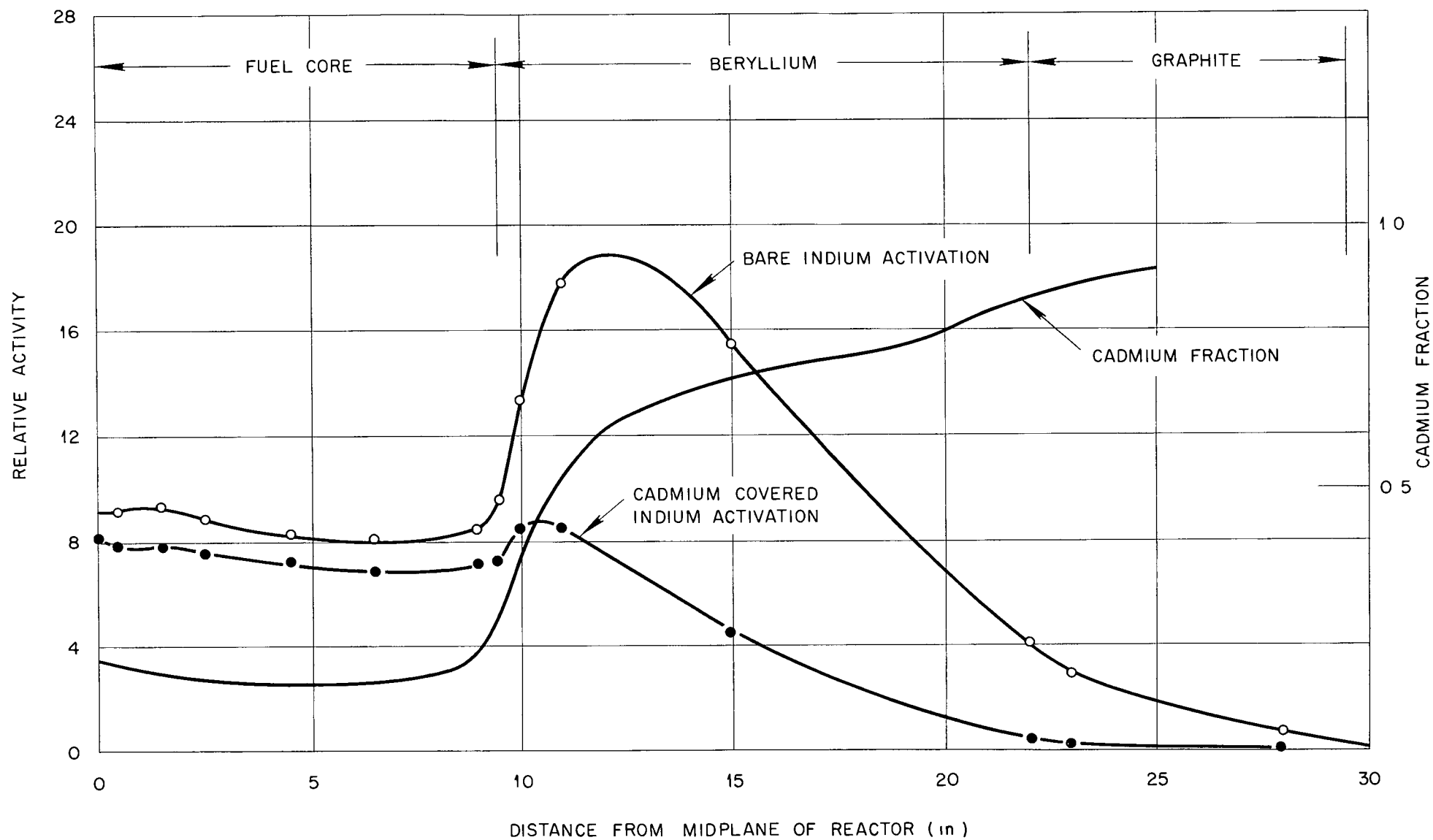


Fig III-7 Bare and Cadmium-Covered Indium Traverses Through Fuel Core

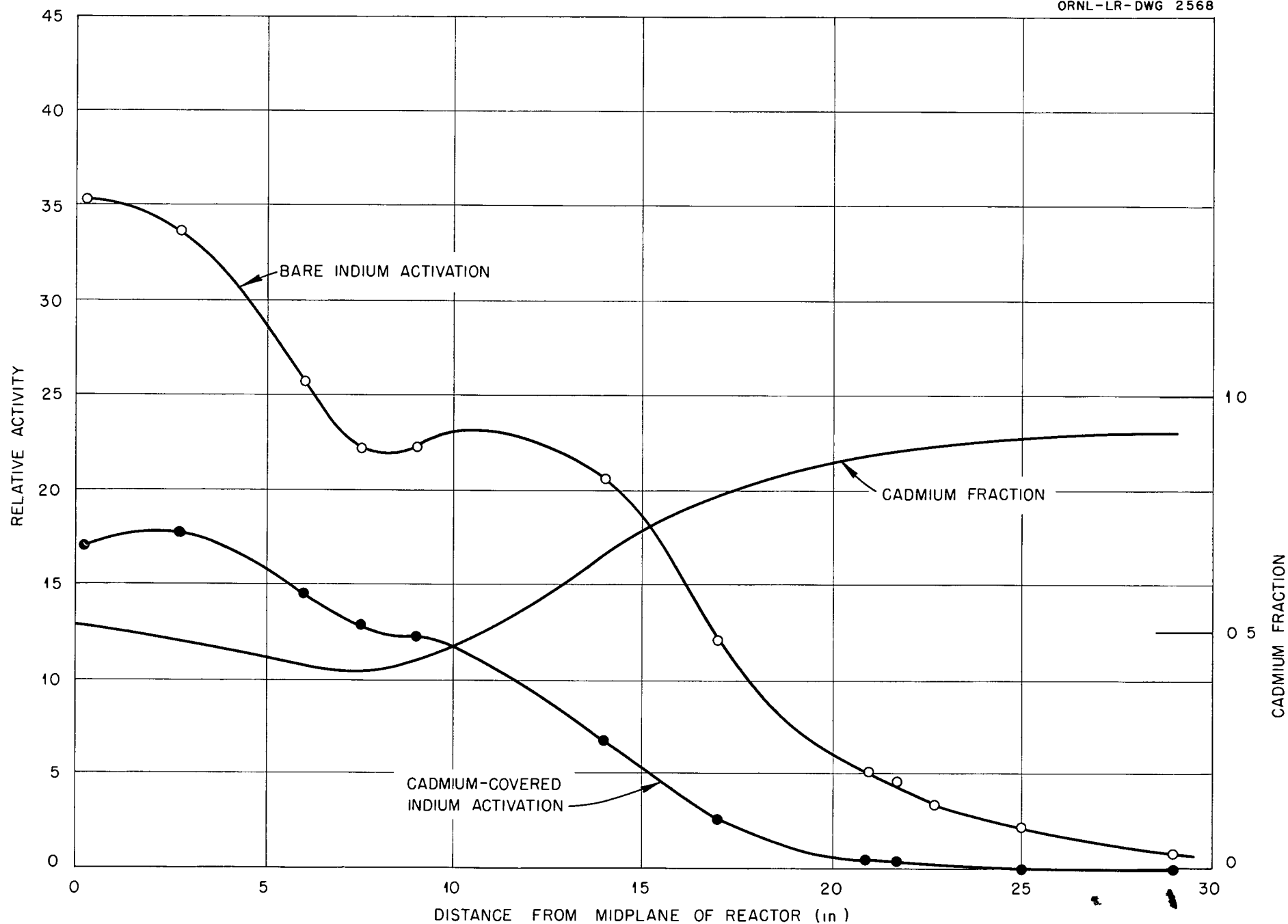


Fig III-8 Bare and Cadmium Covered Indium Traverses Parallel to Axis Through Cell O-12

- 15 -

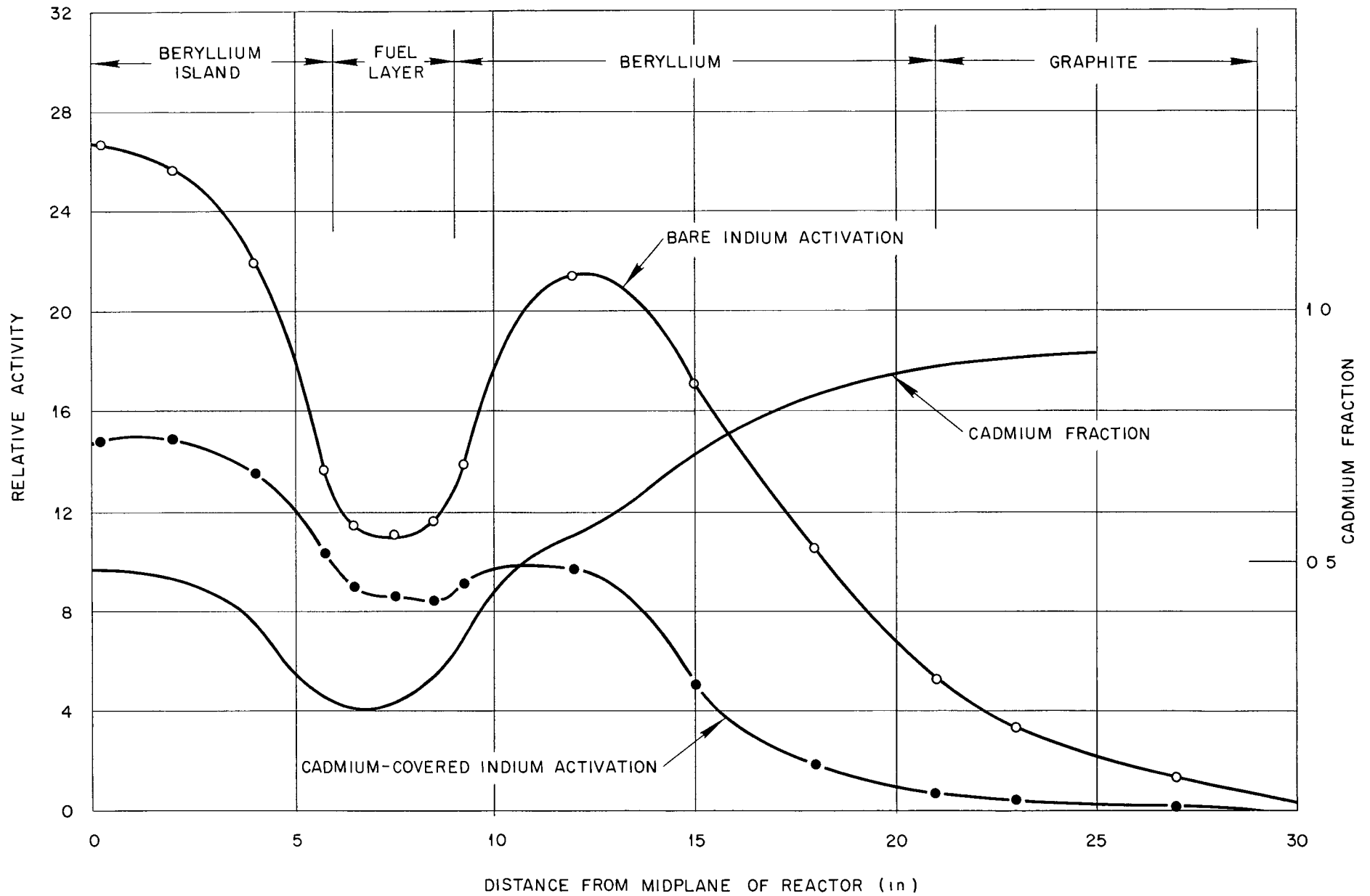


Fig III-9 Bare and Cadmium-Covered Indium Traverses Parallel To Axis Through Beryllium Island and Fuel

relative activity of the various foils and the corresponding Cd fraction* as a function of their distances from the mid-plane of the reactor for the traverses through cells O-12 and P-12 respectively

TABLE III-3

Neutron Flux Traverses in Q-13

Distance of Foil from Mid-plane in Inches	Relative Activity	
	Bare Foils	Cadmium Covered Foils
0 0	10 338	8 084
0 5	9 118	7 889
1 5	9 396	7 959
2 5	8 899	7 663
4 5	8 302	7 393
6 5	8 068	6 910
8 5	8 532	7 160
9 5	9 533	7 370
10 0	13 370	8 569
11 0	17 815	8 580
15 0	15 502	4 578
21 5	4 182	0 464
23 0	2 974	0 341
28 0	0 767	0 078

TABLE III-4

Neutron Flux Traverses Through Cells O-12 and P-12

Cell O-12			Cell P-12		
Distances From Mid-plane in Inches	Relative Activity		Distances From Mid-plane in Inches	Relative Activity	
	Bare	Cd Covered		Bare	Cd Covered
0 3	35 335	17 232	0.3	26 678	14 736
2 7	33 746	17 702	2 0	25 735	14 931
6 0	25 676	14 596	4 0	21 990	13 557
7 5	22 315	13 008	5 7	13 602	10 234
9 0	22.349	12.414	6 5	11.401	8 938
14 0	20 537	6 840	7 5	11.137	8.599
17 0	12 169	2 675	8.5	11 655	8 463
21 0	5 250	0 614	9 2	13.954	9 094
21 7	4.790	0.551	12.0	21.436	9 662
22 7	3 601	0 428	15.0	17 140	5 158
25 0	2.307	0.254	18 0	10 440	1 980
29 0	0 926	0 054	21 0	5 222	0 638
			23 0	3 640	0 406
			27.0	1 388	0 142

*Cd fraction is defined as the fraction of the total activity induced by neutrons with energies less than 0.02" cadmium cut-off

Radial bare and cadmium covered indium traverses were made starting at the axis of the reactor in cell O-12 and extending to cell X-12 Table III-5 contains the data showing the positions and relative activities for both the bare and the cadmium covered foils Figure III-10 is a graph of the relative activities plotted as a function of the distances of the foils from the axis of the reactor

TABLE III-5

Radial Flux Traverse in Mid-plane

Distance of Foil From Axis in Inches	Relative Activity	
	Bare	Cd Covered
0 7	38 543	19 677
2 3	35 595	19 826
4 5	26 173	15 230
6 3	12 137	9 683
7 5	9 889	8 500
8 7	11 861	8 898
10 5	20 692	11 568
13 5	21 483	8 509
16 5	14 764	3 930
19 5	8 310	1 317
22 5	4 125	0 515
25 5	1 675	0 197
27 3	0 542	073

In order to obtain a more detailed pattern of the neutron flux in the fuel region, short radial traverses were made across the fuel in cell N-10 Table III-6 shows the positions of the foils and their relative activities Figure III-11 shows the activities plotted as a function of the distances of the foils from the axis of the reactor

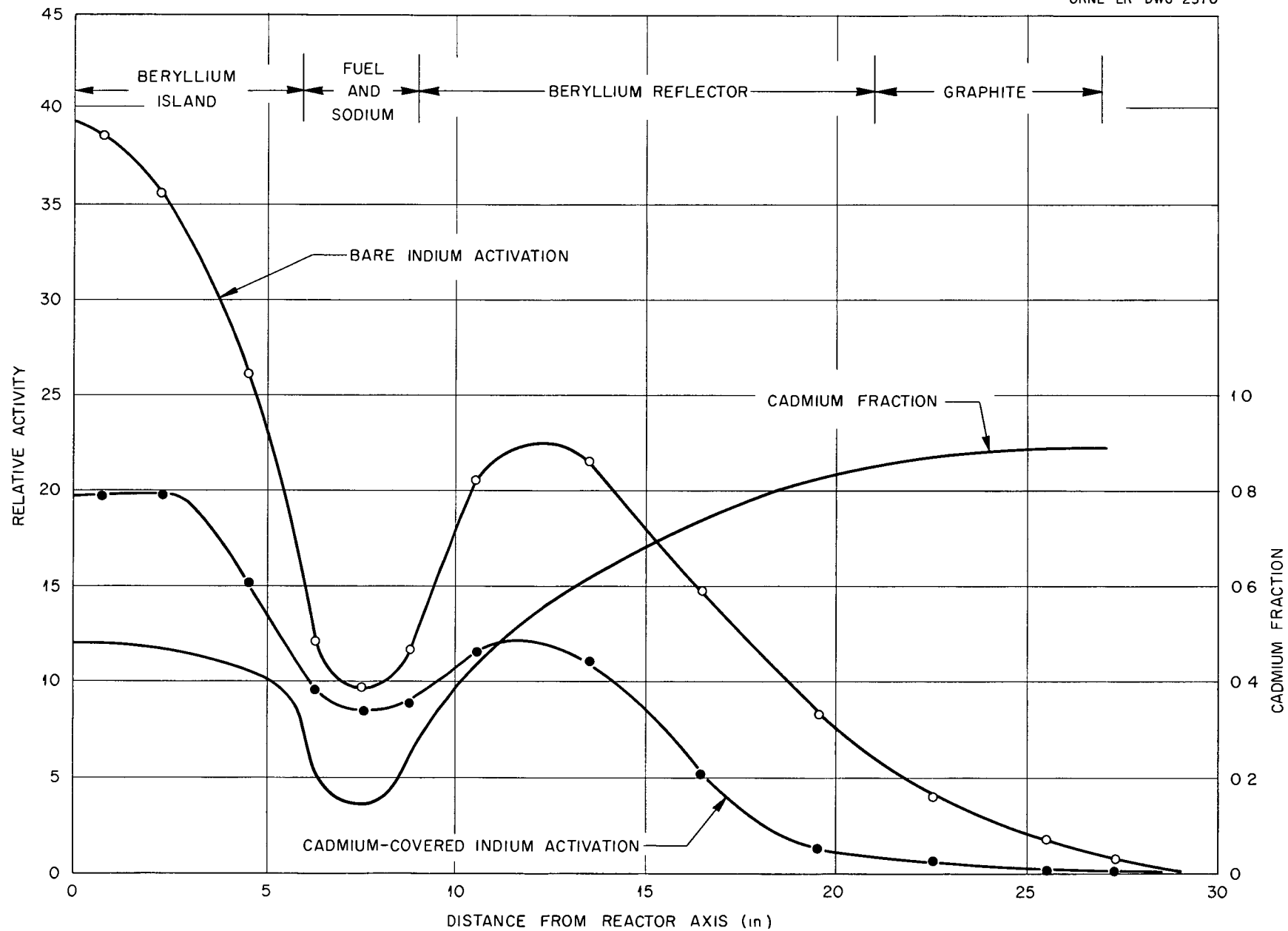


Fig III-10 Indium Traverse Radially in Midplane of Reactor Cell O-12 to X-12

- 19 -

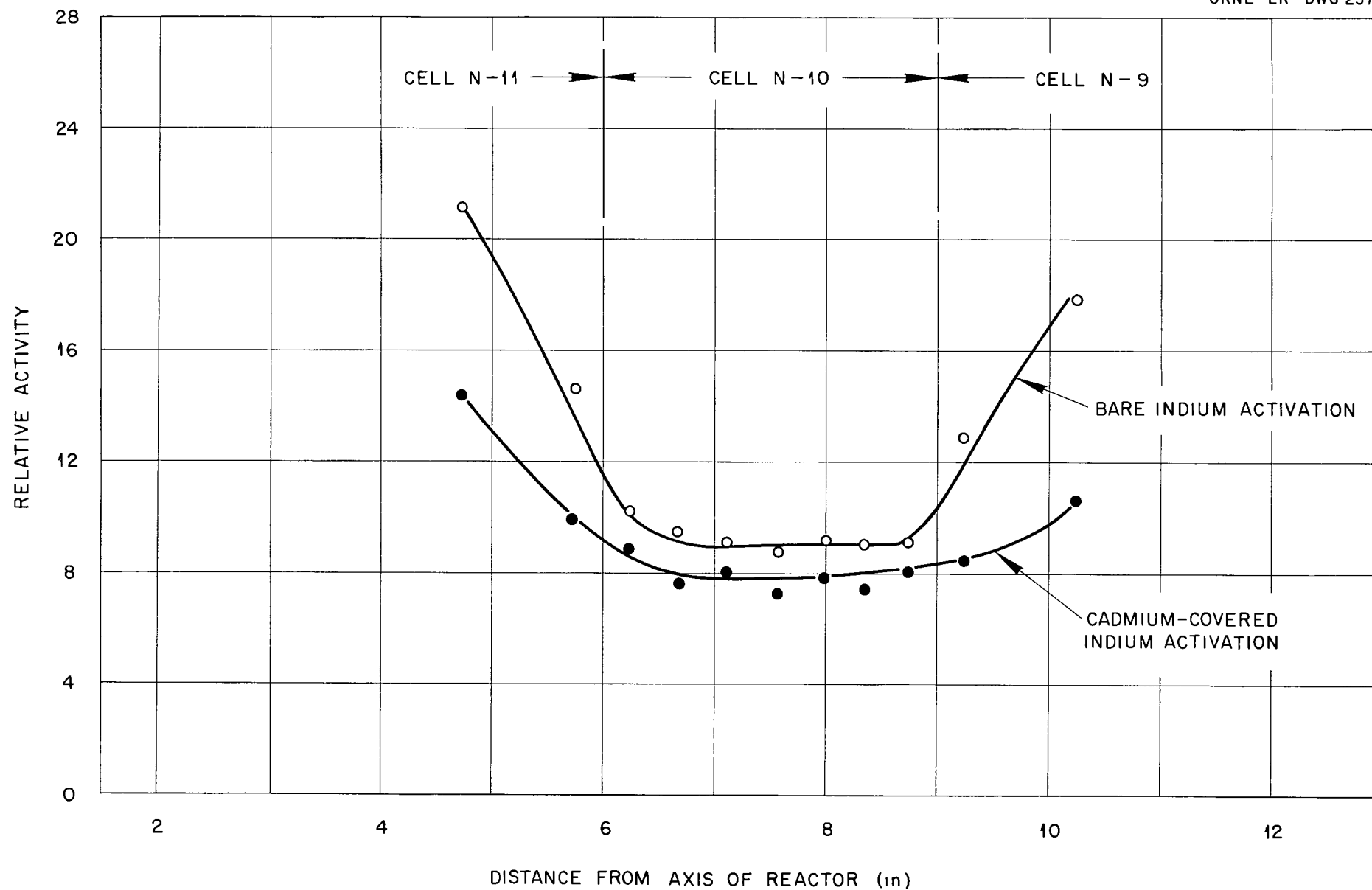


Fig III - 11 Bare and Cadmium-Covered Indium Traverses Across Fuel Annulus

TABLE III-6

Neutron Flux Distribution Across
Fuel Annulus

Distance from Axis of Reactor In Inches	Bare	Cd Covered
4 7	21 172	14 419
5 5	14 603	9 977
6 3	10 242	8 923
6 7	9 554	7 733
7 1	9 038	8 098
7 6	8 799	7 270
8 0	9 200	7 991
8 4	9 060	7 466
8 7	9 104	8 018
9 3	12 837	8 446
10 3	17 857	10 718

2 Power Distributions

The power distribution through the fuel was measured along the axis of cell Q-13. The aluminum catchers were mounted vertically between the uranium fuel disks and the adjacent sodium cans.

Table III-7 contains data showing the distances of the aluminum foils from the mid-plane of the reactor. Figure III-12 is a graph of the relative fission rates plotted as a function of the distance from the mid-plane. The two values shown at 9.5" from the axis indicate different fission rates on the opposite surfaces of the uranium disks which are adjacent to the sodium cans and the beryllium, the higher fission rate occurring on the surface adjacent to the beryllium.

TABLE III-7

Power Distribution in Cell Q-13

Distance from Mid-plane in Inches	Relative Activity
0.5	3182
1.5	3066
3.5	2899
5.5	2563
7.5	2253
9.5	2806
9.5	5318

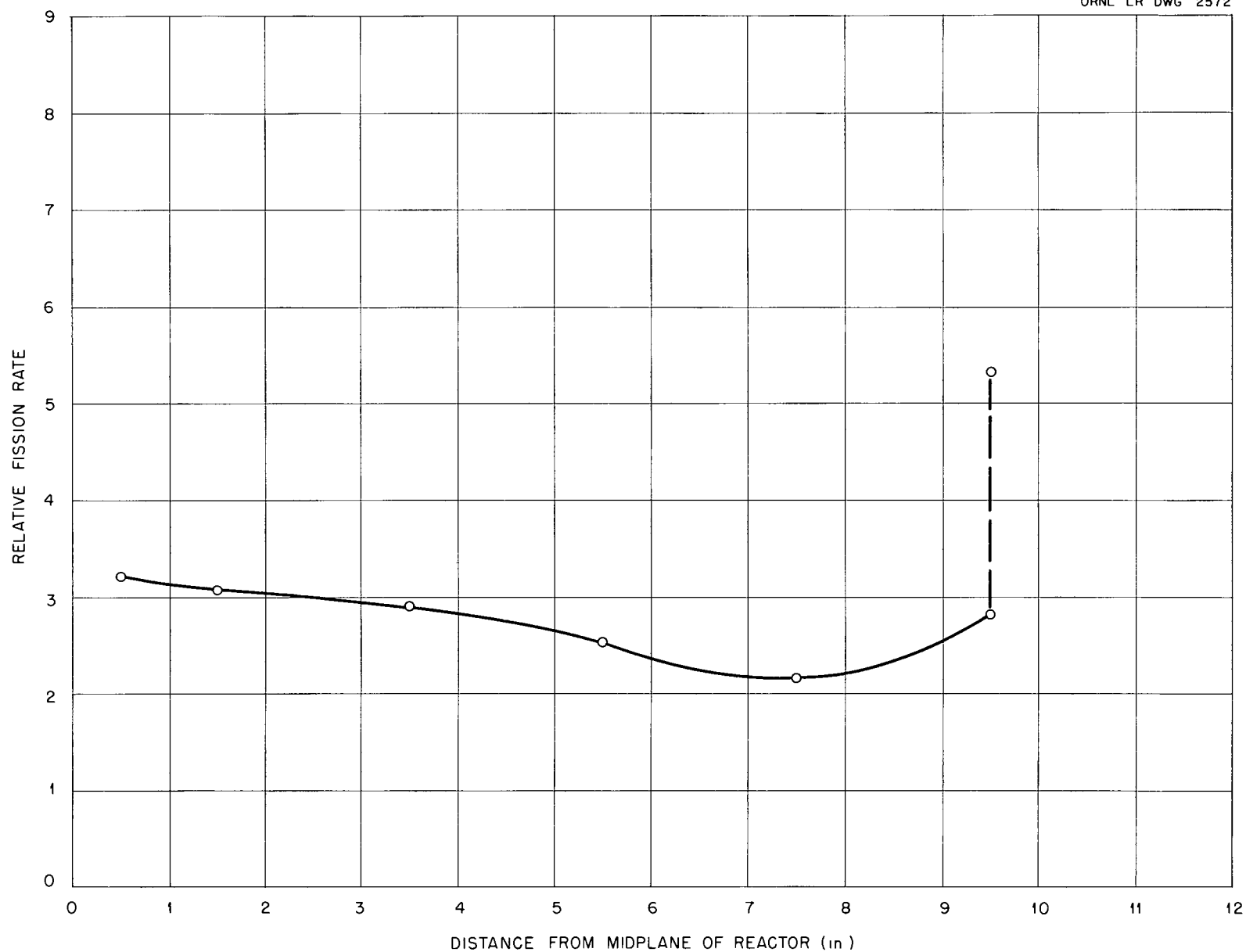


Fig III-12 Power Distribution in Cell Q-13

A power traverse was also made across the fuel annulus using cell Q-13. Two runs were made and the fission fragment counting rates normalized. Table III-8 contains the data showing the distances of the centers of the aluminum catcher foils from the axis of the reactor and the normalized fission fragment activities. Figure III-13 is a graph of the activity plotted as a function of the distances of the centers of the foils from the axis of the reactor. The dotted portions of the curve extrapolate the activities to the edge of the fuel.

TABLE III-8

Power Distribution Across Fuel Annulus

<u>Distance From Axis in Inches</u>	<u>Relative Activity</u>
6 2	661
6 3	596
6 6	588
6 9	508
6 9	511
7 3	485
7 5	469
7 5	475
7 7	482
8 1	501
8 4	562
8 4	570
8 7	629

The depression in the fissioning distribution through two adjacent 0.01" fuel disks was determined by replacing them with ten 2 mil thick fuel disks separated by catcher foils thereby forming a sandwich. This sandwich was inserted in the normal fuel position between two sodium filled cans. The data obtained are shown in Table III-9 and Figure III-14. Two catcher foils were inserted between the internal disks giving the two values reported. To facilitate drawing the curve, symmetry has been assumed and the points reflected.

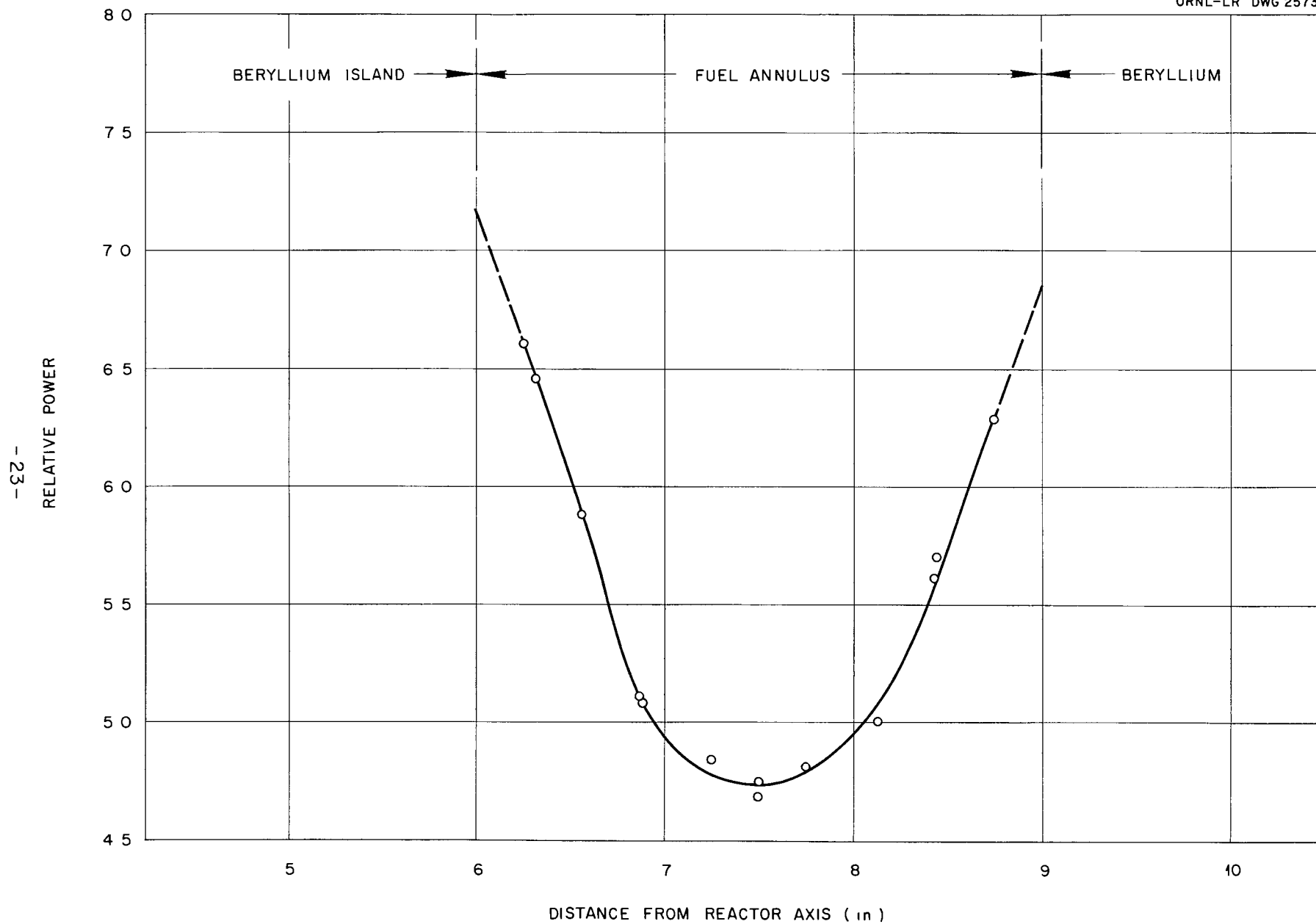


Fig III - 13 Power Distribution Across Fuel Annulus

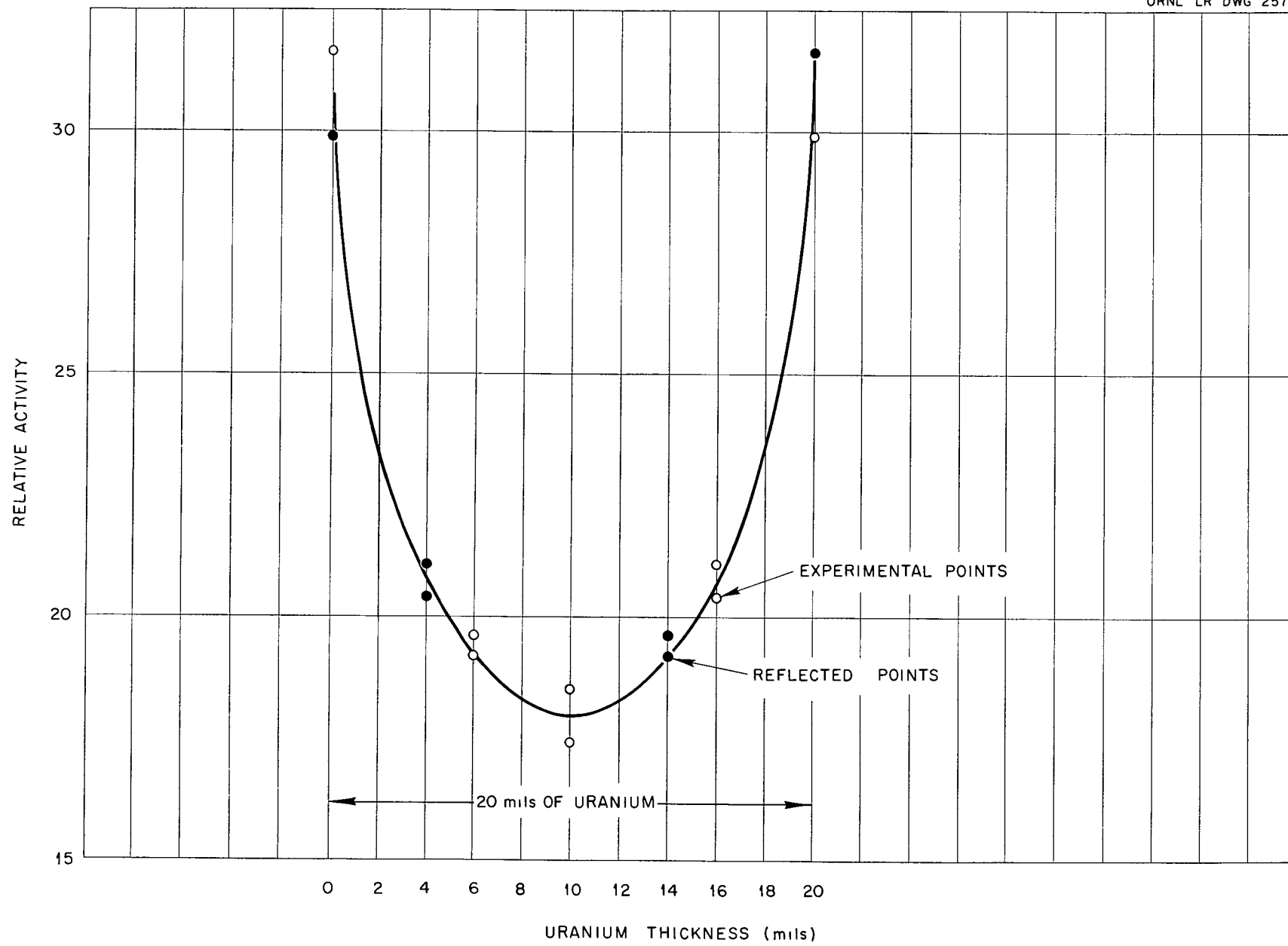


Fig III-14 Power Distribution Through 20 mil Uranium Disk

TABLE III-9

POWER DISTRIBUTION THROUGH 0 02" FUEL DISK

<u>Distance Through Sandwich in Mils*</u>	<u>Relative Activity</u>
0	31 64
6	19 63
6	19 23
10	18 58
10	17 44
16	21 19
16	20 44
20	29 90

*Catcher foil thicknesses have been neglected

3 Fuel Cadmium Fractions

Cadmium fractions for the uranium fuel disks were measured at various positions axially along cell Q-13 Table III-10 contains the values of the cadmium fractions at various distances from the mid-plane The two values listed for the 9 5" position indicate that a measurement was made on both sides of the uranium disk

TABLE III-10

FUEL CADMIUM FRACTIONS FOR CELL Q-13

<u>Distance From Mid-plane in Inches</u>	<u>Fuel Cadmium Fractions</u>
1 5	0 71
5 5	0 68
9 5	0 73
9 5	0 85

4 Effect of Stainless Steel on Power Distribution

In order to determine the effect of a stainless steel core shell on the power distribution across the fuel, the beryllium reflector in cells R-10 through R-15 was rearranged so that a void (5/8" x 2-7/8" x 9") existed adjacent to the fuel annulus extending on one side of the mid-plane only A 3" longitudinal

section in fuel cell Q-13 was rotated 90° about a vertical axis from its normally loaded position. The sodium filled cans were replaced by aluminum spacers and some of the 0.01" fuel disks replaced by 0.002" disks. A radial power distribution was then measured in this 3" section. Stainless steel sheets (9" x 2-7/8" x 0.29") were then inserted in the voids in cells R-10 through R-15, and the power distribution remeasured. The data obtained from both traverses are shown in Table III-11 and Figure III-15.

TABLE III-11

EFFECT OF STAINLESS STEEL ON POWER DISTRIBUTION

Distance of Foil From Reactor Axis In Inches	Relative Activity	
	Without Stainless Steel	With Stainless Steel
6.2	4 885	4 912
6.5 [†]	3 348	3 348
6.91	2.287	2 359
7.2	1 977	1 885
7.5	1 745	1 680
7.5	1 816	1 628
7.7	1 971	1 672
8.3	2 822	2 246
8.5	3 546	2 565
8.7	5 199	3 526

E Danger Coefficient Measurements

1 Stainless Steel

The loss in reactivity due to the presence of stainless steel next to the fuel annulus was determined for three different steel thicknesses inserted* in the void in cells R-10 through R-15 described above. The void itself resulted in a loss in reactivity of 8.7 cents. The loss in reactivity as a function of the stainless steel thickness is plotted in Figure III-16.

2 Bismuth and Lead

A 1-1/8" layer of beryllium adjacent to the fuel surface and extending 8-5/8" on both sides of the mid-plane was removed from cells R-10 through R-15. The introduction of this void

* The fuel region extended slightly beyond the steel inserts so the fuel disks adjacent to the beryllium were not fully shielded.

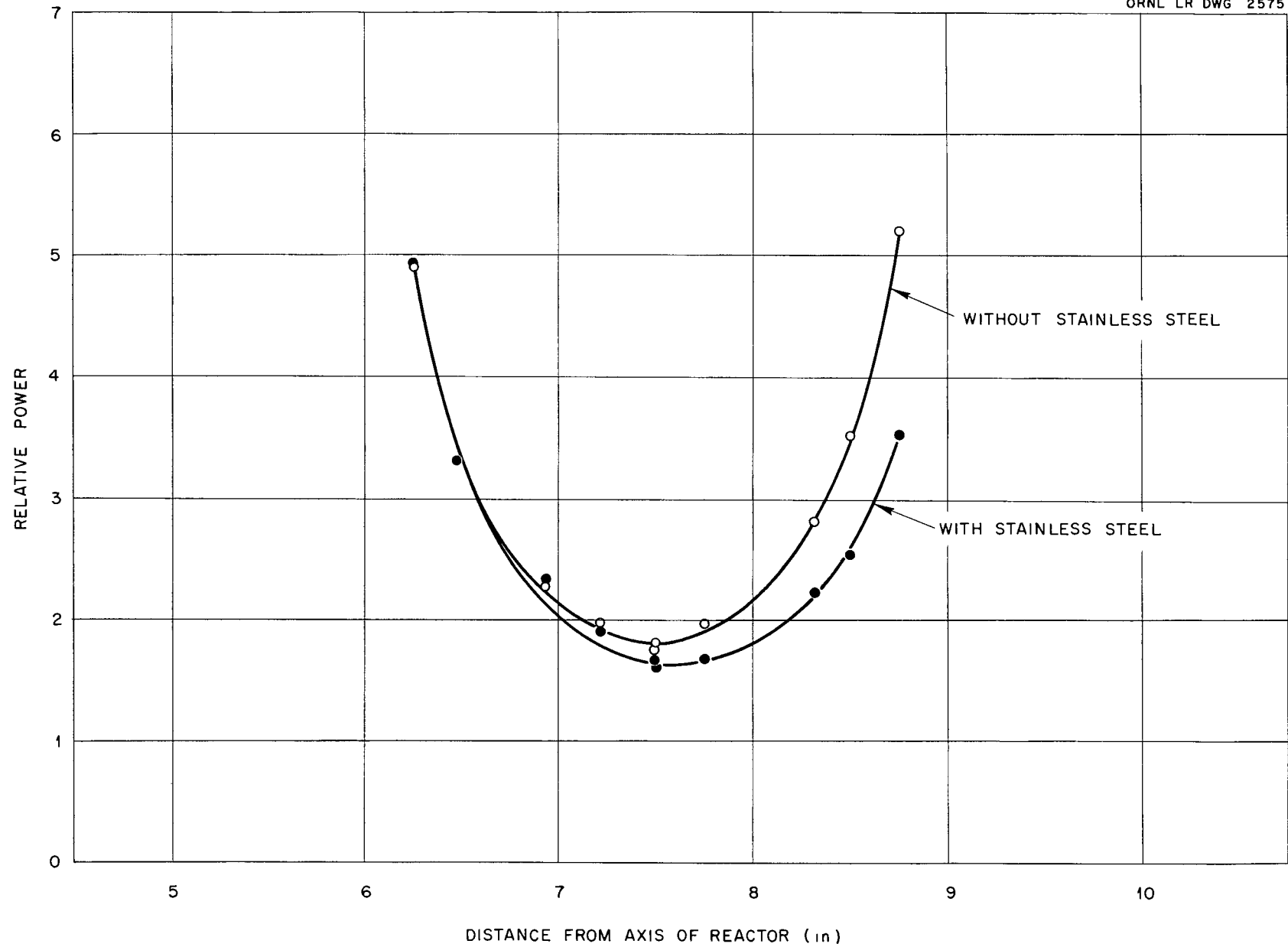


Fig III 15 Effect of Stainless Steel on Power Distribution

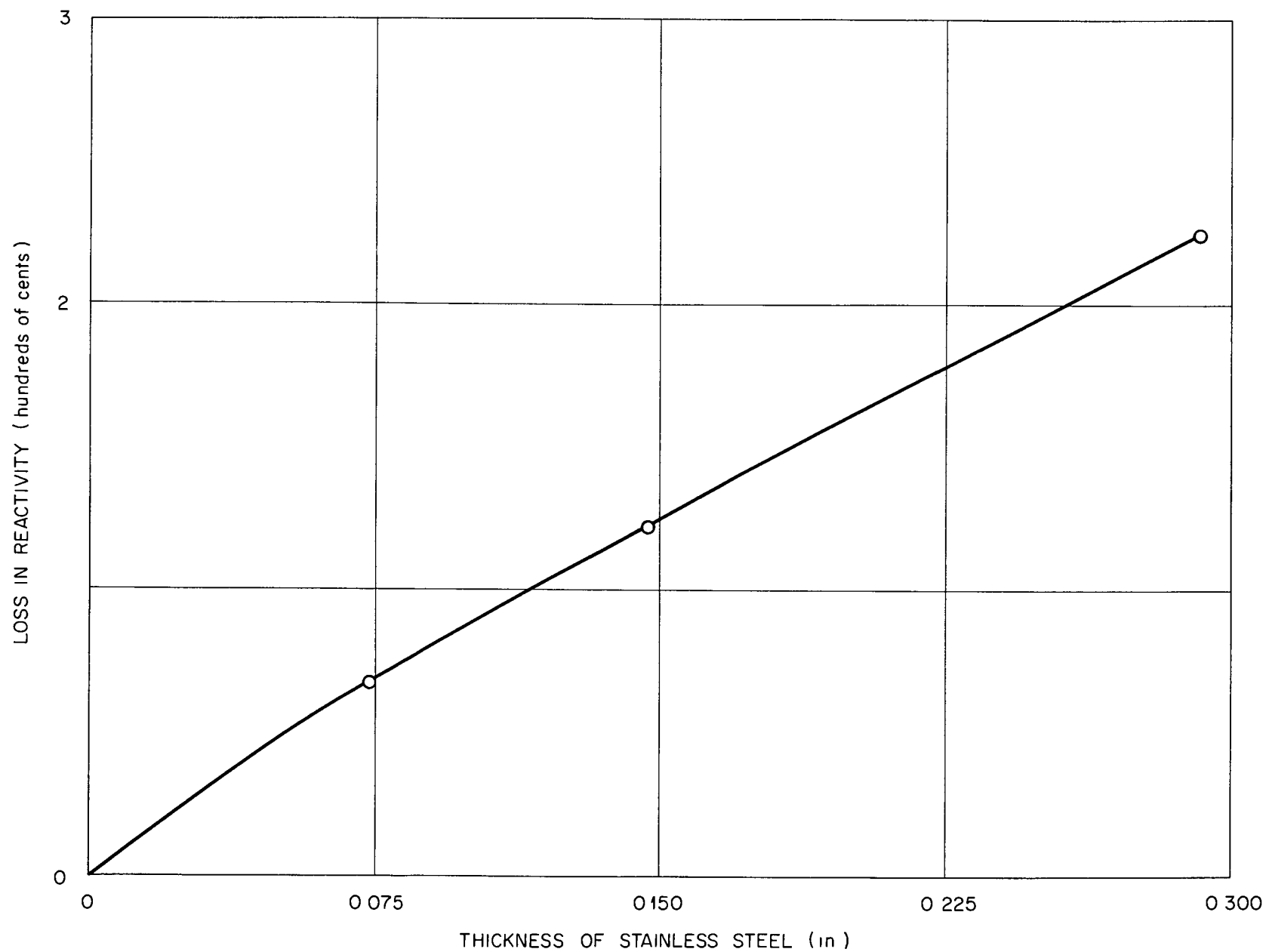


Fig III-16 Loss in Reactivity Due to Addition of Stainless-Steel Core Shells

resulted in a loss in reactivity of 92 cents. Six pieces of bismuth ($2\frac{7}{8}$ " x $2\frac{7}{8}$ " x 1") were then placed in each of these cells to partially fill the void. The additional loss in reactivity due to the bismuth was 32 cents. The bismuth was then removed and replaced by lead, with a resulting loss in reactivity of 121 cents.

3 Stainless Steel and Sodium

Four stainless steel cans filled with sodium were removed from cell Q-13. Four aluminum spacers, each approximately $1\frac{1}{4}$ " x $1\frac{7}{16}$ " x $1\frac{7}{16}$ ", were substituted for each of the sodium filled cans to anchor the fuel disks in place. The change in reactivity due to substituting the aluminum spacers for the cans was determined. The aluminum spacers were then replaced by four empty stainless steel cans similar to those containing the sodium; thus the change in reactivity due to the removal of the sodium alone was obtained. A gain in reactivity of 8.4 cents was obtained by substitution of the aluminum spacers for the sodium filled cans, and a gain of 2.8 cents was realized by the removal of only the sodium.

IV - CA-11

A Assembly Loading

The fuel region of the second assembly (CA-11) had properties that more nearly simulated those of the conceived full scale RMR. The fuel used was an homogeneous mixture of ZrO_2 , NaF, C, UF_4 , and a small amount of adsorbed moisture. The uranium was enriched to 93.2% U-235. The composition of the mixture was

16.2 wt % UF_4

55.0 wt % ZrO_2

19.9 wt % NaF

8.8 wt % C

0.25 wt % H_2O

The uranium density was 0.21 gm U-235/cc and the average packed density of the mixture was 1.8 gm/cc. ZrO_2 was used in place of ZrF_4 with the carbon added to compensate for the difference in the thermal neutron scattering properties of the mixture. The powdered mixture was packed in 1.1/4" O.D. square aluminum tubes.

with a $1/16$ " wall thickness. These fuel tubes were arranged in an annulus around a beryllium island with a beryllium and graphite reflector surrounding the fuel. Figures IV-1 and IV-2 show the loading at the mid-plane and in the vertical plane containing the reactor axis, respectively. Inasmuch as there were no fuel tubes $4-1/2$ " long available, $4-1/2$ " shishes were made using 0.01 " quarter size fuel disks and aluminum spacers. These shishes are shown as vertical lines in Fig IV-2. The fuel annulus was $4-1/2$ " thick in the central region with end ducts that were one fuel tube thick. It should be noted that while the thickness of the fuel region has been reported as $4-1/2$ ", there were three fuel tubes ($3-3/4$ " total thickness) across this dimension. In general the fuel tubes were arranged such that as small a void as possible existed between the fuel tubes themselves. Fig IV-3 shows the arrangement of the fuel tubes. The assembly was critical with 7.7 kg of U-235. In order to gain the additional reactivity required for some of the measurements, 0.01 " thick full size fuel disks were added to the island and/or fuel region as required.

B Evaluation of Control Rod D

Control Rod D was evaluated by subdividing the rod into units of equal reactivity. The evaluation was accomplished by means of the following procedure. The reactor was initially made critical with Rod A all of the way in, Rod D all the way out, and Rod C appropriately located. Rod A was then withdrawn one inch and the reactor returned to the critical condition by inserting Rod D. Rod A was then inserted one inch and the reactor returned to the previous critical condition by withdrawing Rod C. This sequence of operations was continued until Rod D was completely inserted. By this means Rod D was divided into increments of equal reactivity over its entire length. The unit of reactivity was determined from the measurement of the displacement of Rod D equivalent in reactivity to the removal of a safety rod, which had been evaluated previously by the "Rod Drop Method". The data thus obtained for the calibration of Rod D are shown in Table IV-1 and Fig IV-4. The position of the rod is measured from the assembly interface.

C Neutron Flux Distribution

Two radial flux traverses were taken, the first in the mid-plane of the reactor and the second $6-1/4$ " from the midplane. The second traverse passed through the quarter size fuel shishes used instead of the fuel tubes. Tables IV-2 and IV-3 and Figs IV-5 and IV-6 show all the data obtained for both the bare and cadmium covered indium traverses.

- 31 -

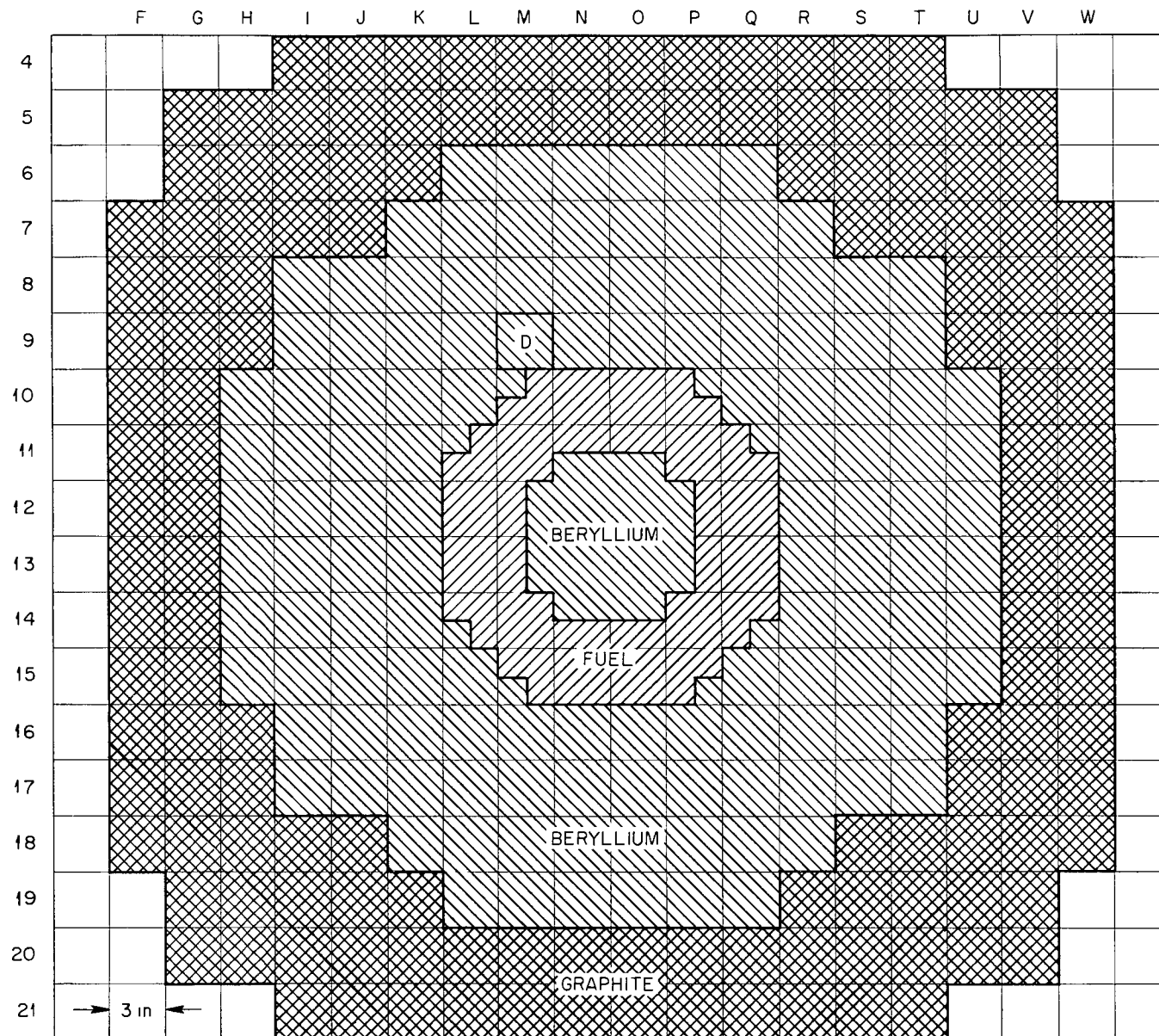


Fig IV-1 Assembly Loading at Mid Plane

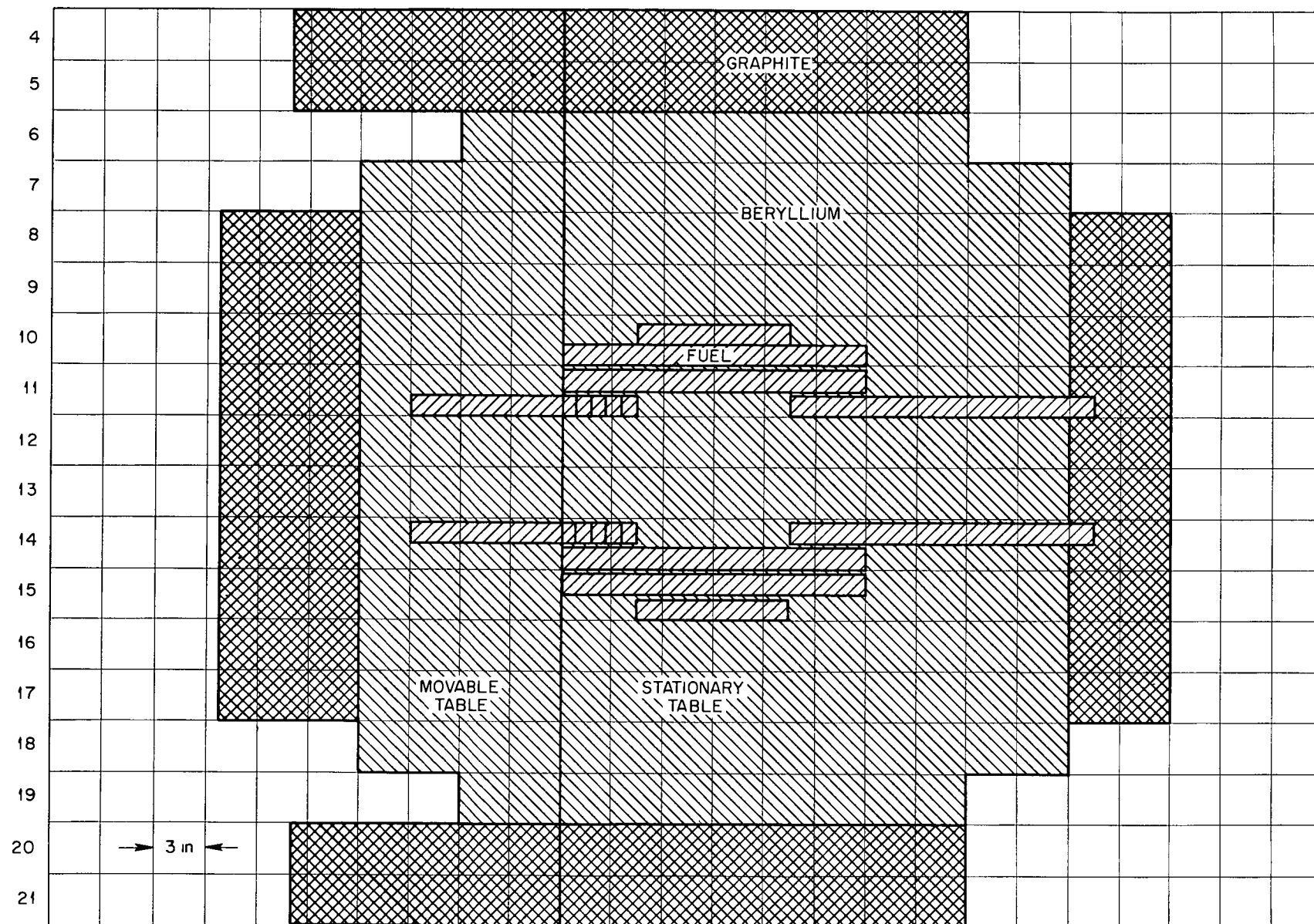


Fig IV-2 Axial Loading of Assembly in Vertical Plane Containing Reactor Axis

~~CONFIDENTIAL~~
PHOTO 12144

-33-

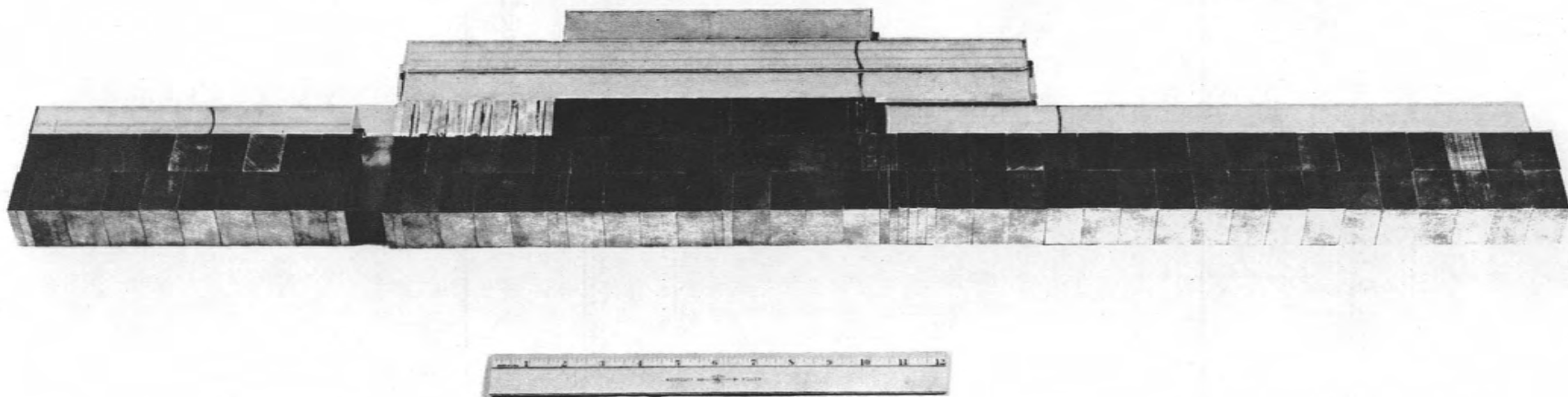


Fig. IV-3. Fuel Tube Arrangement.

TABLE IV-1

Rod D Calibration

Position of Rod From Assembly Interface In Inches	Change in Reactivity in Cents	Average Sensitivity in Cents per Inch
0 0	0 0	0 0
0 530	0 88	1 66
2 930	8 48	3 17
5 660	16 13	2 80
9 264	23 78	2 12
12 980	31 38	2 05
15 980	38 99	2 54
18 740	46 62	2 76
21 880	54 24	2 43
26 120	61 90	1 81
33 774	69 51	0 99

TABLE IV-2

Radial Flux Distribution in Mid-Plane

Distance From Axis in Inches	Relative Indium Activity Bare	Cd Covered
0 00	33 569	21 200
1 25	31 873	20 380
2 75	24 864	16 646
4 63	13 801	10 545
5 87	10 989	9 072
7 25	10 810	9 151
8 50	12 814	9 433
10 25	19 524	10 799
11 75	21 080	9 435
13 25	20 608	7 360
15 0	16 704	4 757
18 0	9 712	1 647
21 0	4 585	0 469
24 0	2 288	0 216
27 0	0 505	0 046

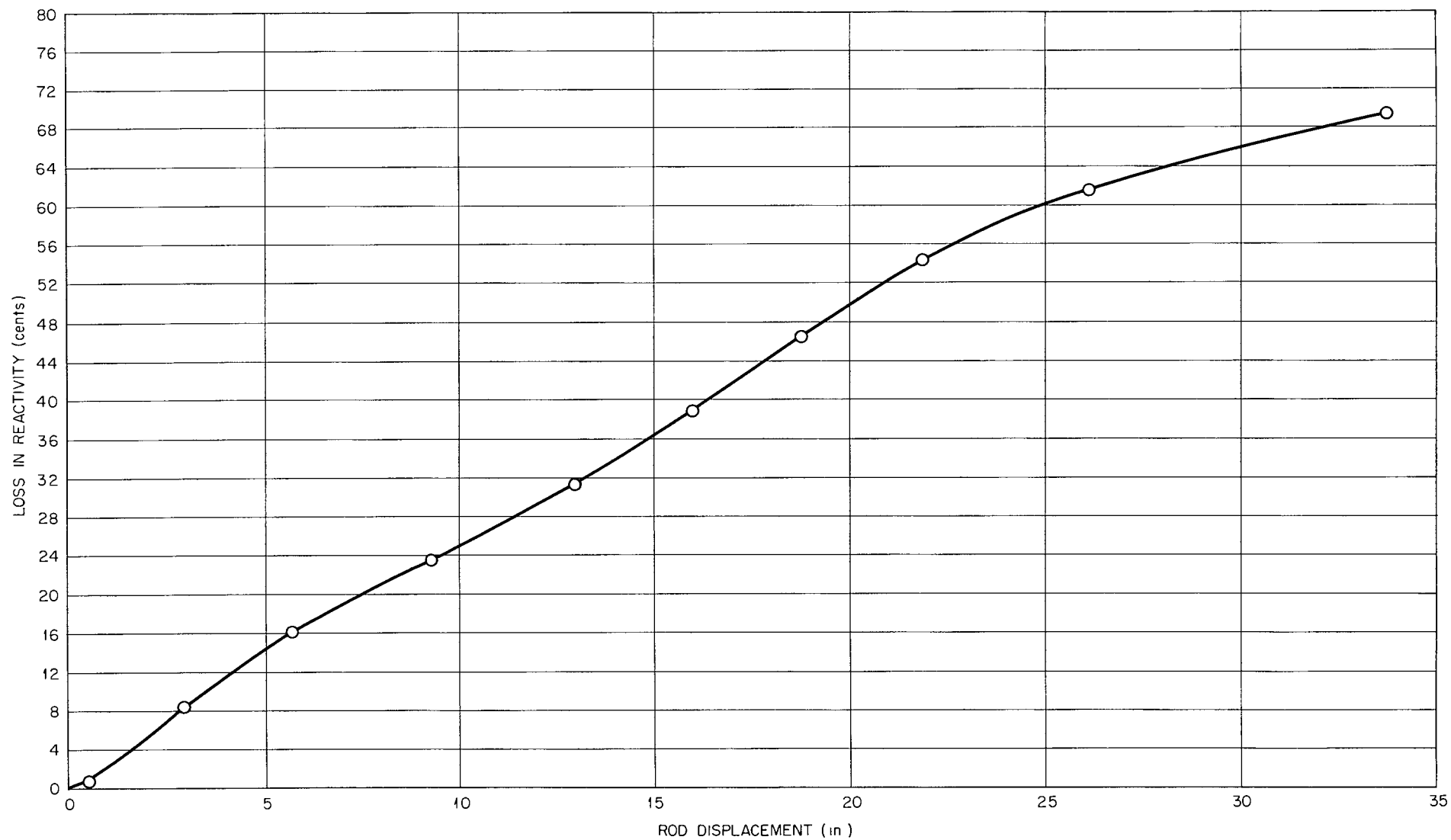


Fig IV-4 Calibration Curve for Control Rod D

-- 96 --

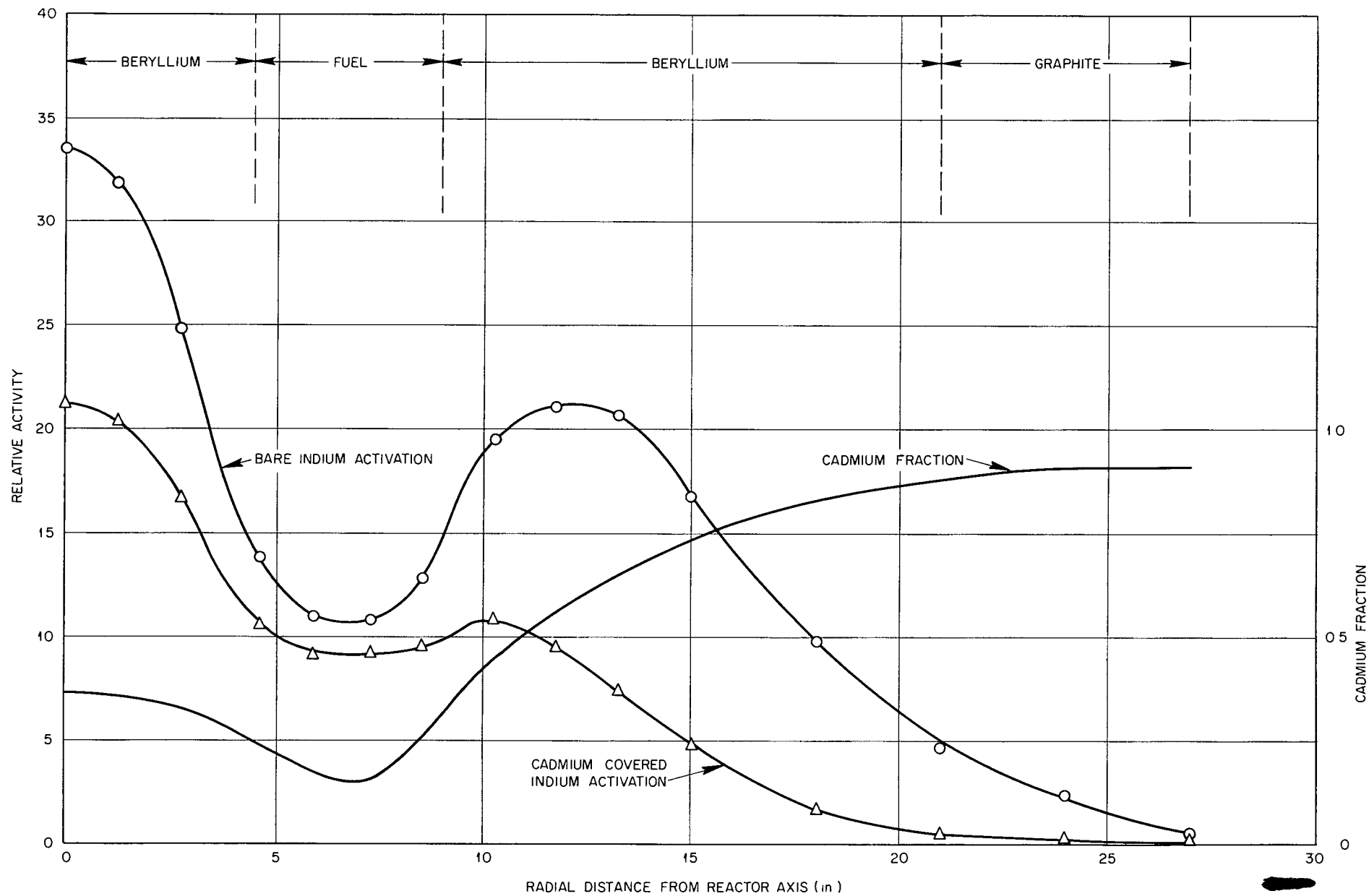


Fig IV 5 Radial Flux Distribution at the Mid plane

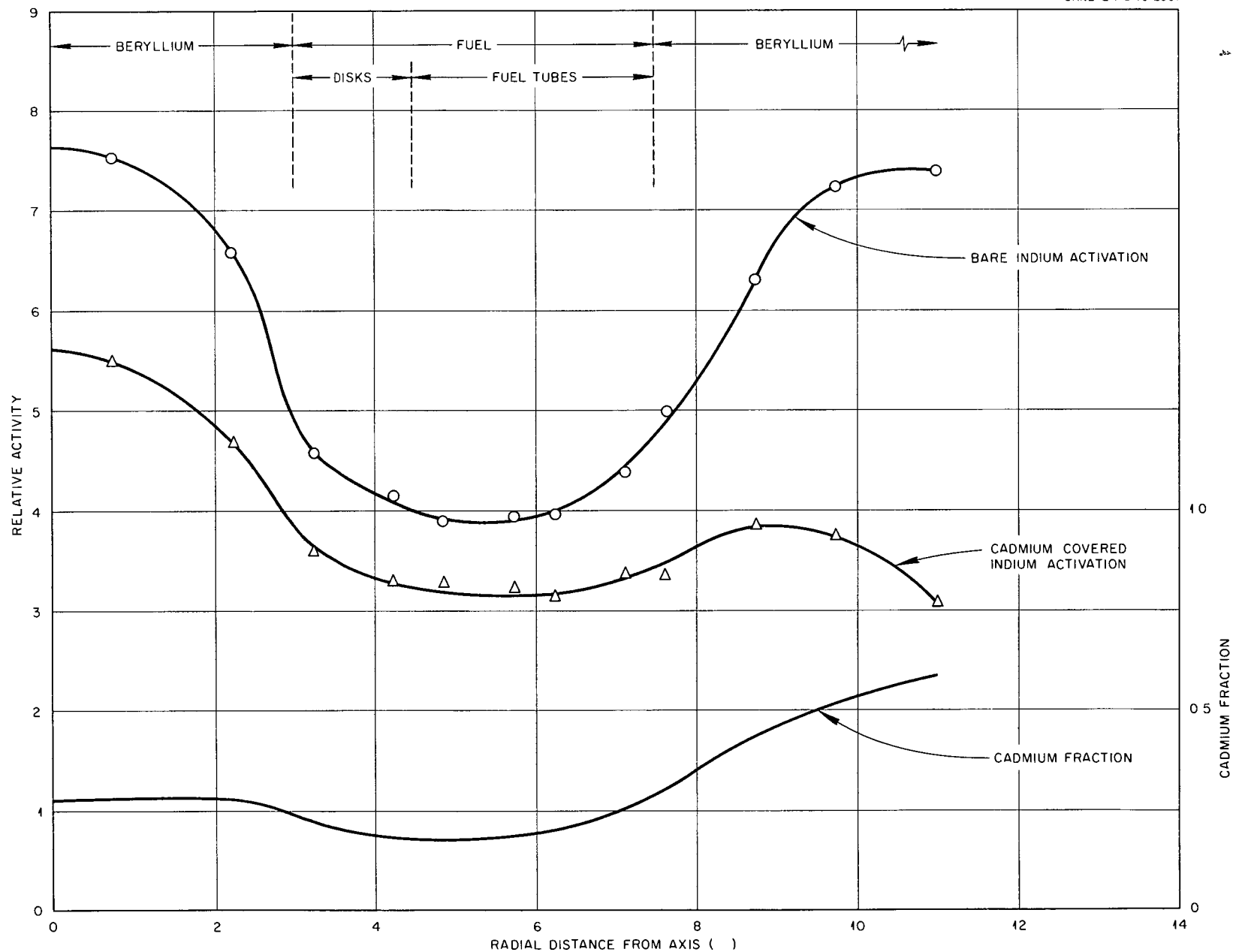


Fig IV 6 Radial Flux Distribution $6\frac{1}{4}$ in from Mid plane

TABLE IV-3

Radial Flux Distribution 6-1/4" from Mid-Plane

Distance from Axis in Inches	Relative Indium Activity	
	Bare	Cd Covered
0 7	7.523	5 484
2 3	6.579	4 679
3 3	4 563	3 589
4 3	4 144	3 292
4 9	3 882	3 274
5 7	3 949	3.202
6 3	3 953	3 120
7 1	4 366	3 364
7 6	4 866	3 346
8 7	6 294	3 634
9 7	7 229	3 532
11 3	7.389	3 076

The associated radial cadmium fractions for indium obtained in the mid-plane from CA-10 and CA-11 are shown in Figure IV-7.

D Power Distributions

Power distributions were obtained by placing 0.002" thick quarter size uranium disks with aluminum catcher foils adjacent to fuel tubes in the desired location. The first was measured parallel to the reactor axis in cell N-14. The 0.002" thick uranium disks and associated catcher foils were placed adjacent to the fuel tube between the fuel tubes and the beryllium island. A second power distribution was taken in the same location with Boral* strips (9" x 2-7/8" x 1/4") placed around the end fuel ducts on the stationary table, replacing some beryllium and graphite as shown in Figure IV-8. The data have been arbitrarily normalized at a point 14.5" from the interface. In order to maintain the reactor critical with the Boral inserted, additional 0.01" fuel disks were added to the beryllium island on the movable table. The data obtained from both runs is shown in Table IV-4 and Figure IV-9.

* The Boral was prepared from a mixture of 35 wt % ~~B₂O₃~~ and aluminum. This mixture is held between two aluminum sheets, each about 0.04" thick forming a 1/4" sandwich containing 250 mg of boron per square centimeter. The boral strips were wrapped in tape to minimize ~~boron~~ contamination.

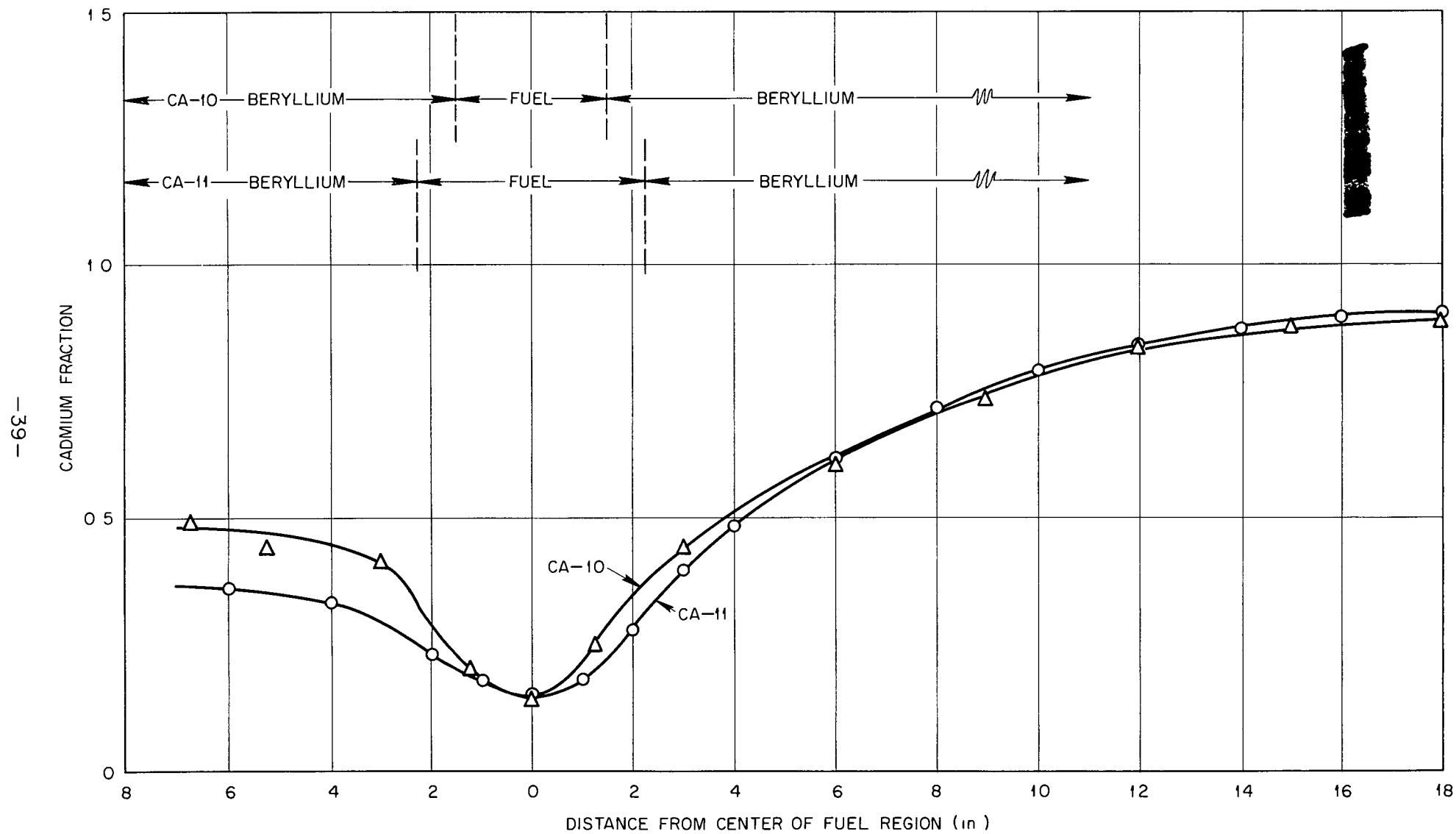


Fig IV-7 Cadmium Fractions in CA-10 and CA-11

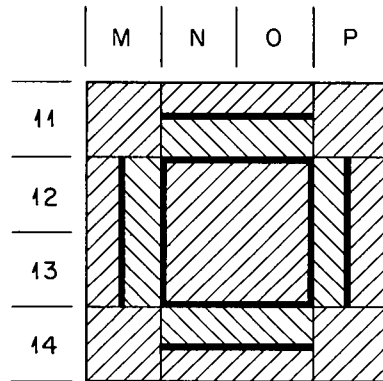
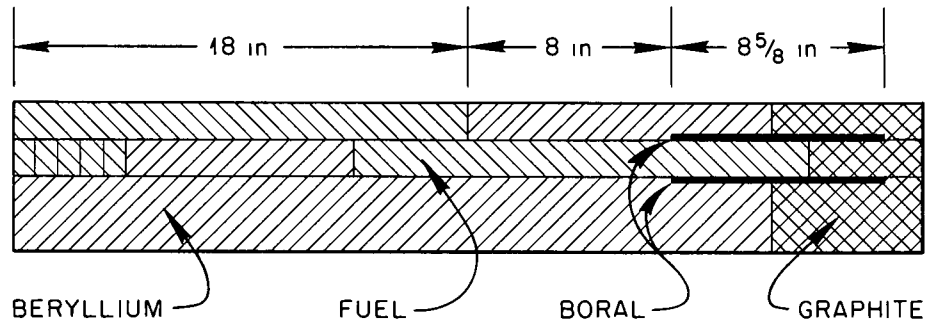


Fig IV-8 Position of Boral Inserted Around End Ducts
on Stationary Table

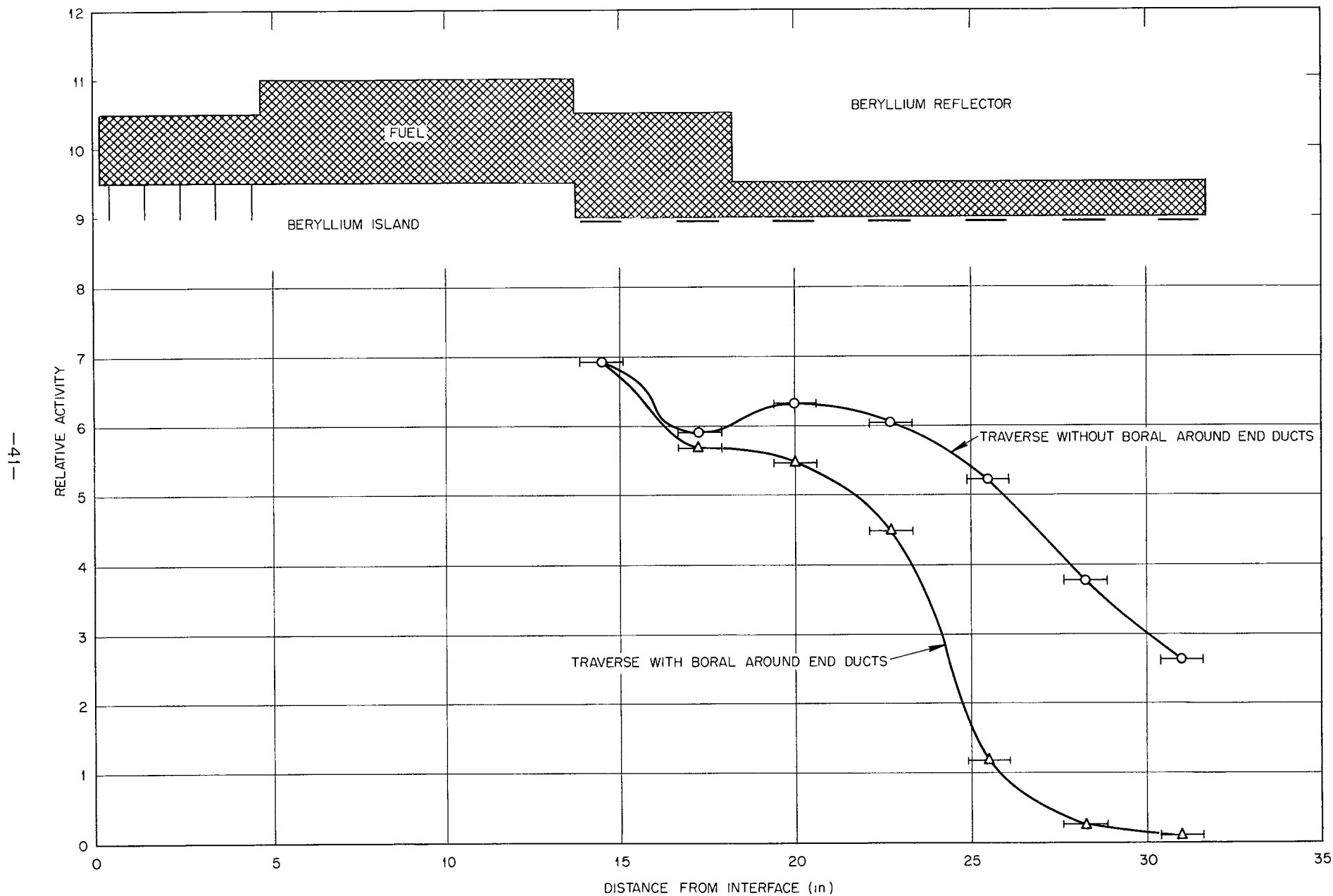


Fig IV-9 Axial Power Distributions in Cell N-14

TABLE IV-4

Axial Power Distribution in N-14

Distance from Interface in Inches	Relative Activity*	
	Without Boral	With Boral
14 5	6 902	6 902
17 3	5 896	5 647
20 0	6 312	5 469
22 7	6 027	4 465
25 5	5 205	1 160
28 3	3 747	0 248
31 0	2 602	0 098

A power distribution was also measured across the fuel annulus in the mid-plane of the reactor. The 0.002" thick uranium disks were placed in the horizontal gap (approximately 1/4") between the fuel tubes of adjacent vertical cells, with eight 5/16" catcher foils distributed across the fuel disks. The data obtained is shown in Table IV-5 and Figure IV-10.

TABLE IV-5

Power Distribution Across Fuel in Mid-Plane

<u>Distance From Reactor Axis</u>	<u>Relative Activity</u>
4 8	6 955
5 3	5 021
5 8	4 213
6 3	3 163
6 8	3 500
7 3	3 880
7 8	5 174
8 4	7 549

* Data normalized at the point 14 5" from the interface

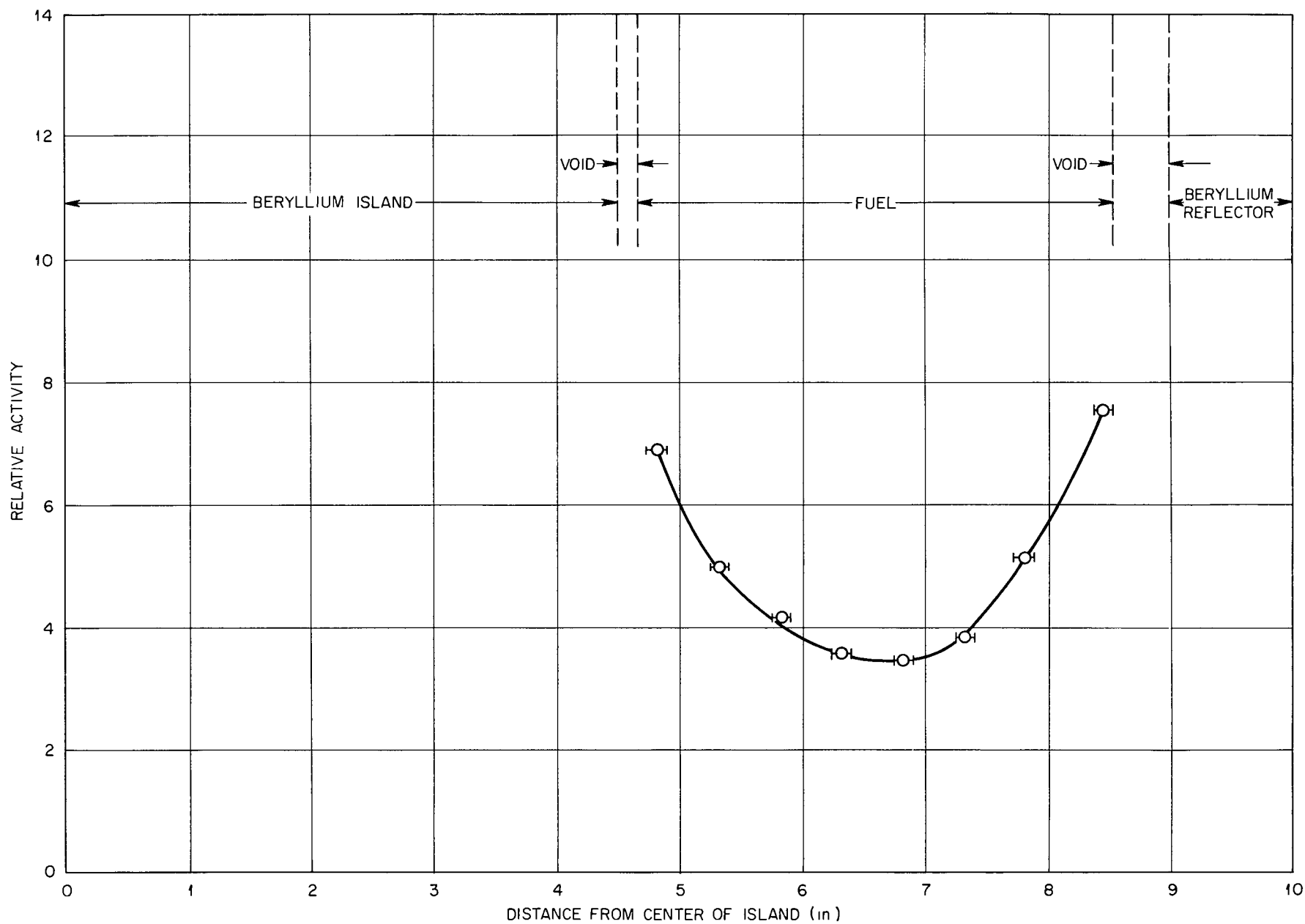


Fig IV-10 Power Distribution Across Fuel in Mid-plane

E Neutron Leakage Measurements

Measurements were obtained in an effort to estimate the ratio of the end to side neutron leakage from the reactor. In the first set of measurements six bare and cadmium covered indium foils were placed on the back surface of the reactor extending from the reactor axis outward 7". Three sets of foils were placed on the outer surface of the graphite side reflector at the mid-plane. These foil measurements were taken without any Boral around the fuel end ducts.

Side and end fast neutron leakage measurements were also obtained using a fast fission chamber. Measurements were taken both with and without Boral around the fuel end ducts, and with a 1/4" of Boral around the fission chamber*. Side leakage was determined by placing the chamber in cell X-12 with the center of the chamber at the mid-plane. The axis of the fission chamber was approximately 1-1/2" from the graphite side reflector. The end leakage was obtained by placing the chamber approximately 7" behind the stationary table with its axis parallel to the mid-plane with the center of the chamber on the projected axis of the reactor. The data obtained are summarized in Table IV-6.

TABLE IV-6

Summary of Neutron Leakage Measurements

	<u>Ratio of End to Side Leakage With Boral Around End Ducts</u>	<u>Ratio of End to Side Leakage Without Boral Around End Ducts</u>
Fission Chamber	6	28
Bare Indium	-	2 3
Cd Covered In	-	1 2
Bare-Cd Covered	-	1 1

* Slabs of Boral, 18" x 2-7/8" x 1/4", were placed around the chamber, which was 10" long, thus approximately 4" of Boral extended beyond either end.

F Evaluation of Boral around Fuel End Ducts

The Boral sheets that were placed around the fuel end ducts as shown in Figure IV-7 were evaluated. The gain in reactivity due to their removal was compensated for by removing fuel disks from the island region on the movable table. The loss in reactivity due to the replacement of beryllium and graphite by Boral around the fuel end ducts amounted to 1.6% in k_{eff} .

G Stainless Steel and Boron Poison Rods

Two 3/16" diameter rods were evaluated in the center of cell O-12 in the island. The first rod was a stainless steel tube 40" long filled with natural boron to a linear density of 0.1 gm B/in. The second was a stainless steel rod 38" long. The loss in reactivity in cents for each rod is shown as a function of the distance of the end of the rod from the mid-plane in Table IV-7 and Figure IV-11.

TABLE IV-7

Reactivity Loss Due to Poison Rods Inserted in O-12

Distance From Mid-Plane in Inches	Loss in Reactivity in Cents	
	Boron Filled Rod*	Stainless Steel Rod
0 0	47 6	5 0
4 5	29 9	3 0
9 0	17 1	-
15 0	4 8	-
21 0	0 4	-

H Cadmium Importance Function

The importance of cadmium as a neutron absorber when placed in the mid-plane of the reactor was obtained by taping a piece of cadmium 2-3/4" square and 0.02" thick weighing 19.09 gm, to either a block of beryllium or a fuel tube, and recording the loss in reactivity for each radial position. The data obtained are shown in Table IV-8 and Figure IV-12.

*Further insertion of the Boron filled rod from the mid-plane to the assembly interface (9") resulted in an additional reactivity loss of 30.2 cents.

-46-

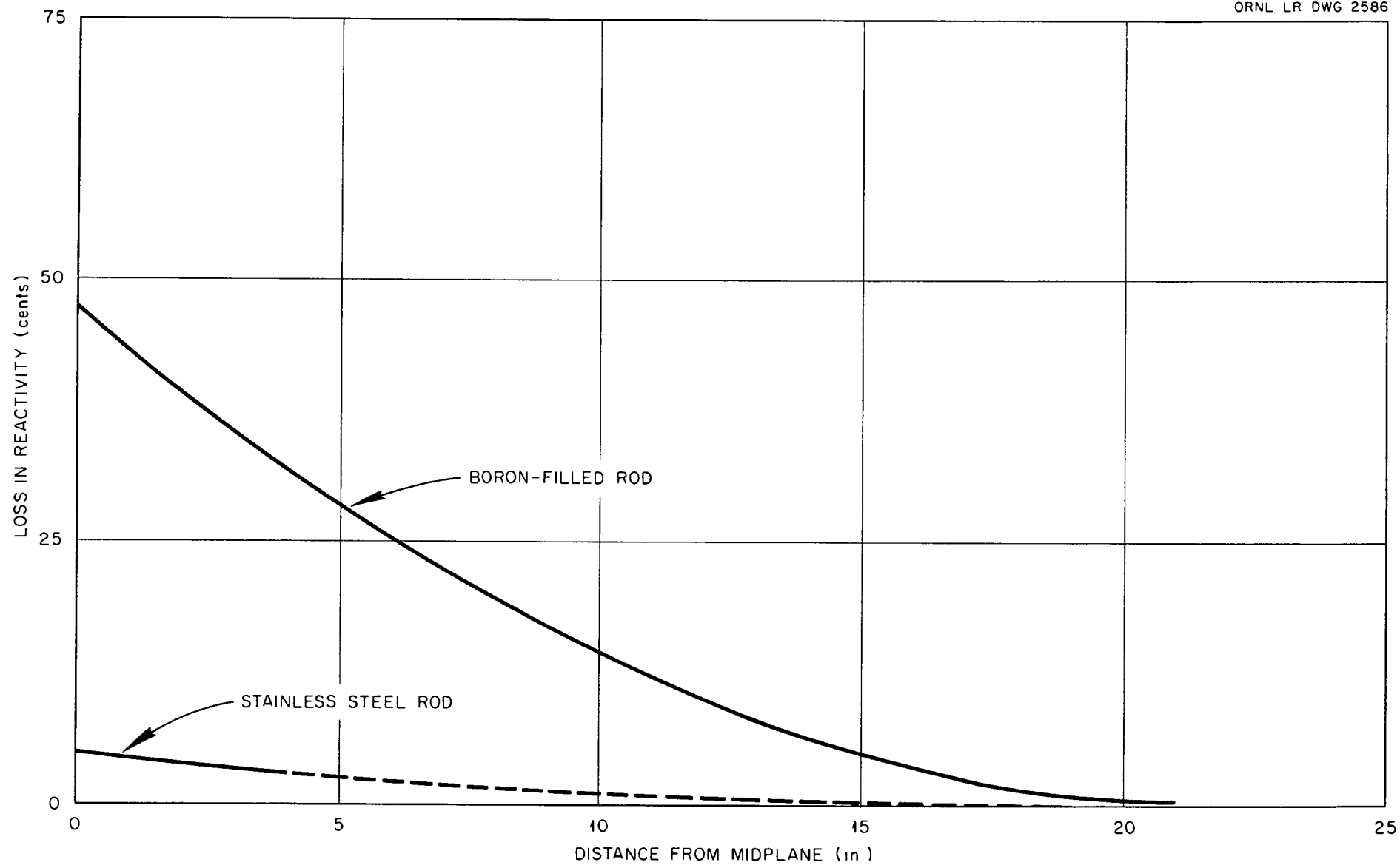


Fig IV-11 Reactivity Loss Due to Poison Rods Inserted in O-12

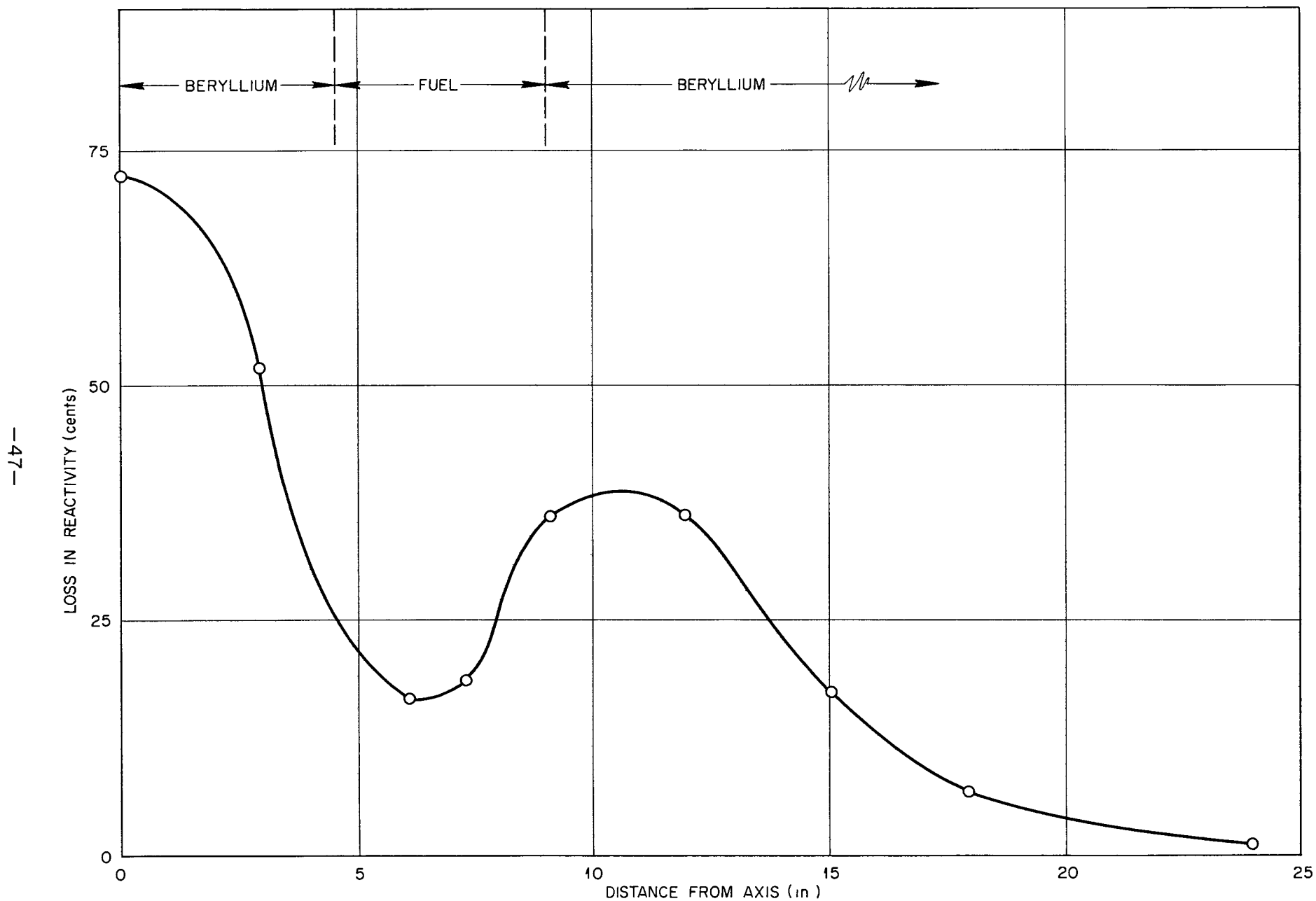


Fig IV-12 Cadmium Importance Function

TABLE IV-8

Cadmium Importance Function

<u>Distance From Axis in Inches</u>	<u>Loss in Reactivity in Cents</u>
0 0	72 2
2.9 ¹ / ₂	51 8
6.1 ¹ / ₂	16 8
7 3 ¹ / ₂	18 7
9.1 ¹ / ₂	36 1
11 9	36 3
15 1	17 5
17 9	6 9
23.9	1 2

I Danger Coefficients

Danger coefficients were obtained for a number of different materials in the reflector and/or fuel regions. Samples were located in cells Q-12 and Q-13 in the fuel region or adjacent to the inner face of cells S-12 and S-13 after removal of some beryllium reflector. All samples were placed symmetrically about the mid-plane. The changes in reactivity, either plus or minus, obtained are shown in Table IV-9 and are referenced to the void. The samples of Li, KF, NaF, Zr, Cr, and RbF were placed in aluminum containers (5/16" x 2-1/2" x 9") with 1/32" wall thickness. It has been assumed that these containers had no significant effect on the reactivity. The sample of sodium was contained in thin walled stainless steel cans, whose reactivity value was measured with the cans empty, thus enabling the reporting of the sodium value. The other samples required no containers. The reactivity changes obtained for these materials are shown in Table IV-9.

The reactivity change due to the substitution of a sample of D₂O for beryllium was measured at three locations in the assembly. The sample was 99.2% D₂O and weighed 2.65 kg. It was placed at the assembly mid-plane in the island adjacent to the fuel, in the reflector adjacent to the fuel and in the reflector 3" from the fuel layer. In each of the first two locations the gain in reactivity due to the substitution was 12 cents, in the latter position the reactivity was decreased by 24 cents.

J Effect of Stainless Steel Around the Fuel Annulus

In order to estimate the effect on reactivity of the fuel containing core shells required in the full scale reactor, two adjacent quadrants of the fuel annulus were partially covered with stainless

TABLE IV-9

Danger Coefficient Measurements

Sample	Sample Weight gm	Sample* Size	Reactivity Change In Fuel Region	cents/gm In Reflector
Li ₂ CO ₃	152 4	A	0 0000	-0 0415
KF	198 0	A	-0 0162	-0 0578
NaF	97 2	A	-0 0058	-0 0354
Zr	287 7	A	+0 0150	-0 0498
Cr	249 4	B	-0 0237	-0 0680
RbF	156 3	B	+0 0118	+0 0026
Inconel	1956 4	A	-0 0276	-0 0448
Ni	2061 0	A	-0 0274	-0 0437
Pb	2544 8	C	-0 0008	-0 0007
Pb	4592 7	D	-	-0 0012
316 Stainless Steel	1990 4	C	-0 0243	-0 0385
310 " "	3195 0	D	-	-0 0233
316 " "	995 2	E	-	-0 0509
Be	753 6	D	-	+0 0090
Na	366 9	D	-	-0 0190
Bi	3931 8	D	-	+0 0006
Graphite	376 2	A	+0 0108	+0 0043
Density 1/72 gm/cc				
Graphite	700 1	D	-	+0 0064
Density 1 72 gm/cc				
Graphite	825 6	D	-	+0 0065
Density 2 0 gm/cc				
BeO	375 0	F	-	+0 0055

*Sample Size

A - 5/16" x 5" x 9"

B - 5/16" x 2-1/2" x 9"

C - 1/4" x 5-3/4" x 9"

D - 1" x 2-7/8" x 8-3/8"

E - 1/8" x 5-3/4" x 9"

F - 7/8" x 2-7/8" x 5"

steel 0.145" thick. The exposed surfaces of the fuel tubes, extending 4-1/2" on either side of the mid-plane, both between the fuel and the island and between the fuel and the reflector, were covered with 9" long plates. The total weight of the steel added was 9.0 kg. The additional reactivity required was provided by adding 0.01" thick fuel disks distributed throughout the fuel region. The addition of this steel to the quadrant first covered resulted in a loss in reactivity of 1.45%* in k_{eff} and requiring the addition of 828 gms of uranium to remake the system critical. The steel added to the second quadrant also resulted in a loss of 1.45%* in k_{eff} and required the addition of 1818 gms of uranium.

*The effect on the control rod calibrations due to the steel and increased fuel loading were not measured, and therefore introduces some doubt as to the accuracy of these data.

V - CA-12

In this assembly three variations of the essential features of the RMR were carried out

- 1 The reactor was first built up with an all graphite island and reflector with a 3" thick 18" long cylindrical fuel annulus separating the two regions. The fuel region contained 1 5' thick 9" long end fuel ducts on both ends of the reactor. The loading is shown in Figure V-1. The fuel loaded in the 1 25" square aluminum tubes, was the same as that used in CA-11 except the ~~U-235~~ density was doubled resulting in the following composition

32.4	wt %	UF ₄
44.2	wt %	ZrO ₂
16.0	wt %	NaF
7.1	wt %	C
0.2	wt %	H ₂ O

The U-235 density was 0.42 gm/cm³, and the mixture was packed to an average density of 1.8 gm/cm³. This reactor loaded with 17.3 kg of U-235 was not critical and an apparent source neutron multiplication of about six was recorded.

- 2 In order to go critical, the assembly was modified by replacing graphite with beryllium in 31 cells of the assembly. Thirteen of these cells were in the island and the remaining 18 were around the periphery of the fuel annulus.

The substitution of beryllium for graphite in the inner reflector region was then completed as is shown in Figure V-2. The excess reactivity gained by this further substitution was absorbed by adding 18.1 kg stainless steel in the form of core shells 0.059" thick around the fuel annulus and covering the central 18" fuel region. A radial flux distribution was measured in the mid-plane of the reactor with the assembly loaded as shown in Figure V-2. The data obtained are shown in Table V-1 and Figure V-3. The cadmium fraction obtained from the two flux curves is also shown in the figure.

- 3 The final variation of CA-12 was a brief exploration of a two region reactor using 17.3 kg of U-235 with the fuel arranged in a central region. The fuel was surrounded by a 3" thick beryllium and thick graphite reflector. For this configuration an apparent source neutron multiplication of about four was recorded. By altering the reflector to provide a 9" layer of

-52-

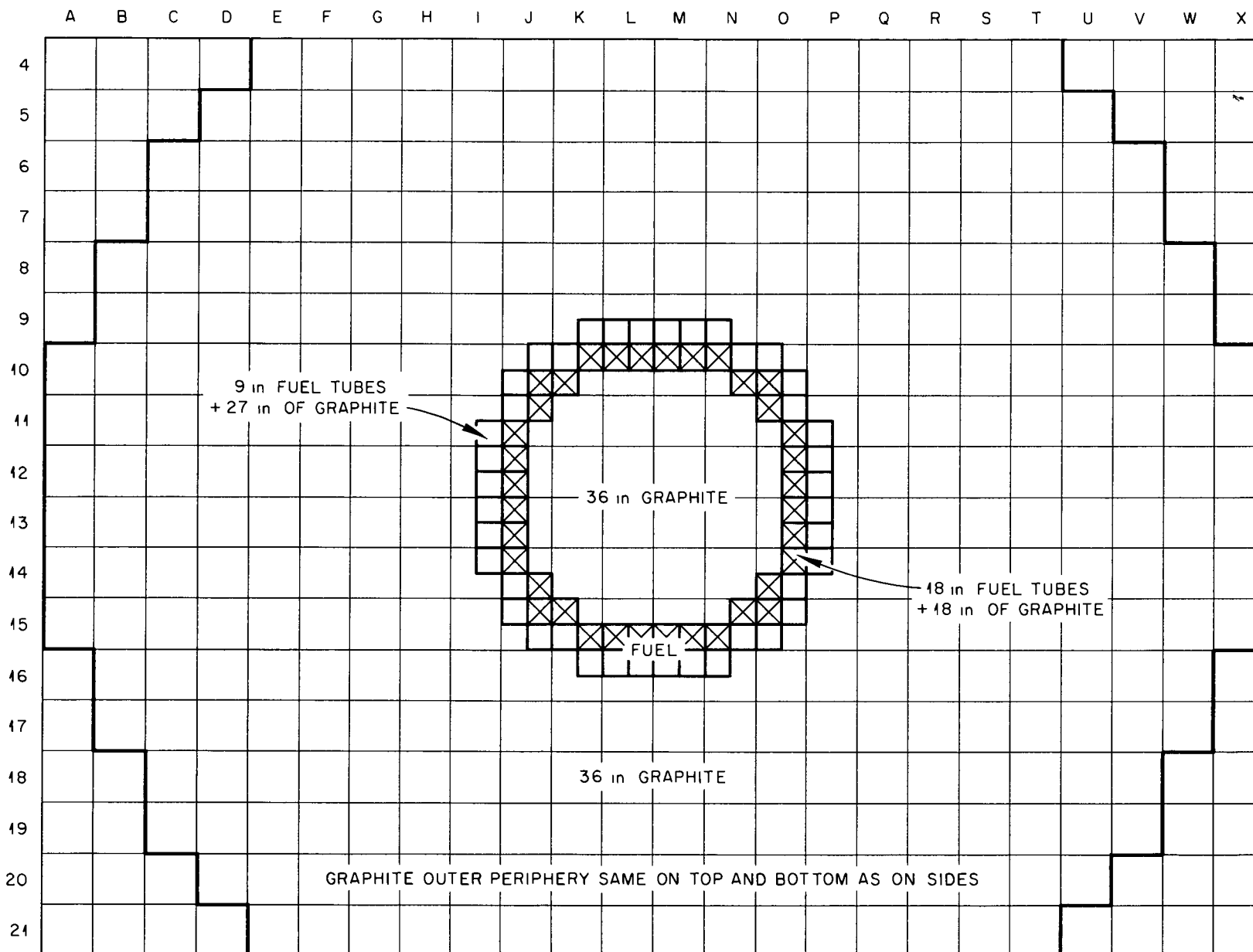


Fig V-1 Assembly Loading at Mid-plane

-53-

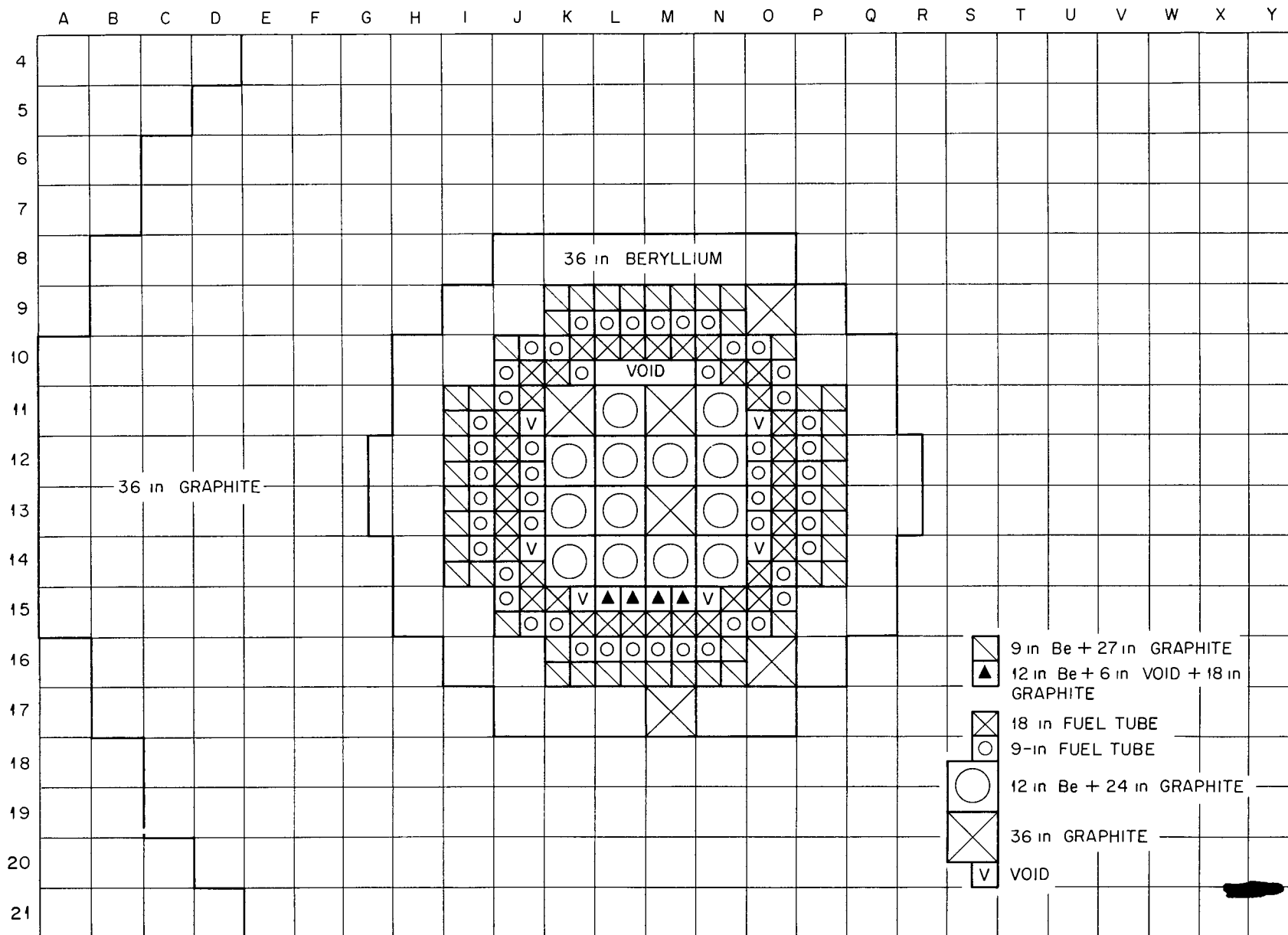


Fig V-2 Assembly Loading at Mid-plane

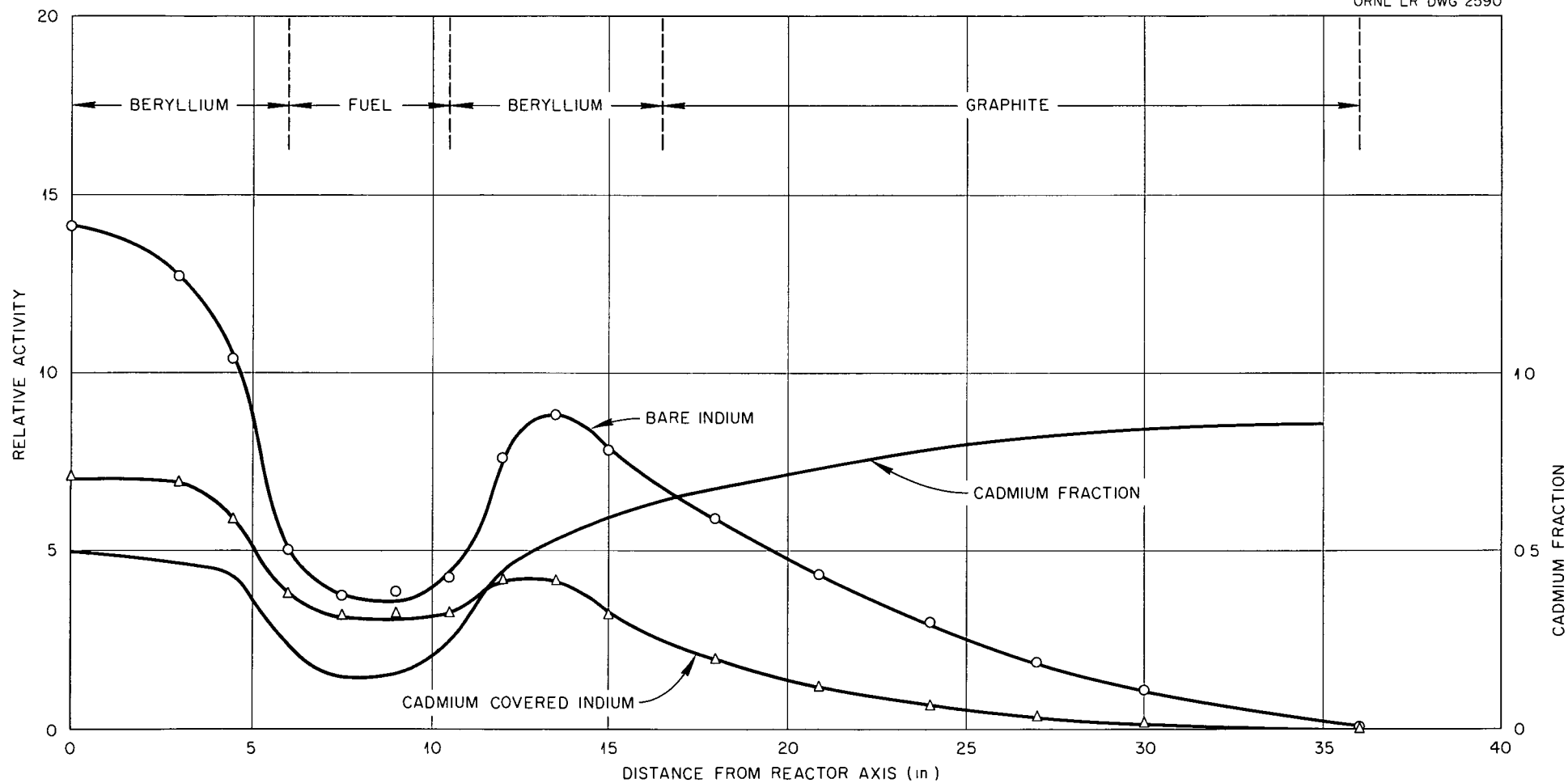


Fig V-3 Neutron Flux Distribution in Mid plane

beryllium surrounding the fuel with the remainder of the reflector graphite, the source neutron multiplication was quadrupled. The assembly was not made critical.

TABLE V-1

Radial Neutron Flux Traverse in Mid-Plane of Reactor

Distance From Axis in Inches	Relative Activity	
	Bare	Cd Covered
0 0	14 118	7 082
3 0	12 711	6 903
4 5	10 385	5 862
6 0	5 003	3 796
7 5	3 744	3 197
9 0	3 889	3 264
10 5	4 291	3 274
12 0	7 604	4 194
13 5	8 835	4 164
15 0	7 822	3 197
18 0	5 926	1 944
20 9	4 360	1 176
24 0	3 045	670
27 0	1 891	356
30 0	1 138	179
36 0	126	017

VI. CA-13

A Assembly Loading

Graphite has been suggested as a high temperature fluoride container for the fissioning volume of the RMR CA-13 was assembled to obtain a check on some of the characteristics of such a reactor. A two region reactor was constructed with a 1/1 graphite to powdered fuel volume ratio in the central core and surrounded by a 12" beryllium and 6" graphite reflector as shown in Figure VI-1. The powdered fuel of CA-12 was used, and the reactor was first critical with 15.2 kg U-235. As additional fuel was added to obtain the configuration shown in Figure VI-1, stainless steel plates 0.059" thick were added around the fuel to take up the excess reactivity. The reactor contained 17.2 kg of U-235 and 11.0 kg of stainless steel when loaded as shown in the figure. The core shell covered 94% of the central fuel region (that is, 9" on either side of the mid-plane) which contained 68% of the fuel.

B Neutron Flux Distribution

With the stainless steel core shell in place, radial bare and cadmium covered indium traverses were taken in mid-plane of the reactor extending from M-12 to W-12. The data are shown in Table VI-1 and Figure VI-2. The associated cadmium fraction is also shown on the figure.

TABLE VI-1

Radial Flux Distribution in the Mid-Plane

Distance From Axis in Inches	Relative Activity	
	Bare Indium	Cd Covered
0 0	0 9628	0 8852
1 5	0 9628	0 9032
3 0	1 036	0 9184
6 0	1 215	1 085
7 5	1 336	-
9 0	1 514	1 330
10 5	2 200	1 515
12 0	3 502	1 842
13 4	3 738	1 561
16 5	2 718	0 7605
22 5	0 7759	0 0776
28 5	0 0815	0 0072

-57-

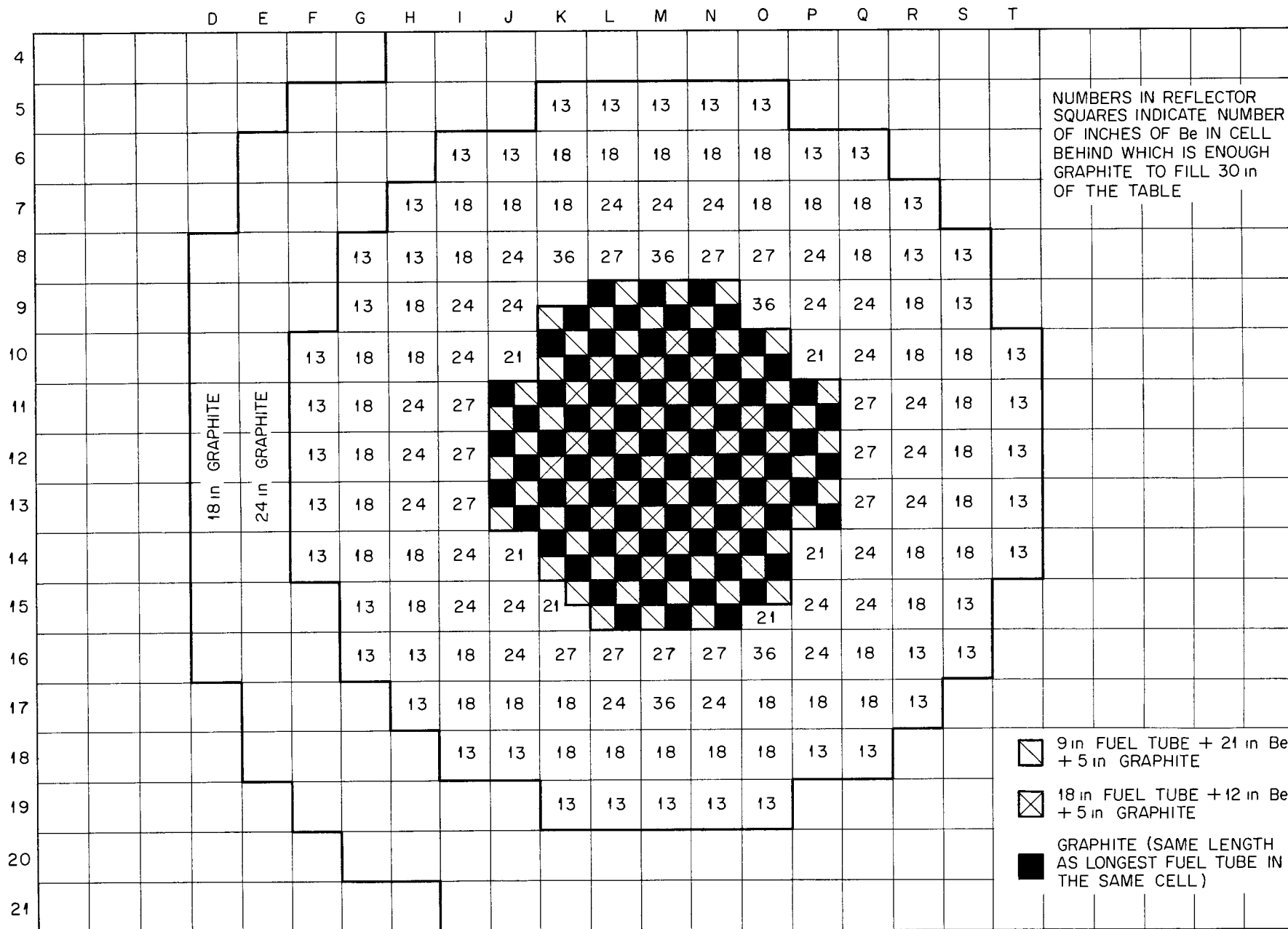


Fig VI-1 Assembly Loading at Mid-plane

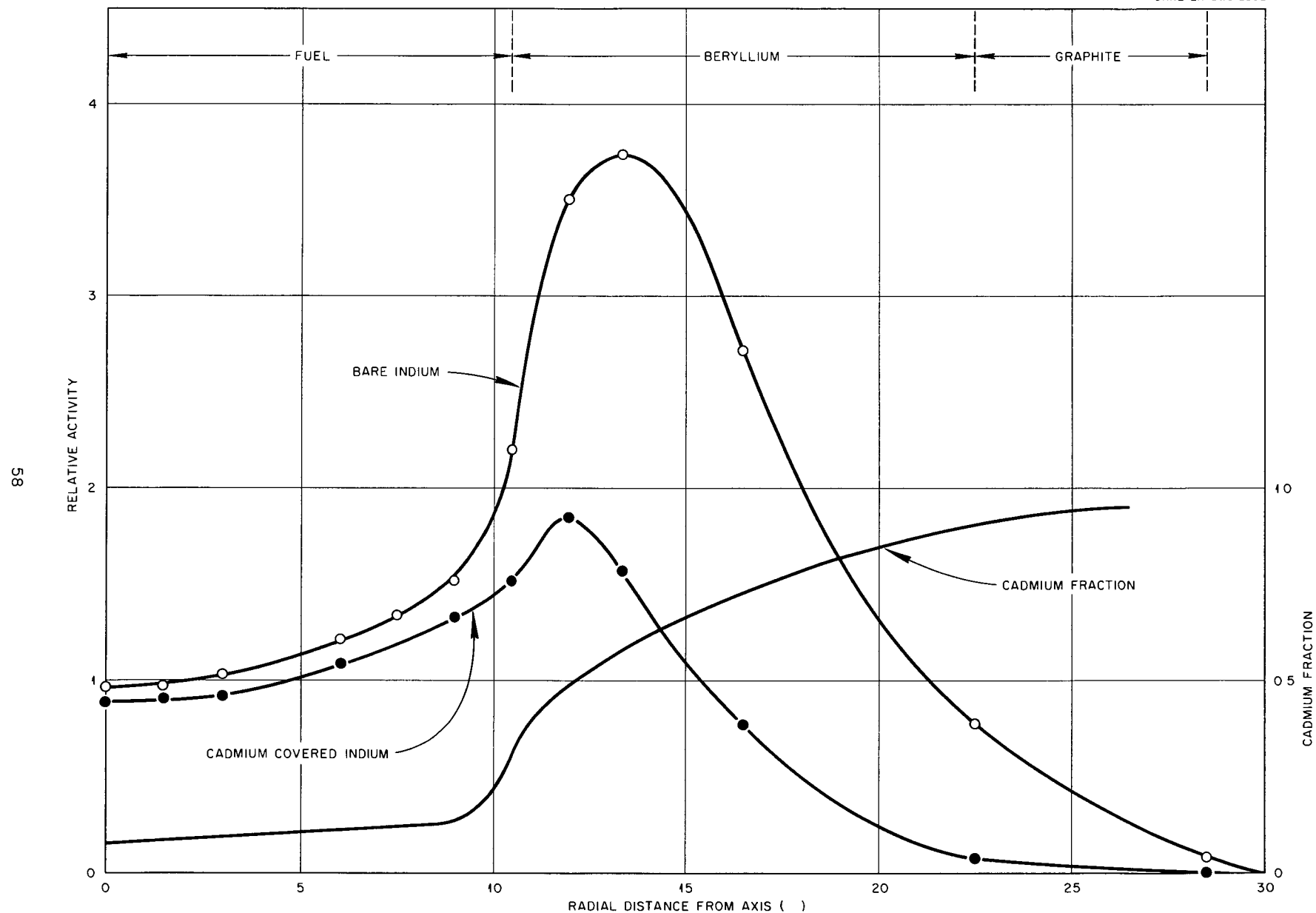


Fig VI 2 Radial Neutron Flux Distribution in Mid plane

C Power Distribution

Power distributions were taken radially in the mid-plane from M-12 to P-12 and axially back through M-12. The traverses were obtained by placing a 0.002" uranium fuel disk and its associated aluminum catcher foil adjacent to a fuel tube. The data obtained for both traverses are shown in Tables VI-2 and VI-3 and Figures VI-3 and VI-4.

TABLE VI-2

Radial Power Distribution in Mid-Plane

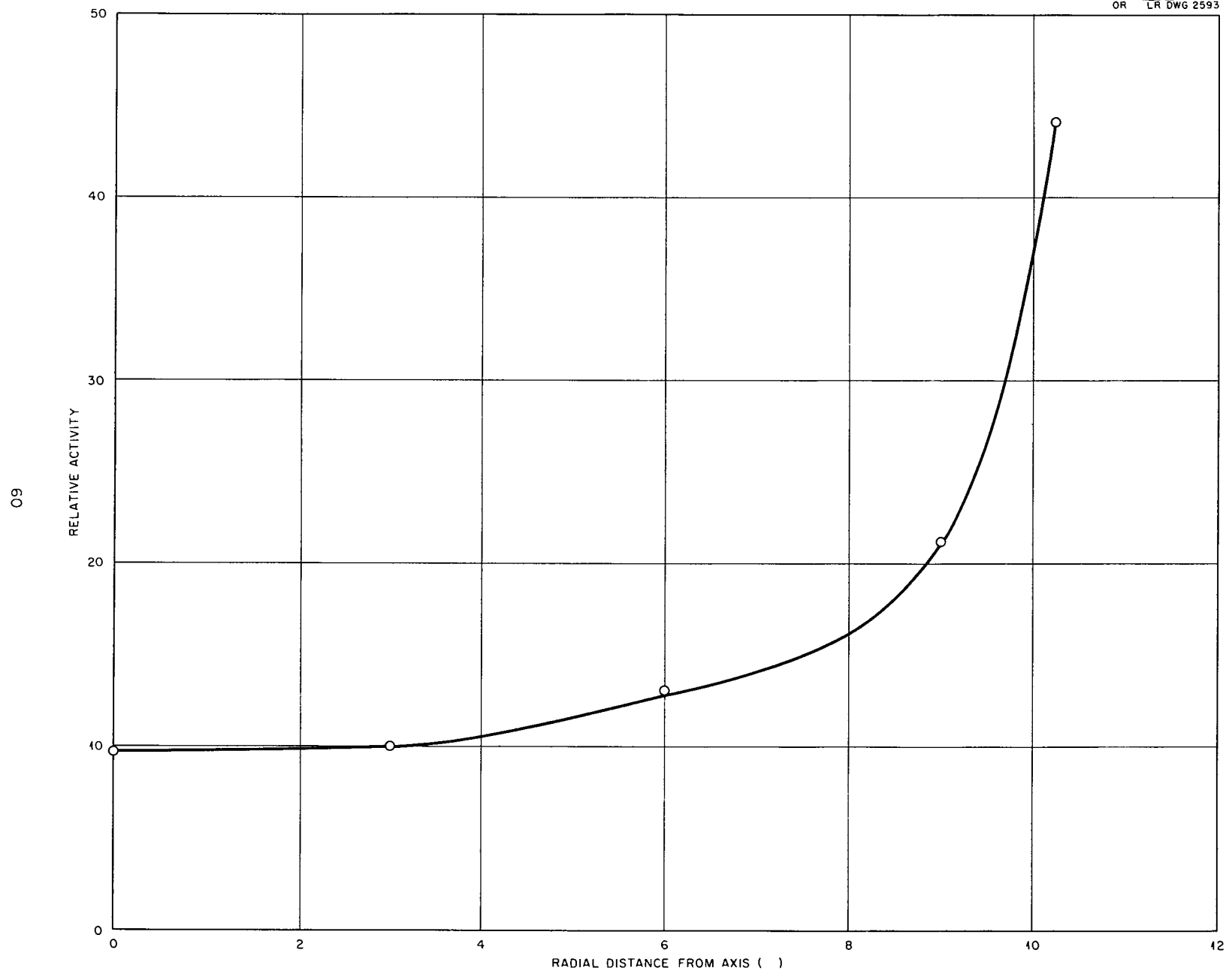
<u>Distance From Axis in Inches</u>	<u>Relative Activity</u>
0 0	9 66
3 0	9 94
6 0	13 09
9.0	21 23
10 3	44 14

TABLE VI-3

Axial Power Distribution Through M-12

<u>Distance From Mid-Plane in Inches</u>	<u>Relative Activity</u>
1 0	9 66
5 1	8 95
9 0	9 18
13 0	10 34
17 0	25 31

Three uranium foils were covered with 0.020" of cadmium and placed in radial positions in the mid-plane. The fuel cadmium fraction, as determined from the activity of these foils together with the activities of similarly placed foils for the radial power distribution, are plotted as a function of the square of the radial distance from the reactor axis in Figure VI-5. Table VI-4 shows the data from which the curve was constructed. This gives an average of very nearly 50% thermal fissions in the mid-plane of the reactor.



F g VI 3 Rad al Power Distribution in Mid plane

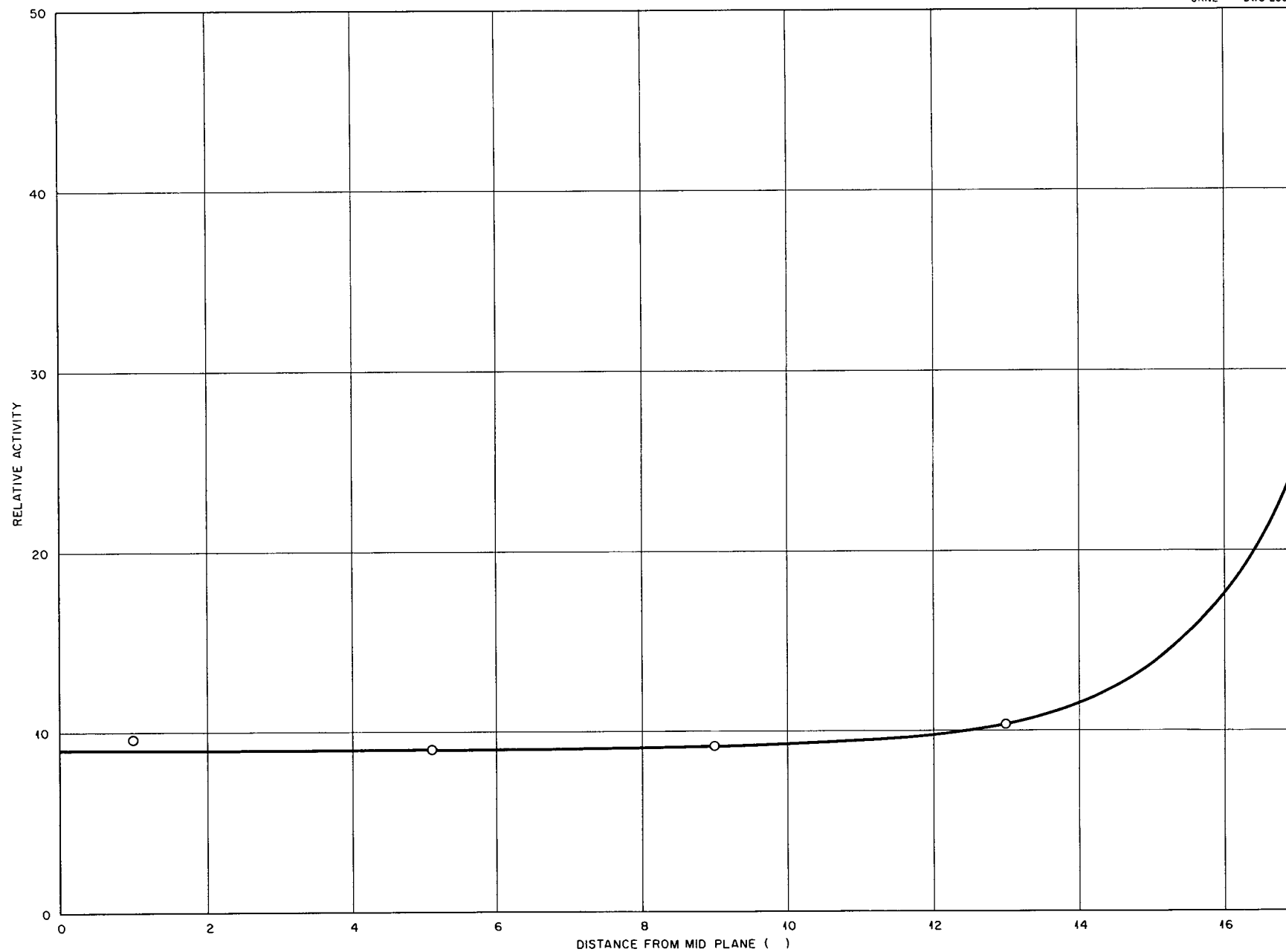
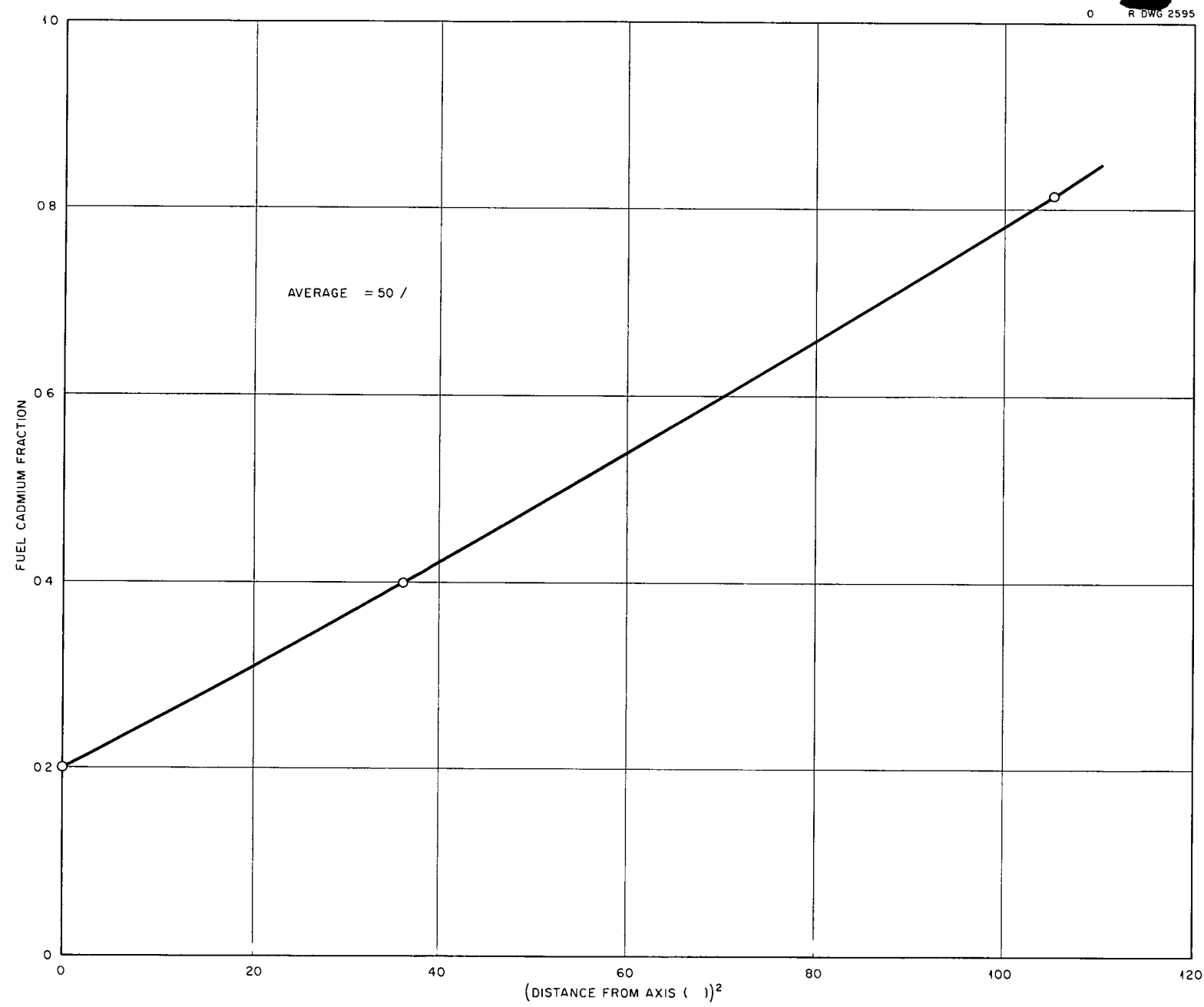


Fig VI 4 Axial Power Distribution Through M 12

62



F g VI 5 Radial Fuel Cadmium F actions

TABLE VI-4

Fuel Cadmium Fractions in the Mid-Plane

<u>Distance From Axis in Inches</u>	<u>Cadmium Fraction</u>
0 0	0 200
6 0	0 399
10 3	0 813

VII CA-14

A Critical Loadings

The final assembly was built up with a geometry similar to that used in CA-11. The aim of the experiment was to insert materials in the reactor that would simulate the structural poisons that would be present in a full scale reactor in the power range of 50 to 200 megawatts. The assembly was loaded as shown in Figures VII-1 and VII-2 and contained 18.2 kg of U-235 in the 0.42 gm U-235/cc fuel mixture described in Section V. In general the reactor was maintained critical with two different sets of poisons. The first set of poisons included

1. Boral sheets (9" x 2-7/8" x 1/4") which surrounded the fuel end ducts on the stationary table. This Boral extended from the end of the assembly to a point 9" from the central fuel region, thus 4-1/2" of the end ducts were covered. Boral sheets (1-1/4" x 2-7/8" x 1/4") were placed around the fuel end ducts on the movable table. These sheets extended from the end of the fuel ducts to a point 7-3/4" from the central fuel region.
2. Stainless steel sheets (0.146" thick) covered 96% of the inside fuel surface. The outside fuel surface was uncovered from the interface of the assembly back 4-1/2" on the stationary table. The fuel surface exposed at the assembly interface and the corresponding surface at the opposite end of the central fuel region were left uncovered. The remaining outside fuel surface was 96% covered with 0.118" thick stainless steel sheets. The total weight of the stainless steel was 25.5 kg.

-64-

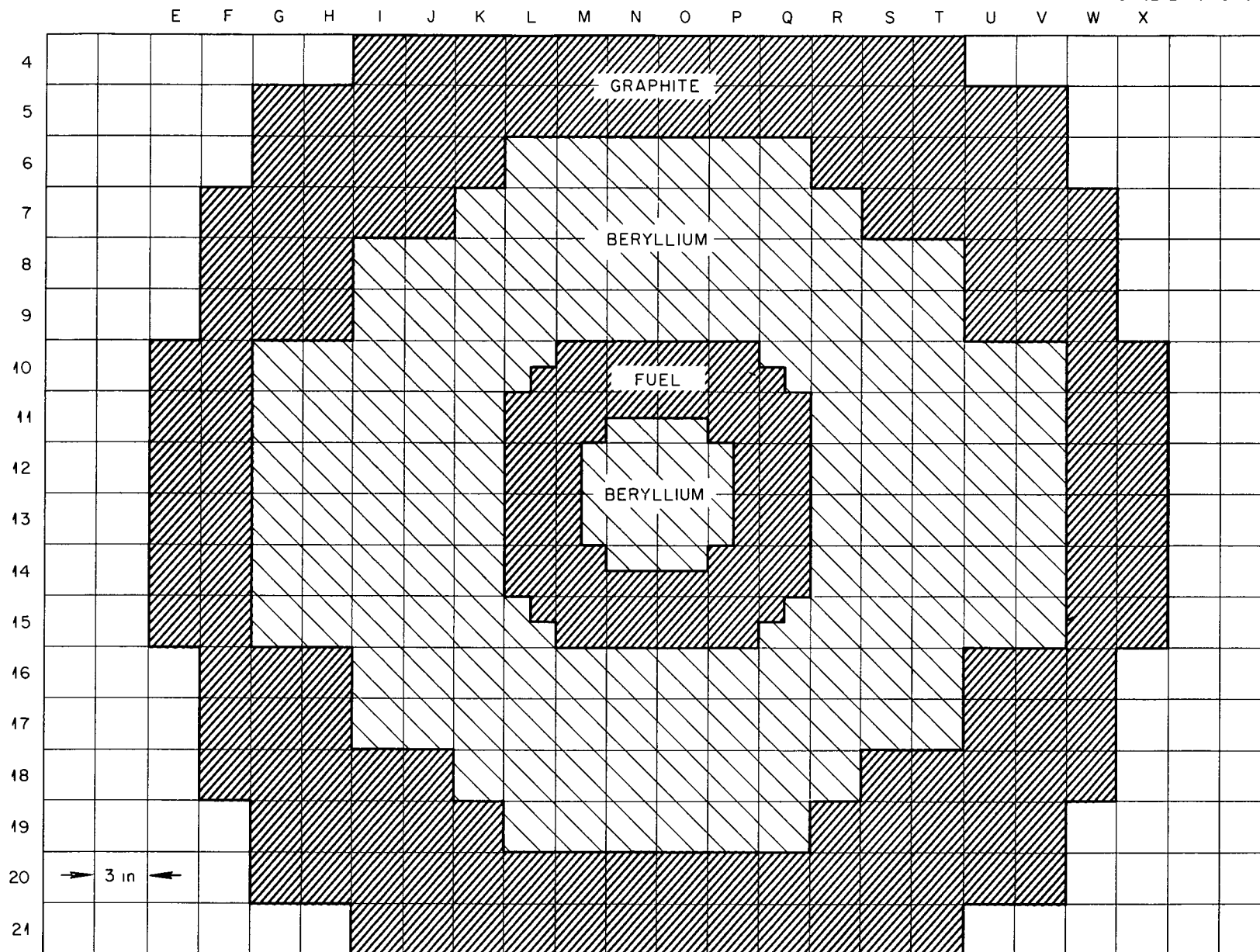


Fig VII-1 Assembly Loading at Mid-plane (No Structure Shown)

-65-

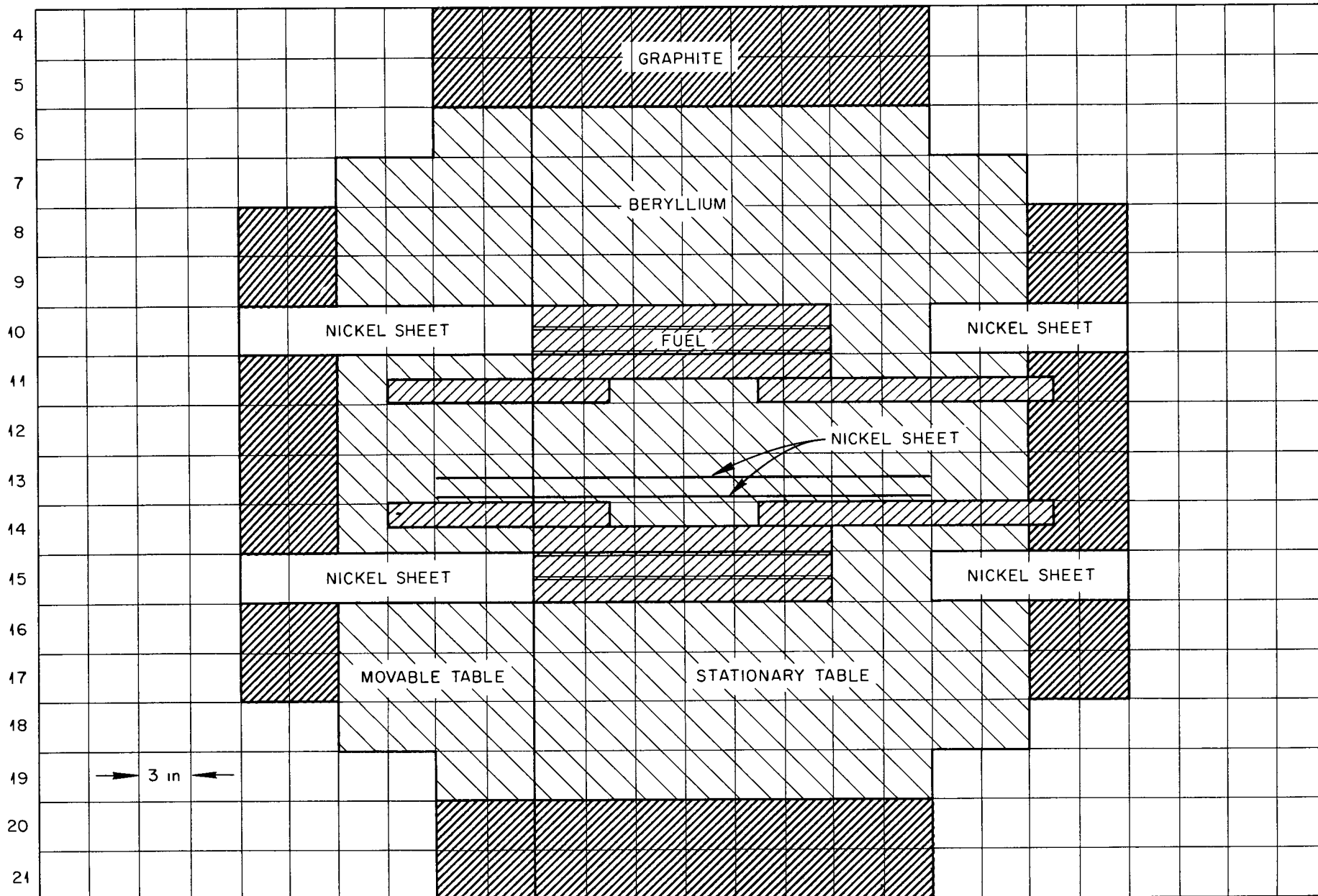


Fig VII-2 Axial Assembly Loading in Vertical Plane Containing Reactor Axis

- 3 Nickel sheets 2-7/8" wide and 0.015" thick were in the positions indicated in Figures VII-2 and VII-3

In addition to the above poisons, 177 in³ of beryllium were added to the fuel region. Of this total, 150 in³ were distributed symmetrically throughout the outer three fuel layers from 0 to 18 inches back on the stationary table. An additional 6 in³ were distributed symmetrically throughout the inner 4-1/2" long fuel layer adjacent to the assembly interface on the stationary table. The remaining 24 in³ of beryllium were symmetrically distributed throughout the fuel region on the movable table.

During this series of experiments reactivity values were obtained for one sheet of nickel (24" x 2-7/8" x 0.010") placed in a horizontal position across the top of cell K-12, and for the extension of the reflector from 9" to 12" of beryllium on the sides of the reactor. The insertion of the nickel sheet resulted in a loss in reactivity of 8 cents. The replacement of graphite by beryllium in cells G-10 through 15 and cells V-10 through 15 and the addition of graphite to cells E-10 through 15 and X-10 through 15 resulted in a gain in reactivity of 9.6 cents.

The second set of poison distributions involved the following changes:

- 1 The entire fuel surface was 95% covered by 27.8 kg of stainless steel
- 2 All the Boral around the end ducts was removed
- 3 The rest of the assembly was as described previously

The remaining measurements described were obtained with the reactor containing this second set of poison distributions.

B Importance Function of Three Stainless Steel Rods

The loss in reactivity due to three 316 stainless steel rods was determined at three radial positions in the reflector and at one position in the island. The rods were 3/16" in diameter, and 36" long and each weighed 132 gm. They were inserted as skewers in the various cells and extended through the entire shish on the stationary table. The data obtained are shown in Table VII-1.

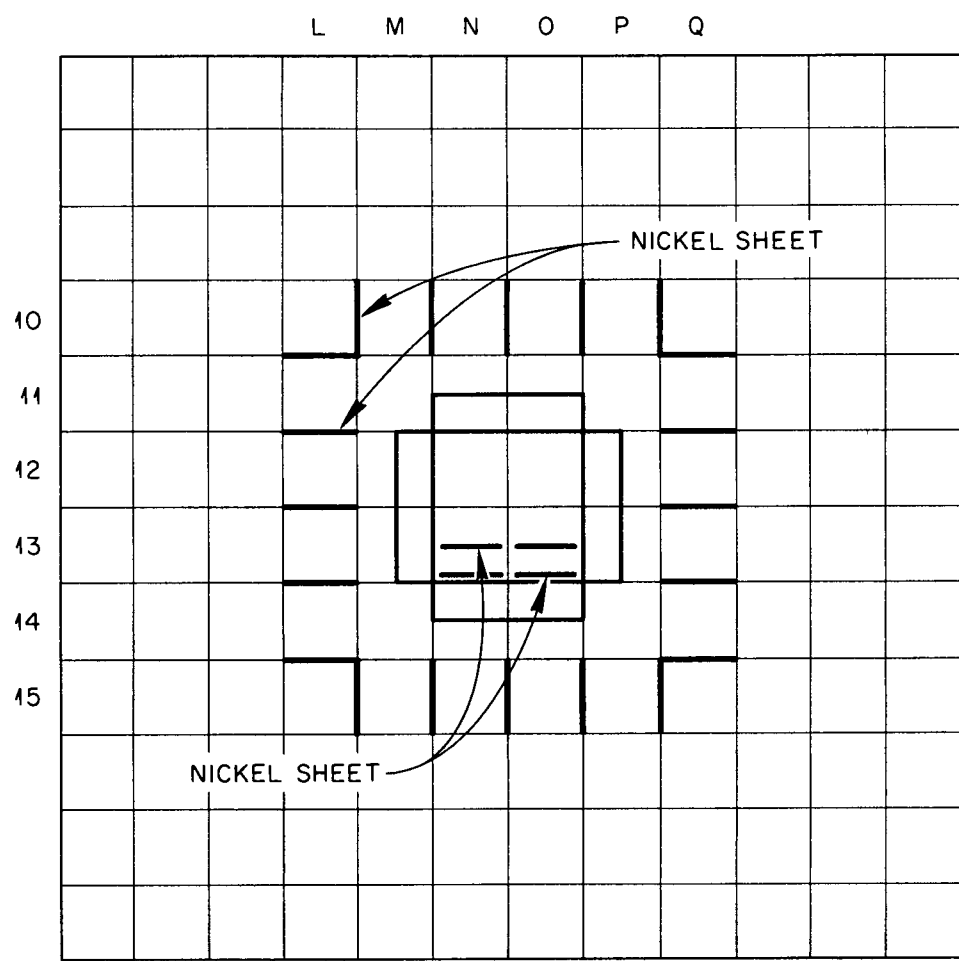


Fig VII-3 Position of Nickel Sheets on the Stationary and Movable Tables

TABLE VII-1

Importance Function of Three Stainless Steel Rods

<u>Average Distance of Rods From Axis in Inches</u>	<u>Loss in Reactivity in Cents</u>
2 3	23 1
10 8	17 6
13 7	12 0
16 7	6 0

C Thermal Neutron Leakage

Thermal neutron leakage was determined at the end and side of the reactor, both with and without Boral shielding around the end fuel ducts. These measurements were taken with 0, 1/8", 1/4", and 3/8" thicknesses of Boral surrounding the U-235 fission chamber that was used.

The side leakage was measured with the U-235 fission chamber located in cell D-12. The geometrical center of the chamber rested 12" back of the interface on the stationary table or 3" back of the mid-plane of the reactor. The axis of the chamber was approximately 1-1/2" from the edge of the graphite side reflector and was parallel to the reactor axis. The Boral layers surrounding the chamber were in the form of concentric cylindrical sleeves that extended from the interface of the stationary table back 24". The inside diameter of the inner most layer was 2", and the outside diameter of the outer most layer, using 3 layers, was about 2-3/4". The ends of the Boral sleeves were not capped.

The end leakage was determined with the fission chamber placed 5-1/2" back of the end graphite reflector. The axis of the chamber was parallel to the floor and perpendicular to the axis of the reactor, which passed through the geometrical center of the chamber. The data obtained are shown in Table VII-2 and Figure VII-4. All measurements are shown relative to the side leakage without any Boral shielding around the chamber or in the reactor.

D Power Distribution

A radial power distribution was taken in the mid-plane across the fuel annulus (cells P-12 and Q-12). The traverse was obtained by placing uranium and aluminum foils between the vertically adjacent fuel tubes in the cells. The data obtained are shown in Table VII-3 and Figure VII-5.

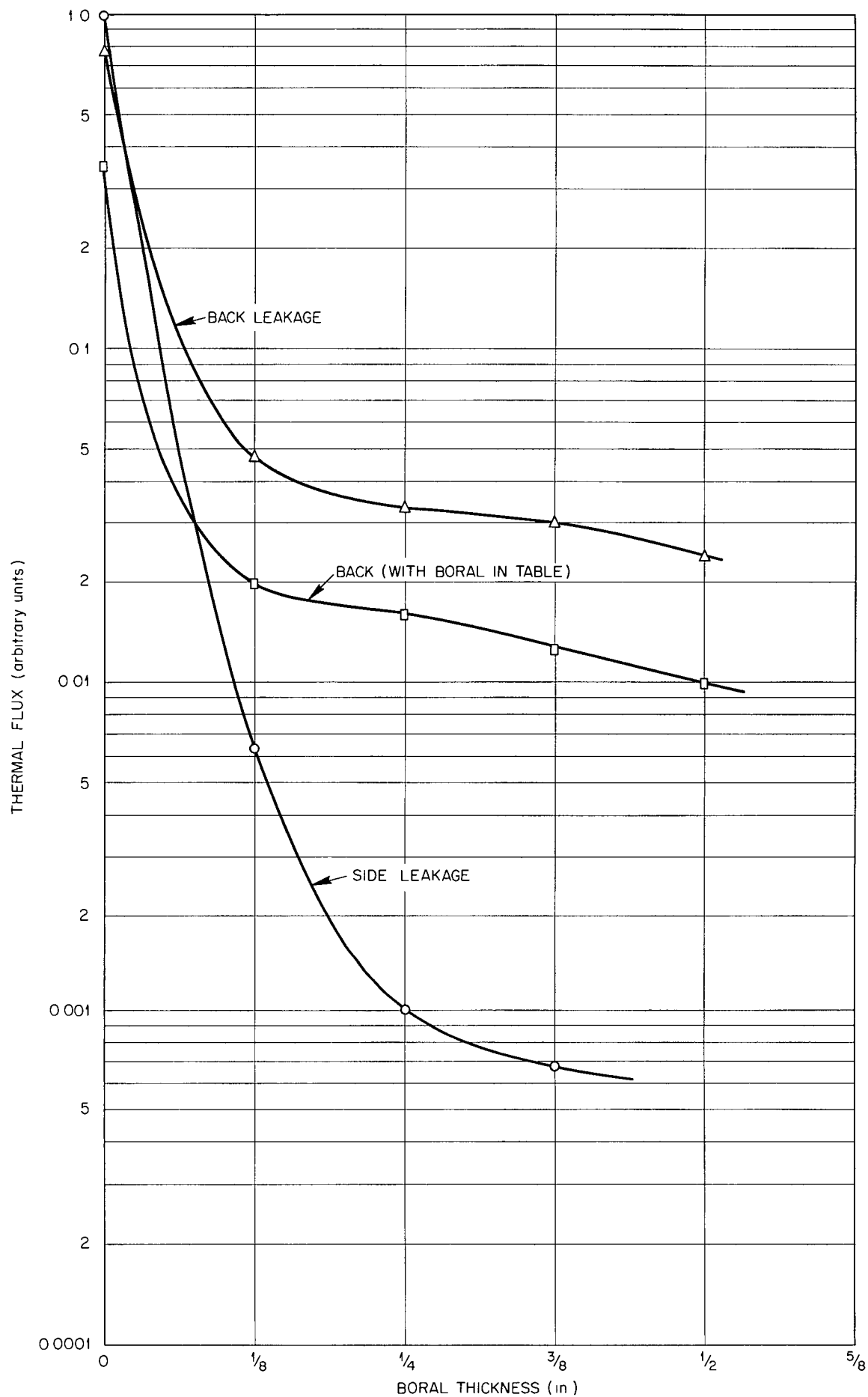


Fig VII-4 Thermal Flux Leakage vs Boral Thickness

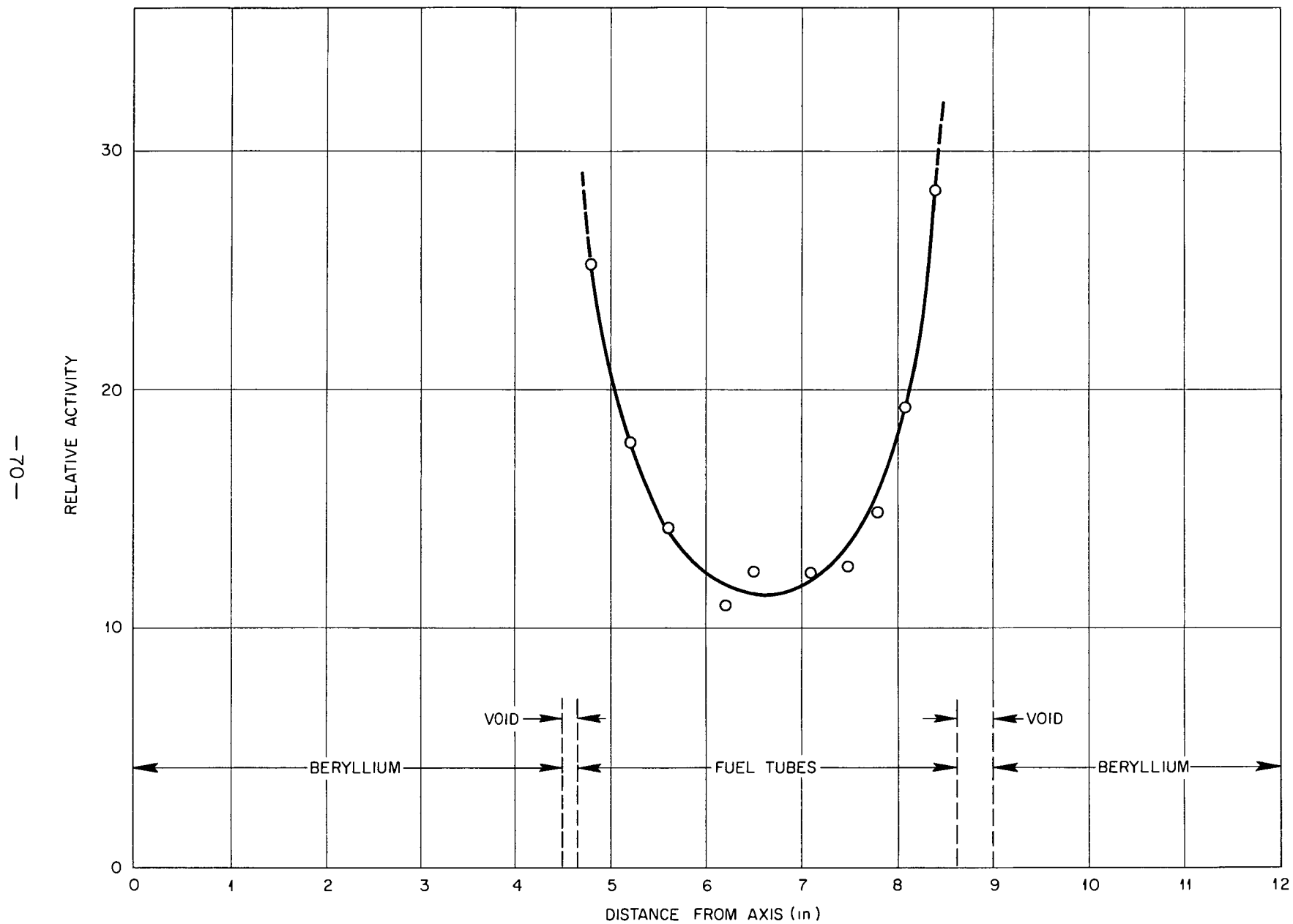


Fig VII-5 Power Distribution across Fuel Annulus at Mid-plane

TABLE VII-2

Thermal Neutron Leakage

<u>Layers of 1/8" Boral*</u> <u>Around Counter</u>	<u>Counter</u> <u>Position</u>	<u>Boral Around</u> <u>End Ducts</u>	<u>Relative</u> <u>Activity</u>
0	Side	No	1 000
1	Side	No	0 00635
2	Side	No	0 00103
3	Side	No	0 000676
0	End	No	0 777
1	End	No	0 0466
2	End	No	0.0332
3	End	No	0 0301
4	End	No	0.0235
0	End	Yes	0 352
1	End	Yes	0 0197
2	End	Yes	0 0160
3	End	Yes	0 0125
4	End	Yes	0 00992

*0.161 gm B/cm²/Layer of Boral present

TABLE VII-3

Power Distribution Across Fuel Annulus at Mid-plane

<u>Distance From Axis</u> <u>in Inches</u>	<u>Relative Activity</u>
4.8	25 30
5.2	17 86
5.6	14 24
6.2	10 97
6.5	12 40
7.1	12 35
7.5	12 63
7.8	14 87
8.1	19 32
8.4	28 34

APPENDIX "A"

Summary of Materials in Reactor Assemblies

CA-10

Island	Mass kg	Volume cm ³ x 10 ⁻³	Mass Fraction	Volume Fraction	Average* Density gm/cm ³
Beryllium	48 1	26 0	911	918	1 699
2S Al Matrix	4 5	1 6	085	058	0 158
24S Al Skewers	0 2	0 1	003	002	0 008
Stainless Steel skewer	-	-	-	-	0 024
Void	-	0 6	-	021	-

The island contained eleven aluminum and one steel skewer They were placed in the outer island cells

Fuel Annulus (Includes beryllium region required to close annulus)

Sodium	52 4	52 5	486	734	0 805
Uranium	16 1	0 9	149	012	0 265
					0 161
304 Stainless Steel Boxes	14 3	1 8	132	025	0 220
2S Al Matrix	11 1	5 4	103	075	0 158
24S Al Skewers	0 6	0 2	005	003	0 008
Stainless Steel skewer	-	-	-	-	0 024
Al Caps	7 4	2 7	068	038	-
Beryllium	6 0	3 3	056	045	1 699
Void	-	4 8	-	067	-

The lower uranium density reported refers to the fuel region behind the island The higher figure refers to the remainder of the fuel region

Reflector (Beryllium)

Beryllium	1521 6	822 5	914	918	1 699
2S Al Matrix	141 6	52 1	085	058	0 158
24S Al Skewers	0 9	0 3	-	-	0 008
Stainless Steel skewers	0 8	0 1	-	-	0 025
Void	-	20 5	-	023	-

CA-10 - Continued

	Mass kg	Volume cm ³ x 10 ⁻³	Mass Fraction	Volume Fraction	Average* Density gm/cm ³
<u>Reflector</u> (Graphite)					
Graphite	1673 5	974 7	907	898	1 542
2S Al Matrix	171 6	63 1	093	058	0 158
Void	-	47 7	-	044	-

* The average densities reported are for a unit cell (9"² cross-sectional area) in which the material was actually present

CA-11

	Mass kg	Volume cm ³ x 10 ⁻³	Mass Fraction	Volume Fraction	Average Density gm/cm ³
<u>Island</u> (Includes Be Region enclosed by end ducts)					
Beryllium	57 1	30 9	912	918	1 699
2S Al matrix	5 3	2 0	085	058	0 158
24S Al skewers	0 2	0 1	003	002	0 008
Void	-	0 7	-	021	-

The island contained 16 skewers, which were placed in the outer beryllium shishes (9" length)

Fuel Annulus (Includes end ducts)

Fuel Mixture					
Including Uranium	64 4	35 0	620	527	-
Uranium	8 2	-	079	-	0 123
UF ₄	-	-	-	-	0 163
ZrO ₂	-	-	-	-	0 553
NaF	-	-	-	-	0 200
C	-	-	-	-	0 088
2S Al Matrix	10 5	3 9	098	058	0 158
Al Fuel Tubes and Spacers	28 6	10 5	275	159	0 443
Stainless Steel					
Nuts	0 8	0 1	007	001	-
Void	-	16 9	-	254	-

The weight of the fuel mixture includes 360 grams of uranium present as disks

Each fuel tube had a stainless steel nut on both ends

Reflector (Beryllium)

Beryllium	1518 6	820 9	914	918	1 699
2S Al Matrix	141 3	52 0	085	058	0 158
24S Al Skewers	0 8	0 3	-	-	0 008
Stainless Steel					
skewers	0 8	0 1	-	-	0 024
Void	-	20 5	-	023	-

Reflector (Graphite)

Graphite	1626 677	947 4	906	898	1 542
2S Al Matrix	166 831	61 3	093	058	0 158

<u>CA-12</u>		Variation I (Graphite island and reflector)			
	Mass	Volume	Mass	Volume	Average
	kg	cm ³ x 10 ⁻³	Fraction	Fraction	Density
					gm/cm ³
<u>Island</u> (Includes region enclosed by fuel annulus)					
Graphite	180 1	104 9	903	898	1 542
2S Al Matrix	18 5	6 8	093	058	0 158
Stainless Steel					
skewers	0 8	0 1	004	001	0 024
Void	-	5 0	-	043	-
<u>Fuel Annulus</u>					
Fuel Mixture	75 3	40 5	622	545	-
(Including Uranium)					
Uranium	18 5	-	153	-	0 249
UF ₄	-	-	-	-	0 329
ZrO ₂	-	-	-	-	0 449
NaF	-	-	-	-	0 163
C	-	-	-	-	0 072
Al Fuel Tubes	33 0	12 1	273	163	0 443
2S Al Matrix	11 8	4 3	097	058	0 158
Stainless Steel					
Nuts	1 0	0 1	008	002	-
Void	-	-	-	232	-
<u>Reflector</u>					
Graphite	6738 5	3965 1	906	900	1 542
2S Al Matrix	696 8	256 2	094	058	0 158
Stainless Steel					
Skewers	0 8	0 1	-	-	0 024
Void	-	185 4	-	042	-

The outer 128 cells were filled with AGHT Graphite in all CA-12 configurations All other graphite is AGOT

Variation II (Combination graphite and beryllium island and reflector)

<u>Island</u>					
Beryllium	82 2	44 4	515	472	1 699
Graphite	61 8	36 1	387	383	1 542
2S Al Matrix	14 9	5 5	093	058	0 158
Stainless Steel					
skewers	0 8	0 1	005	001	0.024
Void	-	8 0	-	085	-

CA-12 - continued

	Mass kg	Volume cm ³ x 10 ⁻³	Mass Fraction	Volume Fraction	Average Density gm/cm ³
<u>Fuel Annulus</u>					
Fuel Mixture Including Uranium	82 0	44 1	608	415	-
Uranium	19 6	-	146	-	-
Al Fuel Tubes	35 0	12 9	260	121	0 443
2S Al Matrix	16 8	6 2	124	058	0 158
Stainless Steel					
Nuts	1 1	0 1	008	001	-
Void	-	42 9	-	404	-

Reflector (Be and Graphite)

Beryllium	681 1	368 2	470	450	1 699
Graphite	639 7	372 6	441	456	1 542
2S Al Matrix	129 3	47 5	089	058	0 158
Void	-	29 3	-	036	-

Reflector (Graphite - includes only the region outside the Be reflector)

Graphite	5674 4	3345 6	906	900	1 542
2S Al Matrix	587 7	216 1	094	058	0 158
Void	-	154 9	-	042	-

Variation III - (Two Region)

Core

Fuel Mixture Including Uranium	75 3	40 5	622	545	-
Uranium	18 5	-	153	-	-
Al Fuel Tubes	33 0	12 1	273	163	0 443
Al Matrix	11 8	4 3	097	058	0 158
Stainless Steel					
Nuts	1 0	0 1	008	002	-
Void	-	19 3	-	232	-

Reflector (Be + Graphite)

Beryllium	559 3	302 3	676	662	1 699
Al Matrix	72 2	26 5	087	058	0 158
Graphite	196 5	114 4	237	251	1 542
Void	-	13 3	-	029	-

CA-12 - Continued

	Mass kg	Volume cm ³ x 10 ⁻³	Mass Fraction	Volume Fraction	Average Density gm/cm ³
<u>Reflector (Graphite)</u>					
Graphite	6362 0	3746 1	906	900	1 542
Al Matrix	658 2	242 0	094	058	0 158
Void	-	174 5	-	042	-

CA-13

Core

Fuel Mixture	75 3	40 5	297	266	-
Including Uranium					
Uranium	18 5	-	073	-	-
UF ₄	-	-	-	-	0 164
ZrO ₂	-	-	-	-	0 224
NaF	-	-	-	-	0 081
C	-	-	-	-	0 036
Graphite	120 7	70 3	475	463	0 771
Al Fuel Tubes	33 0	12 1	130	080	0 221
Al Matrix	24 0	8 8	094	058	0 158
Stainless Steel					
Nuts	1 0	0 1	004	001	-
Void	-	20 0	-	131	-

Reflector (Beryllium)

Beryllium	1654 7	894 4	914	918	1 699
Al Matrix	154 0	56 6	085	058	0 158
Al Skewers	0 4	0 2	-	-	0 008
Stainless Steel					
skewers	1 3	0 2	001	-	0 024
Void	-	22 4	-	023	-

Reflector (Graphite)

Graphite	2071 4	1206 4	907	898	1 542
Al Matrix	212 4	78 1	034	058	0 158
Void	-	59 0	-	044	-

CA-14

Island (Includes Be Region enclosed by End Ducts)

	Mass kg	Volume cm ³ x 10 ⁻³	Mass Fraction	Volume Fraction	Average Density gm/cm ³
Beryllium	57 1	30 9	905	918	1 699
Al Matrix	5 3	2 0	084	058	0 158
Nickel	0 5	0 1	008	002	0 028
Al Skewers	0 2	0 1	003	002	0 008
Void	-	0 7	-	020	-

Fuel Annulus (Including End Ducts)

Fuel Mixture	81 3	43 7	596	544	-
Including Uranium					
Uranium	19 6	-	143	-	0 249
Al Fuel Tubes	36 0	13 2	264	165	0 443
Aluminum Matrix	12 7	4 7	093	058	0 158
Beryllium	5 4	2 9	039	,036	-
Stainless Steel					
Nuts	1 1	0 1	008	002	-
Void	-	15 7	-	195	-

Reflector (Beryllium)

Beryllium	1559 0	842 7	913	918	1 699
Al Matrix	145 1	53 3	085	058	0 158
Nickel	1 8	2	001	0002	0 028
Stainless Steel					
Skewers	0 8	1	0004	0001	0 024
Al Skewers	0 8	3	0005	0003	0 008
Void	-	20 9	-	023	-

Reflector (Graphite)

Graphite	1255 1	731 0	906	898	1 542
Al Matrix	128 7	47 3	093	058	0 158
Nickel	1 2	1	001	-	0 028
Void	-	35 6	-	044	-

APPENDIX B

Analysis of Materials in Weight Per Cent

[illegible]